CALIPSO Lidar Level 2 Vertical Feature Mask Data Description Document
Version 5.00

Last Updated: 5 October 2025

Data Version:	5.00
Data Release Date:	October 01, 2025
Data Date Range:	June 13, 2006 to June 30, 2023

Introduction

The CALIPSO lidar level 2 (L2) vertical feature mask (VFM) data product describes the vertical and horizontal distribution of cloud and aerosol layers observed by the CALIPSO lidar. The primary scientific data set (SDS) in the VFM files is the Feature Classification Flags. The Feature Classification Flags are stored as N × 5515 arrays of bit-mapped 16-bit integers, where N is the number of 15-shot (~5 km along track) data segments in the granule. The data recorded in each 5515-element one-dimensional (1-D) array describes a vertical curtain that extends 5 km horizontally over an altitude range of 30.1 km down to –0.5 km. Each bit-mapped integer in these arrays characterizes the atmospheric state in exactly one of the range bins recorded in CALIOP's downlinked data stream. Applying the Feature Classification Flags bit interpretations given in

Table 3 yields a concise overview of the atmospheric state within each range bin.

As shown in Table 1, the vertical and horizontal resolution of the downlinked CALIOP data varies as a function of altitude above mean sea level. Consequently, the spatial resolution of the elements within the 1-D arrays is nonuniform. Figure 1 illustrates the mapping of the 1-D array of Feature Classification Flags into a two-dimensional (2-D) array of height-resolved averaged lidar data samples. The numbers in each block of this image indicate the 1-D array indices associated with each spatial averaging regime in the 2-D lidar backscatter data. Only the starting and ending indices are shown. Figure 2 shows an example of the information content stored in the Feature Classification Flags. The upper panel shows level 1b (L1b) 532 nm total attenuated backscatter coefficients measured on 28 August 2014 along the west coast of Africa and out into the eastern Atlantic Ocean. The lower panel shows the location and type (e.g., cloud vs. aerosol) for all features identified in the L1b data by the L2 data analysis algorithms. This feature type analysis is only one of several available in the VFM files.

Table 1: Spatial averaging scheme applied to the CALIOP backscatter measurements prior to downlinking the data from the satellite to the ground station. The data shown are taken from Tables 3 and 4 in Hunt et al., 2009 with specifications given only for the 532 nm channel. The VFM Feature Classification Flags are recorded at the spatial resolution of the downlinked 532 nm signals and report samples measured between 30.1 km and –0.5 km.

Nominal Altitude Region (km)	Laser Pulses Averaged	Horizontal Resolution (km)	15-m Digitizer Samples Averaged	Vertical Resolution (m)
40.0 to 30.1	15	5.025	20	300
30.1 to 20.2	5	1.675	12	180
20.2 to 8.2	3	1.005	4	60
8.2 to –0.5	1	0.335	2	30
–0.5 to –2.0	1	0.335	20	300

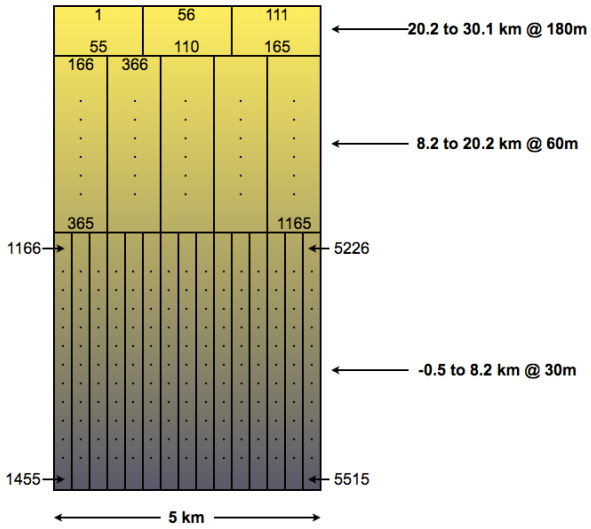

Figure 1: Mapping of the one-dimensional array of feature classification flags into a two-dimensional array of range-resolved lidar data samples. Numbers indicate the (1-based) array index of the elements in 1-D array. To create a pseudo-single-shot matrix, replicate each of the vertical profiles between 30.1 km and 20.2 km five times. Similarly, replicate each of the vertical profiles between 20.2 km and 8.2 km three times.

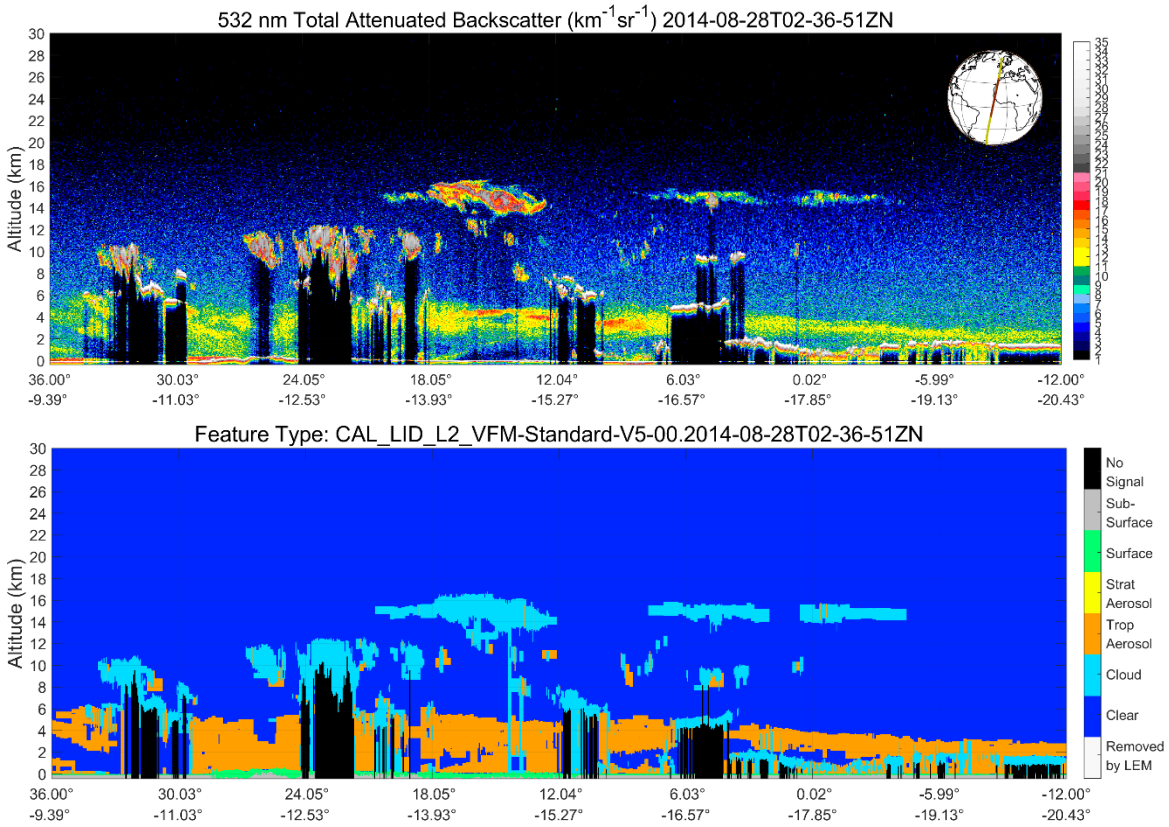

Figure 2: The upper panel shows CALIOP 532 nm total backscatter coefficients measured on 28 August 2014 retrieved from the lidar level 1b file for that date and time. The lower panel shows an image of layer location and type decoded from the Feature Classification Flags in the corresponding VFM file.

Table of Contents

Additional Documentation

Project Documentation

- CALIPSO Data Management Team: CALIPSO Data Products Catalog, PC-SCI-503, Release 5.00.
- Hostetler, C. A., Z. Liu, J. Reagan, M. Vaughan, D. Winker, M. Osborn, W. H. Hunt, K. A. Powell, and C. Trepte, 2006: CALIOP Algorithm Theoretical Basis Document: Calibration and Level 1 Data Products, PC-SCI-201 Release 1.0, https://ntrs.nasa.gov/citations/20250006623.
- Winker, D. M., C. A. Hostetler, M. A. Vaughan, and A. H. Omar, 2006: CALIOP Algorithm Theoretical Basis Document: Part 1 : CALIOP Instrument, and Algorithms Overview, PC-SCI-202 Part 1 Release 2.0, https://ntrs.nasa.gov/citations/20250006626.
- Vaughan, M. A., D. M. Winker, and K. A. Powell, 2005: CALIOP Algorithm Theoretical Basis Document Part 2: Feature Detection and Layer Properties Algorithms, PC-SCI-202 Part 2 Release 1.01, https://ntrs.nasa.gov/citations/20250006627.
- Liu, Z., A. H. Omar, Y. Hu, M. A. Vaughan, and D. M. Winker, 2005: CALIOP Algorithm Theoretical Basis Document: Part 3: Scene Classification Algorithms, PC-SCI-202 Part 3 Release 1.0, https://ntrs.nasa.gov/citations/20250006628.

Peer-Reviewed Algorithm Papers

- Avery, M. A., R. A. Ryan, B. J. Getzewich, M. A. Vaughan, D. M. Winker, Y. Hu, A. Garnier, J. Pelon, and C. A. Verhappen, 2020: CALIOP V4 Cloud Thermodynamic Phase Assignment and the Impact of Near-Nadir Viewing Angles, *Atmos. Meas. Tech.*, **13**, 4539–4563, https://doi.org/10.5194/amt-13-4539-2020.
- Hunt, W. H, D. M. Winker, M. A. Vaughan, K. A. Powell, P. L. Lucker, and C. Weimer, 2009: CALIPSO Lidar Description and Performance Assessment, *J. Atmos. Oceanic Technol.*, **26**, 1214–1228, https://doi.org/10.1175/2009JTECHA1223.1.
- Kim, M.-H., A. H. Omar, J. L. Tackett, M. A. Vaughan, D. M. Winker, C. R. Trepte, Y. Hu, Z. Liu, L. R. Poole, M. C. Pitts, J. Kar, and B. E. Magill, 2018: The CALIPSO Version 4 Automated Aerosol Classification and Lidar Ratio Selection Algorithm, *Atmos. Meas. Tech.*, **11**, 6107-6135, https://doi.org/10.5194/amt-11-6107-2018.
- Liu, Z., J. Kar, S. Zeng, J. Tackett, M. Vaughan, M. Avery, J. Pelon, B. Getzewich, K.-P. Lee, B. Magill, A. Omar, P. Lucker, C. Trepte, and D. Winker, 2019: Discriminating Between Clouds and Aerosols in the CALIOP Version 4.1 Data Products, *Atmos. Meas. Tech.*, **12**, 703–734, https://doi.org/10.5194/amt-12-703-2019.
- Tackett, J. L., J. Kar, M. A. Vaughan, B. Getzewich, M.-H. Kim, J.-P. Vernier, A. H. Omar, B. Magill, M. C. Pitts, and D. Winker, 2023: "The CALIPSO version 4.5 stratospheric aerosol subtyping algorithm", *Atmos. Meas. Tech.*, **16**, 745–768, https://doi.org/10.5194/amt-16-745-2023.
- Vaughan, M., K. Powell, R. Kuehn, S. Young, D. Winker, C. Hostetler, W. Hunt, Z. Liu, M. McGill, and B. Getzewich, 2009: Fully Automated Detection of Cloud and Aerosol Layers in the CALIPSO Lidar Measurements, *J. Atmos. Oceanic Technol*., **26**, 2034–2050, https://doi.org/10.1175/2009JTECHA1228.1.
- Winker, D. M., M. A. Vaughan, A. H. Omar, Y. Hu, K. A. Powell, Z. Liu, W. H. Hunt, and S. A. Young, 2009: Overview of the CALIPSO Mission and CALIOP Data Processing Algorithms, *J. Atmos. Oceanic Technol*., **26**, 2310–2323, https://doi.org/10.1175/2009JTECHA1281.1.

Glossary and Acronym Dictionary

Term	Meaning
CAD	cloud-aerosol discrimination
CALIOP	Cloud-Aerosol Lidar with Orthogonal Polarization

Term	Meaning
CALIPSO	Cloud-Aerosol Lidar and Infrared Pathfinder Satellite Observation
ECR	Earth Centered Rotating coordinates
frame	a fundamental data averaging interval used extensively in CALIOP's level 1 and level 2 data processing. A frame consists of 15 consecutive single-shot profiles spanning an along-track distance of ~5 km. 15 shots is the least common multiple of the along-track averaging intervals defined by CALIOP's vertically varying onboard data averaging scheme (Hunt et al., 2009).
granule	continuous data segment in which all measurements were acquired while the lidar was configured for daytime data acquisition only or nighttime data acquisition only; each granule spans approximately one half of a full orbit, with daytime granules being slightly larger/longer than nighttime granules
HDF	Hierarchical Data Format
IVDR	integrated volume depolarization ratio
L1B	level 1B
LEM	low energy mitigation
nm	nanometer
QA	quality assurance/quality control
QC	quality control/quality assurance
SNR	signal-to-noise ratio
SDS	scientific data set
TAI	International Atomic Time
UTC	Coordinated Universal Time
WRS	Worldwide Reference System

Scientific Data Sets: Measurement Altitudes

Lidar_Data_Altitudes

Units: km

Format: Float_32

Valid Range: -2.0, 30.0

Description: Altitudes (above mean sea level) that specify the vertical midpoints of the 545 range bins in spanned by the measurements reported in the vertical feature mask files. This scientific data set (SDS) is only available in the V5.00 data release. In all prior versions, the lidar data altitude array was stored only in the file metadata.

Scientific Data Sets: Time and Position

Note: the VFM files contain several SDSs that report identical parameters at two different spatial averaging resolutions. To clearly distinguish between the single shot and 5 km (15 shot) resolutions of these identical parameters, a 2-letter prefix ('ss' = single shot) is added to the single shot SDS names.

Profile_Time, ssProfile_Time

Units: TAI seconds

Format: Float_64

Valid Range: 4.203E8, 9.623E8

Description: International Atomic Time (TAI) in elapsed seconds from January 1, 1993. The single shot ssProfile_Time SDS reports TAI times for individual laser pulses. The Profile_Time SDS reports TAI times at the temporal midpoint of each 5 km averaged data segment (i.e., at the 8th of 15 consecutive laser shots).

Profile_UTC_Time, ssProfile_UTC_Time

Units: yymmdd.ffffffff

Format: Float_64

Valid Range: 60428.0, 230701.0

Description: Coordinated Universal Time (UTC), formatted as yymmdd.ffffffff, where yy is a two-digit data acquisition year number (06 to 23), mm is a month number (01 to 12), dd is a day number (1 to 31), and ffffffff is the elapsed fraction of the data acquisition day. The single shot ssProfile_UTC_Time SDS reports UTC times for individual laser pulses. The Profile_UTC_Time SDS reports UTC times at the temporal midpoint of each 5 km averaged data segment (i.e., at the 8th of 15 consecutive laser shots).

Day_Night_Flag, ssDay_Night_Flag

Units: NoUnits

Format: Int_8

Valid Range: 0,1

Description: As CALIPSO approaches the terminator, the lidar is automatically reconfigured to adapt to changing lighting conditions that directly impact signal-to-noise (SNR) levels. These changes occur at Sun-Earth-Satellite (SES) angles of 95° (day-to-night) and 265° (night-to-day), corresponding to sunrise and sunset at an altitude of ~24 km above mean sea level. A 0 in these fields indicates daytime measurement configuration, while a 1 indicates nighttime. The single shot ssDay_Night_Flag SDS reports the lidar configuration status for individual laser pulses. The Day_Night_Flag SDS reports the lidar configuration status at the temporal midpoint of each 5 km averaged data segment (i.e., at the 8th of 15 consecutive laser shots).

Profile_ID, ssProfile_ID

Units: NoUnits

Format: Int_32

Valid Range: 1, 228630

Description: Unique identifier generated sequentially for each individual laser pulse. Profile IDs are unique within each granule but not unique over multiple granules. The single shot ssProfile_ID SDS reports the profile IDs assigned to each individual laser pulses within a granule. The ssProfile_ID SDS reports the single shot profile IDs at the temporal midpoint of each 5 km averaged data segment (i.e., at the 8th of 15 consecutive laser shots).

Latitude, ssLatitude

Units: degrees north

Format: Float_32

Valid Range: -90.0, 90.0

Description: Latitude of the laser footprint on the Earth's surface. The single shot ssLatitude SDS reports footprint latitudes for individual laser pulses. The Latitude SDS reports the laser footprint latitude at the temporal midpoint of each 5 km averaged data segment (i.e., at the 8th of 15 consecutive laser shots).

Longitude, ssLongitude

Units: degrees east

Format: Float_32

Valid Range: -180.0, 180.0

Description: Longitude of the laser footprint on the Earth's surface. Longitudes reported in the 1/3 km layer products are for the individual laser pulses from which the layer statistics were derived. The single shot

ssLongitude SDS reports footprint longitudes for individual laser pulses. The Longitude SDS reports the laser footprint longitude at the temporal midpoint of each 5 km averaged data segment (i.e., at the 8th of 15 consecutive laser shots).

Scientific Data Sets: Lidar Operating Mode

Minimum_Laser_Energy_532

Units: J

Format: Float_32

Typical Range: 0.003…0.135

Fill Value: -9999.0

Description: Minimum laser energy at 532 nm measured within each 80 km along-track data segment (80 km = 240 single-shot laser pulses). The 80 km distance matches the largest horizontal extent considered in CALIOP's standard level 2 data analyses. Since layers can be detected at horizontal resolutions as large as 80 km, anomalously low laser energies in coarse resolution upper layers can potentially introduce biases in the spatial and optical property retrievals of underlying layers detected at finer spatial resolutions. The Minimum_Laser_Energy_532 SDS enables ready identification of these problematic situations.

ssLaser_Energy_532

Units: J

Format: Float_32

Typical Range: 0.003...0.135

Description: 532 nm laser energy measured for each laser pulse by a dedicated onboard laser energy monitor.

Scientific Data Sets: Surface Information

Land_Water_Mask

ssLand_Water_Mask

Units: NoUnits

Format: Int_8

Valid Range: 0, 7

Fill Value: -9

Description: Surface type at the laser footprint provided by the CloudSat science team digital elevation model.

Table 2: Interpretation of the Land Water Mask

value	interpretation
0	shallow ocean
1	land
2	coastlines
3	shallow inland water
4	intermittent water
5	deep inland water
6	continental ocean
7	deep ocean

Scientific Data Sets: Feature Detection

Feature_Classification_Flags

Units: NoUnits

Format: UInt_16

Valid Range: 1, 49146

Description: For each layer detected in the CALIPSO backscatter data, a set of feature classification flags is assembled to provide a high-level description of feature type. These feature classification flags are stored as bit-mapped 16-bit integers, with bit 0 being the least significant bit. For each granule processed by the level 2 data analyses, the VFM data product maps these flags onto a 2D matrix of 16-bit integers recorded at CALIOP's altitude-dependent data downlink resolution between 30.1 km and –0.5 km and extending along the full granule ground track. As illustrated in Figure 2 (feature type) and Figure 3 (horizontal averaging required for feature detection), the feature classification flags for individual layers are replicated vertically and horizontally in all matrix elements in which the feature was detected.

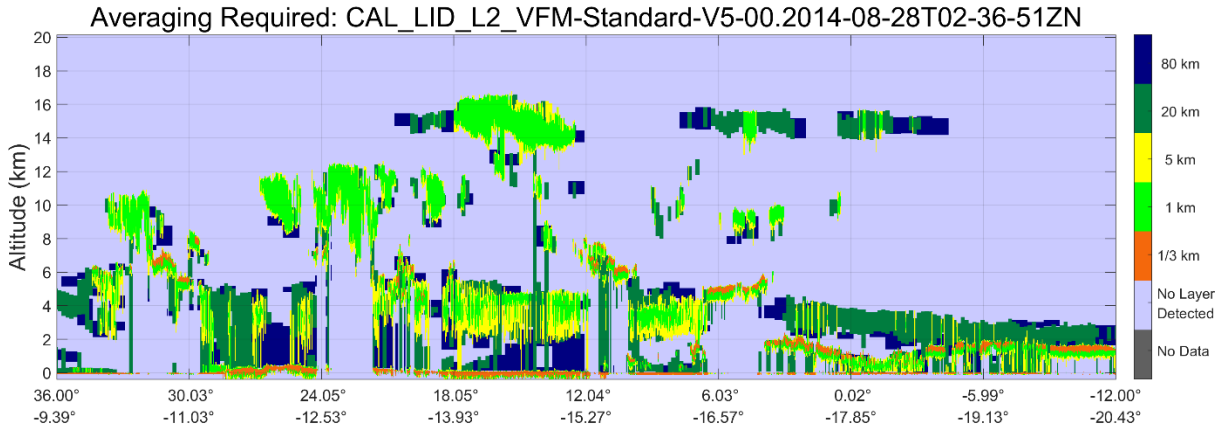

Figure 3: VFM image showing the amount of horizontal averaging required to detect the features in the CALIOP 532 nm total backscatter scene shown in Figure 2.

The interpretations of the bit fields in the feature classification flags are given in Table 3. The first three bits (bits 0–2) specify the feature type. Bits 9–11 identify the feature subtype for clouds, tropospheric aerosols, and stratospheric aerosols. For regions identified as "clear air", in which no atmospheric features were detected, bits 9–11 report additional LEM analyses of the range bin (Tackett et al., 2025). Correct interpretation of the feature subtype bits depends entirely on the feature type identified in bits 0–2, and the interpretations are different for clouds, aerosols, and clear air. Distinguishing between features and clear air is accomplished by the CALIOP layer detection algorithms (Vaughan et al., 2009). Cloud-aerosol discrimination (CAD) is accomplished using 5-dimensional probability distribution functions (PDFs), as described in Liu et al., 2019. Aerosol layers in the troposphere are partitioned into eight subtypes: undetermined, marine, dust, polluted continental/ smoke, clean continental, polluted dust, elevated smoke, and dusty marine. Five subtypes of stratospheric aerosols are identified: invalid, polar stratospheric aerosol, volcanic ash, sulfate, elevated smoke, and unclassified. Comprehensive descriptions of the tropospheric and stratospheric aerosol subtyping algorithms are given in, respectively, Kim et al., 2018 and Tackett et al., 2023. The CALIOP cloud subtyping algorithm recognizes eight cloud types: low, overcast, and optically thin (e.g., transparent stratus); low, overcast, and optically thick (e.g., opaque stratus); transition stratocumulus; low, broken clouds (e.g., trade wind cumulus); transparent altocumulus; opaque altostratus; transparent cirrus; and deep convective (e.g., cumulonimbus and nimbostratus). Further details are given in the CALIOP Scene Classification ATBD.

Table 3: Interpretation of the bits in the V5.00 Feature Classification Flags. Bit 0 is the least significant bit.

Bits	Field Description	Bit Interpretation
0–2	Feature Type	0 = rejected by LEM 1 = "clear air" 2 = cloud 3 = tropospheric aerosol 4 = stratospheric aerosol 5 = surface 6 = subsurface 7 = no signal (totally attenuated)
3–4	Feature Type QA	0 = none 1 = low 2 = medium 3 = high
5–6	Ice/Water Phase	0 = unknown / not determined 1 = ice 2 = water 3 = oriented ice crystals
7–8	Ice/Water Phase QA	0 = none 1 = low 2 = medium 3 = high
9–11	Feature Sub-type	
	If feature type = tropospheric aerosol, bits 10-12 will specify the tropospheric aerosol type	0 = not determined 1 = marine 2 = desert dust 3 = polluted continental/smoke 4 = clean continental 5 = polluted dust 6 = elevated smoke 7 = dusty marine
	If feature type = cloud, bits 10-12 will specify the cloud type.	0 = low overcast, transparent 1 = low overcast, opaque 2 = transition stratocumulus 3 = low, broken cumulus 4 = altocumulus (transparent) 5 = altostratus (opaque) 6 = cirrus (transparent) 7 = deep convective (opaque)
	If feature type = stratospheric aerosol, bits 10-12 will specify stratospheric aerosol type.	0 = invalid 1 = polar stratospheric aerosol 2 = volcanic ash 3 = sulfate 4 = elevated smoke 5 = unclassified 6 = spare 7 = spare

Bits	Field Description	Bit Interpretation
	If feature type = clear-air, bits 10-12 will specify horizontal averages not searched for features due to low energy mitigation	0 = not applicable 1 = not searched at 80 km 2 = not searched at 20 and 80 km
12	Feature Subtype QA	0 = not confident 1 = confident
13-15	Horizontal Averaging Required	0 = not applicable 1 = 1/3 km 2 = 1 km 3 = 5 km 4 = 20 km 5 = 80 km

Additional notes on feature classification flag usage

Bits 0-2: Feature Type = Rejected by LEM

Layer data in profiles rejected by the low energy mitigation (LEM) algorithm are assigned a special value indicating that the profile was excluded from all level 2 analyses. For floating point parameters (e.g., layer base and top altitudes and integrated attenuated backscatters) and some integer parameters (e.g., CAD scores), this special value is –111. In bit-mapped parameters, LEM rejection is identified differently, depending on the information conveyed by the parameter. The feature classification flags in LEM-rejected profiles are set to zero, and hence the assigned feature type will also be zero. Any information gleaned from these LEM-rejected profiles should be excluded from all science data analyses. In previous data releases, a zero in the feature type field indicated bad or missing data.

Bits 0-2: Feature Type = Clear Air

Atmospheric regions where the signal has not been totally attenuated by overlying layers and in which no feature is detected are classified as being clear air. Because the determination of clear air depends not only on the cloud/aerosol content of the atmosphere, but also on the minimum detectable backscatter of the CALIOP layer detection scheme (McGill et al., 2007), regions containing especially weak layers can be misclassified as clear air. Detection threshold issues are addressed in detail in the CALIPSO Layer Detection ATBD.

Bits 0-2: Feature Type = Cloud / Tropospheric Aerosol / Stratospheric Aerosol

For each feature detected, the CALIOP CAD algorithm computes a CAD score based on layer altitude, layer latitude, and three altitude-and-latitude-dependent measured optical properties (i.e., layer-mean total attenuated color ratio, χ'; layer-mean volume depolarization ratio, δ_v; and layer mean attenuated backscatter coefficient, $<\beta'_{532}>$). The sign of the CAD score indicates whether a feature is classified as a cloud (positive scores) or an aerosol (negative scores). The confidence in each classification is given by the magnitude of the CAD score (between 0 and 100). The measured optical properties depend on the quality of the calibrations at 532 nm and 1064 nm. Significant errors in the calibration of either channel may result in the misclassification of a particular feature. The same CAD algorithm is applied to layers detected at all horizontal averaging resolutions in both the troposphere and the stratosphere.

Bits 0-2: Surface

Earth's surface is detected by a dedicated surface detection algorithm independently executed at averaging resolutions of 1/3 km (single shot), 1 km (3 sorts), and 5 km (15 shots).

Bits 0-2: Subsurface

Altitude regions lying below the surface echo detected by the CALIOP surface detection algorithm are classified as subsurface regions.

Bits 0-2: Totally attenuated / no signal

Regions where the CALIOP backscatter signals have been totally attenuated by opaque, overlying atmospheric layers are classified as having "totally attenuated / no signal".

Bits 3-4: Feature Type QA

For atmospheric features, the feature type QA bits define ranges of CAD score magnitudes corresponding to high, medium, low, and no confidence classifications. QA evaluations for all other feature types are constant for all features identified within each class. Table 4 defines the range of possible QA assignments for each feature type.

Table 4: Interpretations for the Feature Type QA bits (bits 3–4) in the CALIOP feature classification flags

Feature Type	QA Interpretation
0 = LEM-rejected	N/A (always 0)
1 = clear air	N/A (always 0)
2 = cloud	0 = no confidence = |CAD score| < 20 1 = low confidence = 20 ≤ |CAD score| < 50 2 = medium confidence = 50 ≤ |CAD score| < 70 3 = high confidence = |CAD score| ≥ 70
3 = tropospheric aerosol	
4 = stratospheric aerosol	
5 = surface	N/A (always 3)
6 = subsurface	N/A (always 0)
7 = no signal	N/A (always 0)

Bits 5-6: Ice-Water Phase

The classification of cloud ice-water phase is based on layer-integrated volume depolarization ratios, backscatter intensities, temperatures, and total attenuated backscatter color ratios (Avery et al., 2020). The CALIOP algorithm recognizes water and ice phases (both randomly oriented ice (ROI) and horizontally oriented ice (HOI)) but does not identify mixed phase layers (see Mace et al., 2020). In those cases where the classification is ambiguous, cloud phase is reported as “unknown/not determined”.

CALIOP’s ability to identify horizontally oriented ice clouds depends very strongly on the instruments off nadir angle. From launch until 28 November 2007, CALIOP pointed at 0.3° off nadir, and hence specular reflections from oriented ice crystals were most often scattered back into the receiver. This phenomenon produces a characteristic HOI signature: very high attenuated backscatter coefficients coupled with very low volume depolarization ratios (Hu et al., 2007). On 28 November 2007, the nominal CALIOP off nadir angle was changed to 3.0°, almost completely suppressing the specular backscatter from oriented crystals. Users will thus see a marked difference in phase classification distributions before and after CALIOP’s change in off nadir angle.

Bits 7-8: Ice-Water Phase QA

Ice-water phase classification confidence estimates are derived using the same parameters used to determine cloud thermodynamic phase. Cloud phases reported as “unknown/not determined” are automatically evaluated as having no confidence (i.e., phase QA = 0). Distributions of cloud phase QA segregated according to cloud phase for all clouds detected during September 2007 are shown in Figure 4.

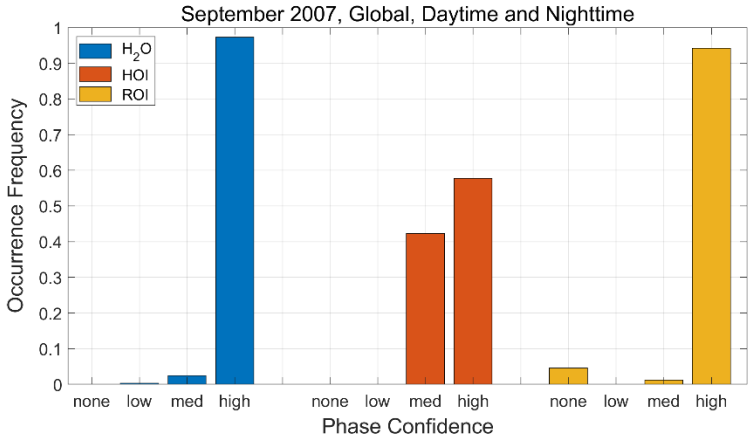

Figure 4: Distributions of cloud phase QA segregated according to cloud phase for all clouds detected during September 2007. Phase classification confidence for water clouds and ROI clouds is almost always high. However, classification confidence for HOI clouds is less certain.

Bits 9-11: Feature Subtype, Clouds

Cloud subtypes are assigned by the CALIOP cloud subtyping algorithm illustrated in Figure 5. High, middle, and low clouds are defined according to the International Satellite Cloud Climatology Project (ISCCP) cloud top pressure (P(top)) boundaries at 680 mb and 440 mb. Further discrimination is done using along track cloud fraction (cf) and cloud opacity.

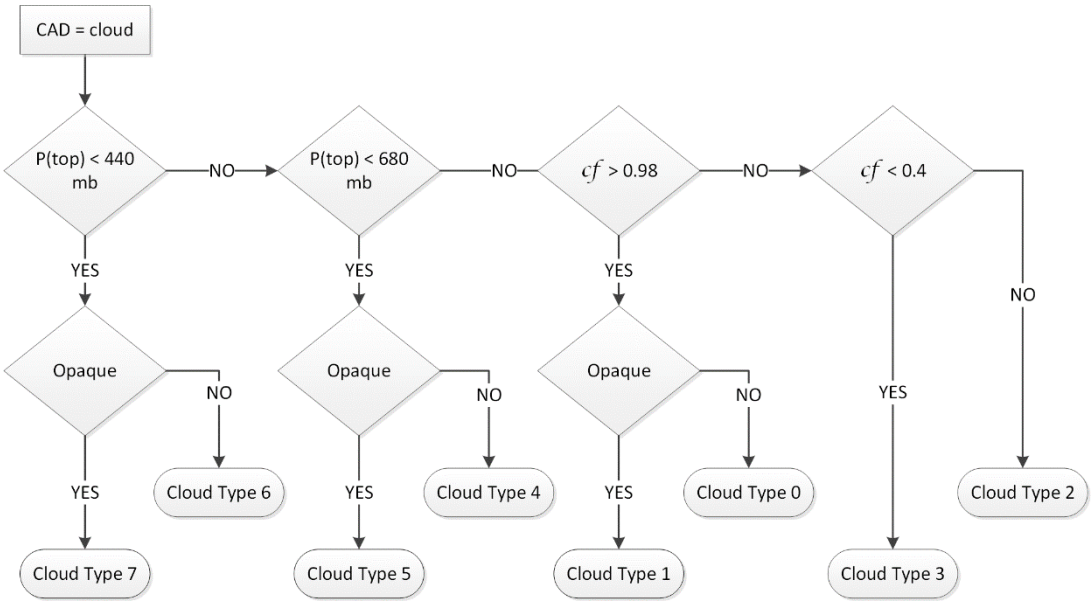

Cloud Type 0 = Low, overcast, thin (transparent stratus, stratocumulus, and fog)
Cloud Type 1 = Low, overcast, thick (opaque stratus, stratocumulus, and fog)
Cloud Type 2 = Transition stratocumulus
Cloud Type 3 = Low, broken (trade cumulus and shallow cumulus)
Cloud Type 4 = Altocumulus (transparent)
Cloud Type 5 = Altostratus (opaque, altostratus, nimbostratus, altocumulus)
Cloud Type 6 = Cirrus (transparent)
Cloud Type 7 = Deep convective (opaque altostratus, cumulonimbus, nimbostratus)

Figure 5: Diagram of the CALIOP cloud subtyping algorithm, adapted from the CALIOP Scene Classification ATBD. P(top) represents cloud top pressure and cf represents along track cloud fraction.

Bits 9-11: Feature Subtype, Tropospheric Aerosols

As illustrated in Figure 6, CALIOP's aerosol subtype designation is derived using the estimated particulate depolarization for the layer (δ_p^{est}), layer height information (Z_{top} and Z_{base}), estimated aerosol loading, as characterized by the 532 nm integrated attenuated backscatter (γ'_{532}), and the underlying surface type. The first three of these parameters are CALIOP observables. δ_p^{est} is largely an intrinsic property, whose magnitude ideally depends on particle shape (i.e., $\delta_p^{est} \approx 0$ for spherical particles and $\delta_p^{est} \approx 0.4$ for ice crystals), which is directly related to aerosol type. However, because δ_p^{est} is also influenced by aerosol hydration, it functions at least partially as an extrinsic property whose value depends on the amount of available water in the atmosphere. Similarly, γ'_{532} is typically considered as a purely extrinsic property that varies according to aerosol loading (i.e., aerosol optical depth (AOD)). Taken together, δ_p^{est} and γ'_{532} are not sufficient to fully constrain aerosol model selection. Additional discriminatory power is provided by the layer base and top altitudes, which are used to establish vertical extent and to distinguish between lofted layers and surface-attached layers. Finally, the selection process uses surface type information obtained from ancillary data sources as a coarse estimate of local aerosol origins. δ_p^{est} is the primary parameter used to identify aerosol types that have a substantial concentration of non-spherical particles (e.g., dust and mixtures of dust and smoke). γ'_{532} is used to constrain aerosol type selection in instances of high aerosol loading (e.g., a CALIOP measurement of $\gamma'_{532} = 0.01$ sr^{-1} is physically impossible for a smoke layer with a lidar ratio of 70 sr, but entirely plausible for a marine layer with a lidar ratio of 25 sr.) Surface type is typically the deciding factor when identifying marine aerosols.

As suggested by the red paths and labels in Figure 6, CALIOP's V5.00 identification of surface type in the Arctic now accounts for differences between the aerosol types situated above open oceans, which generally contain a substantial marine component, and those lying over extended over-ocean ice sheets, which are largely dominated by anthropogenic aerosol arriving in the polar regions via long range transport from continental sources.

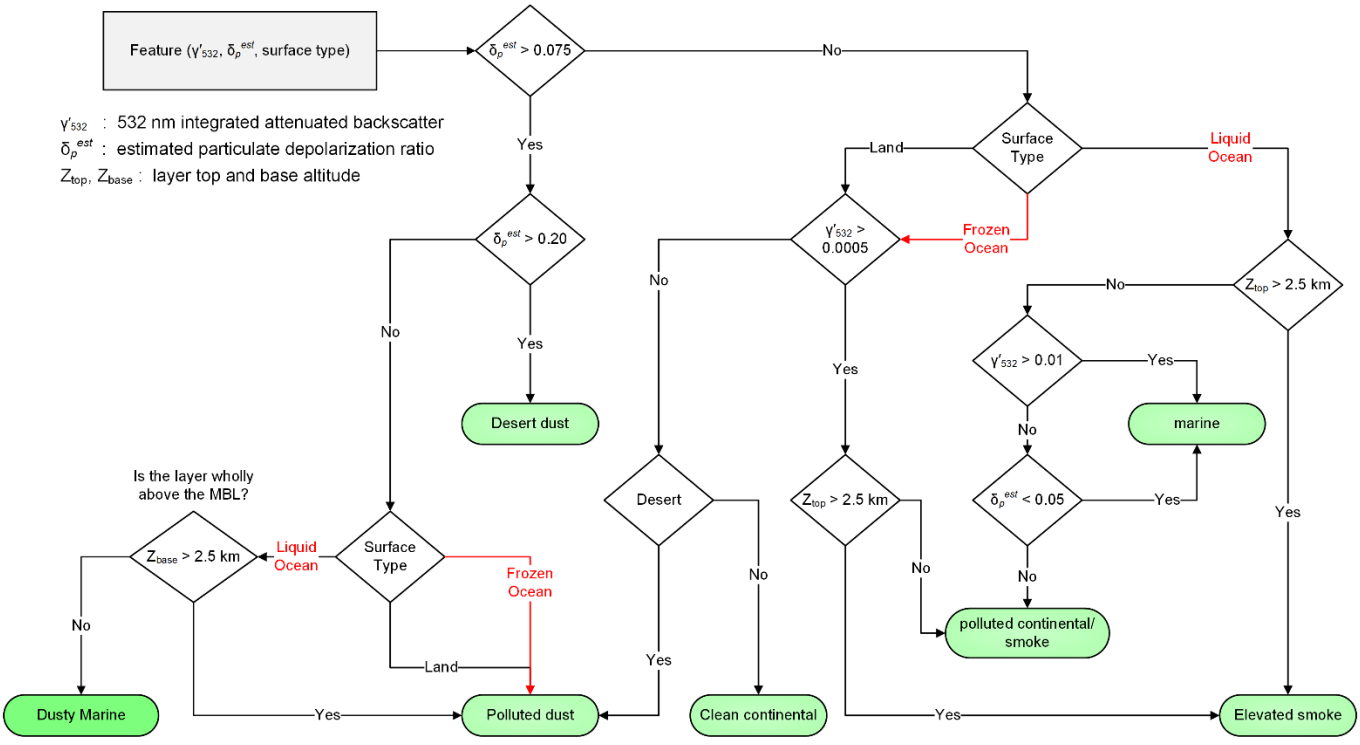

Figure 6: Flowchart illustrating the selection of aerosol subtypes in the CALIOP V5.00 data products. The red pathways and labels indicate changes relative to the V4.51 subtype selection scheme.

Aerosol layers having δ_p^{est} above 0.2 are classified as dust. Layers for which $0.075 < \delta_p^{est} \leq 0.2$ are either polluted dust or dusty marine, depending on layer base height and the surface type along the lidar ground track. Polluted dust is modeled as a mix of dust and urban pollution and is not identified solely over desert

regions. Likewise, layers detected over oceans and classified as dusty marine could also contain both dust and urban pollution components. Of the non-depolarizing aerosols, tropospheric layers with top altitudes greater than 2.5 km above the Earth's surface are assumed to be smoke. Non-depolarizing layers with tops below 2.5 km are classified as either clean continental, when γ'_{532} is small, or polluted continental/smoke when γ'_{532} is large. Because it is not possible to unambiguously discriminate smoke from urban pollution based on CALIOP measurables, the polluted continental/smoke class can potentially contain smoke, urban pollution, or a mixture of the two types. Marine layers, which are only identified over oceans and other large water bodies, have layer tops below 2.5 km and either $\gamma'_{532} > 0.01\ sr^{-1}$ or, if $\gamma'_{532} \leq 0.01\ sr^{-1}$, $\delta_p^{est} \leq 0.05$.

With the exception of marine and dusty marine, once the aerosol subtype has been determined, a globally constant, wavelength-specific aerosol lidar ratio, S_a, is chosen from a lookup table that currently consists of five pairs of 532 nm and 1064 nm values (Kim et al., 2018). New in V5.00, marine and dusty marine lidar ratios are interpolated from seasonally and regionally varying lidar ratio maps that were derived empirically by constraining the solution of the lidar equation using collocated MODIS retrievals of AOD (Toth et al., 2025).

Bits 9-11: Feature Subtype, Stratospheric Aerosols

The stratospheric aerosol type selection scheme, illustrated in Figure 7, first identifies polar stratospheric aerosol (PSA) as aerosol layers with 532 nm attenuated backscatter centroid temperatures less than -70C that are detected during polar stratospheric cloud (PSC) seasons, assumed to be December to February in the Arctic and May to October in the Antarctic. Non-PSC related stratospheric aerosol layers are identified as one of three stratospheric aerosol species based on δ_p^{est} and γ'_{532}. Thresholds for these three subtypes were developed empirically from CALIOP observations of volcanic plume events and several smoke events which were detected above the tropopause. Weakly scattering layers are immediately relegated to the unclassified category. Layers having high depolarization ratios are classified as volcanic ash while layers with moderate to low δ_p^{est} are classified as smoke. Layers for which $\delta_p^{est} < 0.075$ are classified as sulfates.

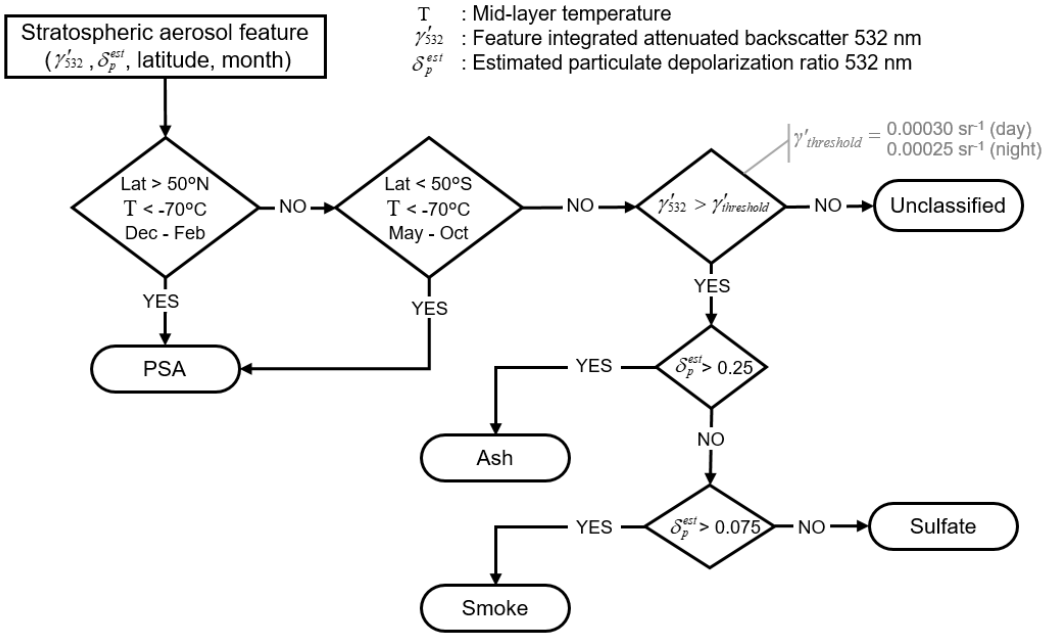

Figure 7: Flowchart for determining stratospheric aerosol subtypes (Tackett et al., 2023)

Distinguishing Tropospheric Aerosol from Stratospheric Aerosol

The distinction between tropospheric aerosol layers and stratospheric aerosol layers is made by comparing the centroid altitude of the 532 nm attenuated backscatter profile within the layer to the local tropopause height retrieved from the MERRA-2 reanalysis data. When the bulk of the attenuated backscatter lies above the tropopause – i.e., when the centroid altitude is higher than the tropopause altitude – layers are

classified as stratospheric. Tropospheric aerosols have centroid altitudes below the tropopause. The success of this classification scheme relies on the accuracy of the MERRA-2 tropopause. At times aerosols appear to straddle the tropopause, and in these cases the layer typing and subtyping can oscillate between tropospheric and stratospheric. Figure 8 shows an example from 1 July 2011 where clouds, stratospheric aerosol, and tropospheric aerosol are all detected in the same scene.

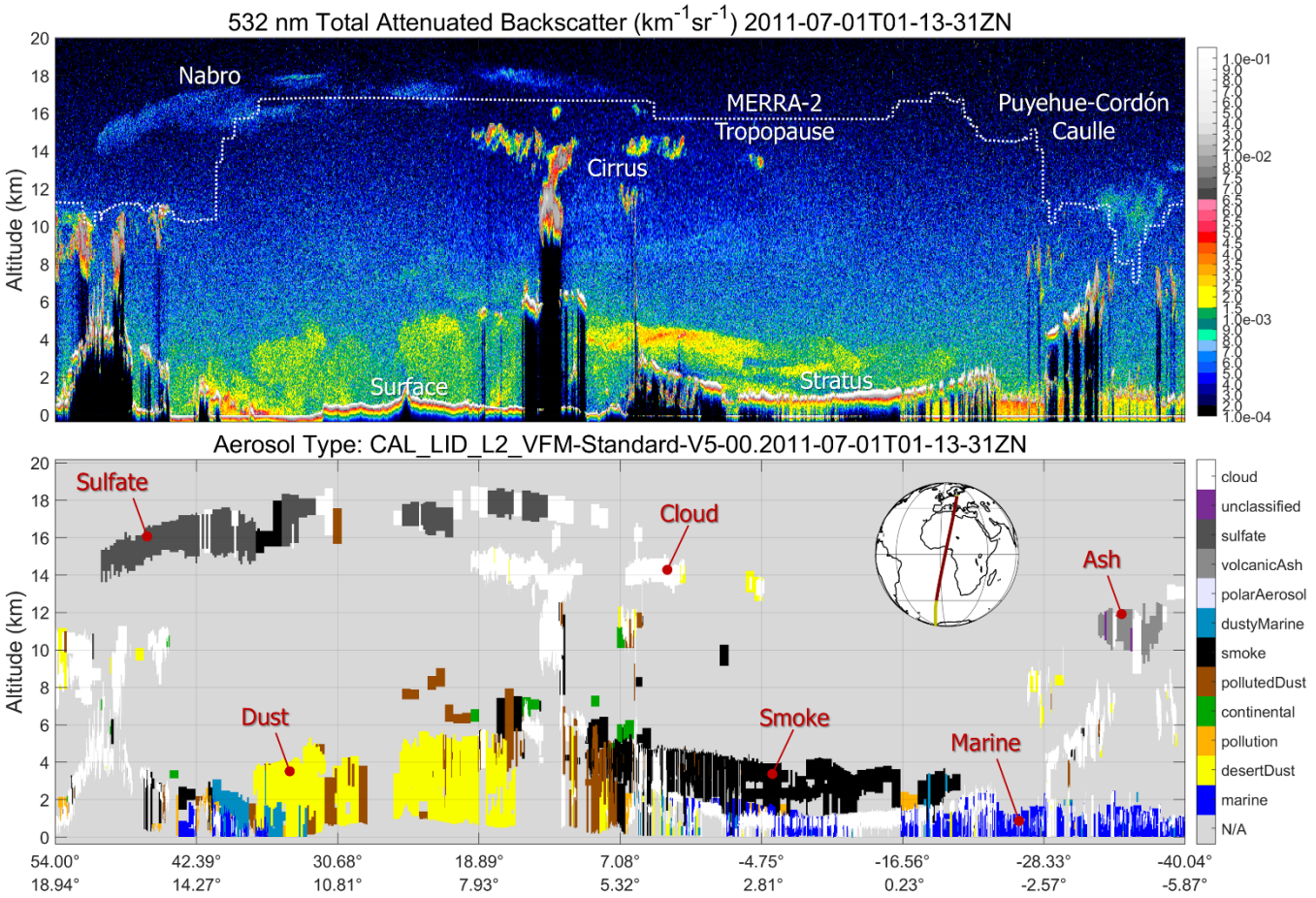

Figure 8: The upper panel shows CALIOP 532 nm total attenuated backscatter coefficients measured during a night-time orbit on 1 July 2011. This scene captures stratospheric aerosol injections from the June 2011 eruptions of the Nabro volcano in Eritrea (northern hemisphere) and the Puyehue-Cordón Caulle volcano in Chile (southern hemisphere). The lower panel shows the aerosol subtypes assigned by the CALIOP aerosol subtyping algorithm. CALIOP reliably detects the stratospheric aerosols and a substantial majority of the tropospheric aerosols, but only detects intermittent hints of the faint tropospheric aerosol layer seen in the upper panel between ~5°N and ~9°S at altitudes between ~6 km and ~11 km. Localized variability in feature type is most prominent for weakly scattering layers.

Bits 9-11: Feature Subtype, Clear Air

For any range bin, a value of 1 in this field indicates that CALIOP's low energy mitigation (LEM) algorithm identified a valid 5 km horizontal average using the backscatter data in this range bin. However, because the surrounding profiles contained too many low energy laser pulses, the LEM algorithm could not subsequently identify a valid 80 km horizontal average that also used this range bin. As a result, the data in this range bin were never searched for the presence of features at CALIOP's 80 km resolution. A value of 2 indicates that, in addition to not identifying a valid 80 km horizontal average, the LEM algorithm also failed to identify a valid 20 km horizontal average that used this range bin. Range bins with values of 2 are thus never evaluated to determine whether they contain faint features that could only be detected at either of the coarser resolutions.

Bit 12: Feature Subtype QA

This bit was intended to provide a binary confidence evaluation (i.e., confident vs. not confident) of feature subtype. However, because suitable tests of classification confidence have not been well-developed for all feature subtypes, and because the existing tests are not uniformly applied, values in this field should be ignored.

Bits 13-15: Horizontal Averaging Required for Feature Detection

One or more of these bits will be toggled on in every matrix element of the feature classification flags in which a feature was detected. Bit decoding is given in Table 3.

VFM_Feature_Detection_Quality_Flag

Units: NoUnits

Format: UInt_16

Valid Range: 1, 32767

Description: Quality control flag, used to directly map the actions of the low energy mitigation (LEM) algorithm for each range bin in the VFM feature classification flags.

Table 5: Interpretation of the Vertical Feature Mask (VFM) Feature Detection Quality flag

bit	interpretation
0	First single-shot profile has low energy or missing data
1	Second single-shot profile has low energy or missing data
2	Third single-shot profile has low energy or missing data
3	Fourth single-shot profile has low energy or missing data
4	Fifth single-shot profile has low energy or missing data
5	Bin in first single-shot profile is rejected by LEM
6	Bin in second single-shot profile is rejected by LEM
7	Bin in third single-shot profile is rejected by LEM
8	Bin in fourth single-shot profile is rejected by LEM
9	Bin in fifth single-shot profile is rejected by LEM
10	Contributed to feature detection at resolution 1 (1/3-km)
11	Contributed to feature detection at resolution 2 (1-km)
12	Contributed to feature detection at resolution 3 (5-km)
13	Contributed to feature detection at resolution 4 (20-km)
14	Contributed to feature detection at resolution 5 (80-km)

Scientific Data Sets: Spacecraft Position

Spacecraft_Position

Units: km

Format: Float_64

Valid Range: -8000, 8000

Fill Value: -9999.0

Description: Position of the CALIPSO satellite expressed in Earth Centered Rotating (ECR) coordinates (also known as Earth-centered, Earth-fixed (ECEF) coordinates).

Vgroup: Single Shot Detection

In the earliest iteration of the VFM data products, time and position parameters were reported at 5 km (15 shot) resolution, consistent with the temporal and spatial resolution of the arrays reported in the Feature Classification Flags SDS. To allow analysis and plotting of the single shot results directly from the VFM files, CALIOP's version 4.10 release added the Single Shot Detection Vgroup. The SDS names and data reported in this Vgroup are the single shot (333 m) analogs of the 15-shot (5.025 km) resolution SDS names and data reported in the HDF file root directory. To clearly distinguish between single shot and resolutions 5 km of identical parameters, 2-letter prefix ('ss' = single shot) is added to the SDS names in the Single Shot Detection Vgroup. Table 6 lists the 5 km SDSs that are replicated at single shot resolution. Descriptions of these parameters are found in the Scientific Data Sets: Time and Position section. The one exception is the laser energy information which is described in the Scientific Data Sets: Lidar Operating Mode section.

Table 6: Correspondence between the SDSs in the Single Shot Detection Vgroup and the SDSs in the HDF file root directory.

5 km (15 shot) SDS name	333 m (1 shot) SDS name
Latitude	ssLatitude
Longitude	ssLongitude
Profile_Time	ssProfile_Time
Profile_UTC_Time	ssProfile_UTC_Time
Profile_ID	ssProfile_ID
Day_Night_Flag	ssDay_Night_Flag
Minimum_Laser_Energy_532	ssLaser_Energy_532

Metadata Parameters

Product_ID

An 80-byte character string containing the product name.

Date_Time_at_Granule_Start

A 27-byte character string that specifies the UTC start date and time for the first single shot profile in each granule. The format is yyyy-mm-ddThh:nn:ss.ffffffZ, where yyyy is the year, mm is the month, dd is the day, hh is the hour, nn is the minute, ss is the second, and ffffff is the fractional second. Date and time are separated by the character 'T'. The 'Z' indicates that time is given in UTC.

Date_Time_at_Granule_End

A 27-byte character string that specifies the UTC start date and time for the last single shot profile in each granule. The format is yyyy-mm-ddThh:nn:ss.ffffffZ, where yyyy is the year, mm is the month, dd is the day, hh is the hour, nn is the minute, ss is the second, and ffffff is the fractional second. Date and time are separated by the character 'T'. The 'Z' indicates that time is given in UTC.

Date_Time_of_Production

A 27-byte character string that specifies the granule UTC start date and time. The format is yyyy-mm-ddThh:nn:ss.ffffffZ, where yyyy is the year, mm is the month, dd is the day, hh is the hour, nn is the minute, ss is the second, and ffffff is the fractional second. Date and time are separated by the character 'T'. The 'Z' indicates that time is given in UTC.

Number_of_Bad_Profiles

A 32-bit integer specifying the number of bad attenuated backscatter profiles contained in the level 1b file used to generate the level 2 analyses. Profiles are considered bad if (a) any of the three measurement channels are missing (see bits 0, 1, and 2 in the QC Flags SDS reported in the CALIOP Level 1 files); (b) the measurement data could not be geolocated (see bit 3 in the QC flags SDS); or (c) the energy in either the 532 nm or 1064 nm channel falls below the low energy threshold (see bits 5 and 6 in the QC Flags SDS).

Number_of_Good_Profiles

A 32-bit integer specifying the number of good (i.e., not identified as being bad) attenuated backscatter profiles contained in the level 1b file used to generate the level 2 analyses.

Initial_Subsatellite_Latitude

This field reports the first subsatellite latitude of the granule.

Initial_Subsatellite_Longitude

This field reports the first subsatellite longitude of the granule.

Final_Subsatellite_Latitude

This field reports the last subsatellite latitude of the granule.

Final_Subsatellite_Longitude

This field reports the last subsatellite longitude of the granule.

Orbit_Number_at_Granule_Start

Orbit_Number_at_Granule_Stop

Orbit_Number_Change_Time

Orbit Number consists of three fields that define the number of revolutions by the CALIPSO spacecraft around the Earth. This number is incremented each time the spacecraft passes the equator on the ascending node. To maintain consistency between the CALIPSO and CloudSat orbit parameters, the Orbit Number is keyed to the CloudSat orbit 2121 at 23:00:47 on 2006/09/20. Because the CALIPSO data granules are organized according to the day and night conditions, based on fixed Sun-Earth-Satellite angles, day/night boundaries do not coincide with transition points for defining orbit number. As such, three parameters are needed to describe the orbit number for each granule as:

- **Orbit Number at Granule Start:** orbit number at the granule start time.
- **Orbit Number at Granule End:** orbit number at the granule stop time.
- **Orbit Number Change Time:** time at which the orbit number changes in the granule.

Path_Number_at_Granule_Start

Path_Number_at_Granule_Stop

Path_Number_Change_Time

Path Number consists of three fields that define an index ranging from 1-233 that references orbits to the Worldwide Reference System (WRS). This global grid system was developed to support scene identification for LandSat imagery. Since the A-Train is maintained to the WRS grid within +/- 10 km, the Path Number provides a convenient index to support data searches, instead of having to define complex latitude and longitude regions along the orbit track. The Path Number is incremented after the maximum latitude in the orbit is attained and changes by a value of 16 between successive orbits. Because the CALIPSO data granules are organized according to the day and night conditions, based on fixed Sun-Earth-Satellite angles, day/night boundaries do not coincide with transition points for defining path number. As such, three parameters are needed to describe the path number for each granule as:

- **Path Number at Granule Start:** path number at the granule start time.
- **Path Number at Granule End:** path number at the granule stop time.
- **Path Number Change Time:** time at which the path number changes in the granule.

Lidar_Data_Altitudes

Altitudes (above mean sea level) that specify the vertical midpoints of the 545 range bins in the profile measurements downlinked from the CALIPSO satellite. The values in this field are identical to those in the Lidar_Data_Altitudes SDS and are retained in V5.00 for backward compatibility with existing software.

GEOS_Version

Specifies the version of the meteorological data used in the level 2 analyses. For the version 5.0 data release, this field is always "MERRA2".

GMAO_Files_Used

Lists the four MERRA2 meteorological data files used to create the level 2 data files for this granule.

Classifier_Coefficients_Version_Number

Version number of the classifier coefficients file that stores the five-dimensional probability distribution functions used by the cloud-aerosol discrimination (CAD) algorithm.

Classifier_Coefficients_Version_Date

Creation date of the classifier coefficients file that stores the five-dimensional probability distribution functions used by the cloud-aerosol discrimination (CAD) algorithm.

Production_Script

Provides the configuration information and command sequences that were executed during the processing of the CALIOP Lidar Level 2 data products. Documentation for many of the control constants found within this field is contained in the CALIPSO Lidar Level 2 Algorithm Theoretical Basis Documents.

CALIPSO Data Quality Information

Relevant External Documentation

This section lists CALIPSO Algorithm Theoretical Basis Documents (ATBDs) and peer-reviewed journal articles that provide detailed descriptions of the algorithms used to calibrate the lidar and retrieve the CALIOP level 2 science data products.

ATBDs and Project Documentation

- CALIPSO Data Management Team: CALIPSO Data Products Catalog, PC-SCI-503, Release 5.00.
- Vaughan, M. A., D. M. Winker, and K. A. Powell, 2005: CALIOP Algorithm Theoretical Basis Document, Part 2: Feature Detection and Layer Properties Algorithm, PC-SCI-202.02, https://ntrs.nasa.gov/citations/20250006627.
- Liu, Z., A. H. Omar, Y. Hu, M. A. Vaughan, and D.M. Winker, 2005: CALIOP Algorithm Theoretical Basis Document, Part 3: Scene Classification Algorithms, PC-SCI-202.03, https://ntrs.nasa.gov/citations/20250006628.
- Winker, D. M., C. A. Hostetler, M. A. Vaughan, and A. H. Omar, 2006: CALIOP Algorithm Theoretical Basis Document, Part 1: CALIOP Instrument and Algorithms Overview, PC-SCI-202.01, https://ntrs.nasa.gov/citations/20250006626.

Peer-Reviewed Journal Papers

- Liu, Z., M. J. McGill, Y. Hu, C. A. Hostetler, M. Vaughan, and D. Winker, 2004: "Validating lidar depolarization calibration using solar radiation scattered by ice clouds", *IEEE Geosci. Remote Sens. Lett.*, **1**, 157–161, https://doi.org/10.1109/LGRS.2004.829613.
- Liu, Z., M. Vaughan, D. Winker, C. A. Hostetler, L. R. Poole, D. L. Hlavka, W. D. Hart, and M. J. McGill, 2004: Use of probability distribution functions for discriminating between cloud and aerosol in lidar backscatter data, *J. Geophys. Res.*, **109**, D15202, https://doi.org/10.1029/2004JD004732.
- Liu, Z., W. Hunt, M. Vaughan, C. Hostetler, M. McGill, K. Powell, D. Winker, and Y. Hu, 2006: Estimating Random Errors Due to Shot Noise in Backscatter Lidar Observations, *Appl. Opt.*, **45**, 4437–4447, https://doi.org/10.1364/AO.45.004437.
- Hu, Y., M. Vaughan, Z. Liu, K. Powell, and S. Rodier, 2007: Retrieving Optical Depths and Lidar Ratios for Transparent Layers Above Opaque Water Clouds From CALIPSO Lidar Measurements, *IEEE Geosci. Remote Sens. Lett.*, **4**, 523–526, https://doi.org/10.1109/LGRS.2007.901085.
- Hu, Y., D. Winker, M. Vaughan, B. Lin, A. Omar, C. Trepte, D. Flittner, P. Yang, W. Sun, Z. Liu, Z. Wang, S. Young, K. Stamnes, J. Huang, R. Kuehn, B. Baum, and R. Holz, 2009: CALIPSO/CALIOP Cloud Phase Discrimination Algorithm, *J. Atmos. Oceanic Technol*., **26**, 2293–2309, https://doi.org/10.1175/2009JTECHA1280.1.
- Hunt, W. H, D. M. Winker, M. A. Vaughan, K. A. Powell, P. L. Lucker, and C. Weimer, 2009: CALIPSO Lidar Description and Performance Assessment, *J. Atmos. Oceanic Technol.*, **26**, 1214–1228, https://doi.org/10.1175/2009JTECHA1223.1.
- Liu, Z., M. A. Vaughan, D. M. Winker, C. Kittaka, R. E. Kuehn, B. J. Getzewich, C. R. Trepte, and C. A. Hostetler, 2009: The CALIPSO Lidar Cloud and Aerosol Discrimination: Version 2 Algorithm and Initial Assessment of Performance, *J. Atmos. Oceanic Technol*., **26**, 1198–1213, https://doi.org/10.1175/2009JTECHA1229.1.
- Omar, A., D. Winker, C. Kittaka, M. Vaughan, Z. Liu, Y. Hu, C. Trepte, R. Rogers, R. Ferrare, R. Kuehn, and C. Hostetler, 2009: The CALIPSO Automated Aerosol Classification and Lidar Ratio Selection Algorithm, *J. Atmos. Oceanic Technol*., **26**, 1994–2014, https://doi.org/10.1175/2009JTECHA1231.1.
- Powell, K. A., C. A. Hostetler, Z. Liu, M. A. Vaughan, R. E. Kuehn, W. H. Hunt, K. Lee, C. R. Trepte, R. R. Rogers, S. A. Young, and D. M. Winker, 2009: CALIPSO Lidar Calibration Algorithms: Part I - Nighttime 532 nm Parallel Channel and 532 nm Perpendicular Channel, *J. Atmos. Oceanic Technol*., **26**, 2015–2033, https://doi.org/10.1175/2009JTECHA1242.1.
- Vaughan, M., K. Powell, R. Kuehn, S. Young, D. Winker, C. Hostetler, W. Hunt, Z. Liu, M. McGill, and B. Getzewich, 2009: Fully Automated Detection of Cloud and Aerosol Layers in the CALIPSO Lidar Measurements, *J. Atmos. Oceanic Technol*., **26**, 2034–2050, https://doi.org/10.1175/2009JTECHA1228.1.
- Winker, D. M., M. A. Vaughan, A. H. Omar, Y. Hu, K. A. Powell, Z. Liu, W. H. Hunt, and S. A. Young, 2009: Overview of the CALIPSO Mission and CALIOP Data Processing Algorithms, *J. Atmos. Oceanic Technol*., **26**, 2310–2323, https://doi.org/10.1175/2009JTECHA1281.1.
- Young, S. A. and M. A. Vaughan, 2009: The retrieval of profiles of particulate extinction from Cloud Aerosol Lidar Infrared Pathfinder Satellite Observations (CALIPSO) data: Algorithm description, *J. Atmos. Oceanic Technol*., **26**, 1105–1119, https://doi.org/10.1175/2008JTECHA1221.1.
- Garnier, A., J. Pelon, M. A. Vaughan, D. M. Winker, C. R. Trepte, and P. Dubuisson, 2015: Lidar multiple scattering factors inferred from CALIPSO lidar and IIR retrievals of semi-transparent cirrus cloud optical depths over oceans, *Atmos. Meas. Tech.*, **8**, 2759–2774, https://doi.org/10.5194/amt-8-2759-2015.
- Getzewich, B. J., M. A. Vaughan, W. H. Hunt, M. A. Avery, K. A. Powell, J. L. Tackett, D. M. Winker, J. Kar, K.-P. Lee, and T. Toth, 2018: CALIPSO Lidar Calibration at 532-nm: Version 4 Daytime Algorithm, *Atmos. Meas. Tech.*, **11**, 6309–6326, https://doi.org/10.5194/amt-11-6309-2018.
- Kar, J., M. A. Vaughan, K. P. Lee, J. Tackett, M. Avery, A. Garnier, B. Getzewich, W. Hunt, D. Josset, Z. Liu, P. Lucker, B. Magill, A. Omar, J. Pelon, R. Rogers, T. D. Toth, C. Trepte, J-P. Vernier, D. Winker, and S. Young, 2018:

CALIPSO Lidar Calibration at 532 nm: Version 4 Nighttime Algorithm, *Atmos. Meas. Tech.*, **11**, 1459–1479, https://doi.org/10.5194/amt-11-1459-2018.

- Kim, M.-H., A. H. Omar, J. L. Tackett, M. A. Vaughan, D. M. Winker, C. R. Trepte, Y. Hu, Z. Liu, L. R. Poole, M. C. Pitts, J. Kar, and B. E. Magill, 2018: The CALIPSO Version 4 Automated Aerosol Classification and Lidar Ratio Selection Algorithm, *Atmos. Meas. Tech.*, **11**, 6107-6135, https://doi.org/10.5194/amt-11-6107-2018.
- Lu, X., Y. Hu, Y. Yang, M. Vaughan, Z. Liu, S. Rodier, W. Hunt, K. Powell, P. Lucker, and C. Trepte, 2018: Laser pulse bidirectional reflectance from CALIPSO mission, *Atmos. Meas. Tech.*, **11**, 3281–3296, https://doi.org/10.5194/amt-11-3281-2018.
- Young, S. A., M. A. Vaughan, J. L. Tackett, A. Garnier, J. B. Lambeth, and K. A. Powell, 2018: Extinction and Optical Depth Retrievals for CALIPSO's Version 4 Data Release, *Atmos. Meas. Tech.*, **11**, 5701–5727, https://doi.org/10.5194/amt-11-5701-2018.

  Supplement: https://doi.org/10.5194/amt-11-5701-2018-supplement
- Liu, Z., J. Kar, S. Zeng, J. Tackett, M. Vaughan, M. Avery, J. Pelon, B. Getzewich, K.-P. Lee, B. Magill, A. Omar, P. Lucker, C. Trepte, and D. Winker, 2019: Discriminating Between Clouds and Aerosols in the CALIOP Version 4.1 Data Products, *Atmos. Meas. Tech.*, **12**, 703–734, https://doi.org/10.5194/amt-12-703-2019.
- Vaughan, M., A. Garnier, D. Josset, M. Avery, K.-P. Lee, Z. Liu, W. Hunt, J. Pelon, Y. Hu, S. Burton, J. Hair, J. Tackett, B. Getzewich, J. Kar, and S. Rodier, 2019: CALIPSO Lidar Calibration at 1064 nm: Version 4 Algorithm, *Atmos. Meas. Tech.*, **12**, 51–82, https://doi.org/10.5194/amt-12-51-2019.
- Avery, M. A., R. A. Ryan, B. J. Getzewich, M. A. Vaughan, D. M. Winker, Y. Hu, A. Garnier, J. Pelon, and C. A. Verhappen, 2020: "CALIOP V4 Cloud Thermodynamic Phase Assignment and the Impact of Near-Nadir Viewing Angles", *Atmos. Meas. Tech.*, **13**, 4539–4563, https://doi.org/10.5194/amt-13-4539-2020.
- Ryan, R. A., M. A. Vaughan, S. D. Rodier, J. L. Tackett, J. A. Reagan, R. A. Ferrare, J. W. Hair, and B. J. Getzewich, 2024: "Total Column Optical Depths Retrieved from CALIPSO Lidar Ocean Surface Backscatter", *Atmos. Meas. Tech.*, **17**, 6517–6545, https://doi.org/10.5194/amt-17-6517-2024.
- Tackett, J. L., J. Kar, M. A. Vaughan, B. Getzewich, M.-H. Kim, J.-P. Vernier, A. H. Omar, B. Magill, M. C. Pitts, and D. Winker, 2023: "The CALIPSO version 4.5 stratospheric aerosol subtyping algorithm", *Atmos. Meas. Tech.*, **16**, 745–768, https://doi.org/10.5194/amt-16-745-2023.
- Tackett, J. L., R. A. Ryan, A. E. Garnier, J. Kar, B. Getzewich, X. Cai, M. A. Vaughan, C. R. Trepte, R. Verhappen, D. M. Winker and K.-P. A. Lee, 2025: Mitigating Impacts of Low Energy Laser Pulses on CALIOP Data Products, *EGUsphere* [preprint], https://doi.org/10.5194/egusphere-2025-2376.
- Toth, T. D., G. Schuster, M. Clayton, Z. Li, D. Painemal, S. Rodier, J. Kar, T. Thorsen, R. Ferrare, M. Vaughan, J. Tackett, H. Bian, M. Chin, A. Garnier, E. Welton, R. Ryan, C. Trepte and D. Winker, 2025: "Mapping CALIPSO Marine and Dusty Marine Aerosol Lidar Ratios using MODIS AOD Constrained Retrievals and GOCART Model Simulations" *EGUsphere* [AMTD], https://doi.org/10.5194/egusphere-2025-2832.

Data Release Information

At the conclusion of the mission, the CALIPSO project had released five major versions of the lidar level 2 data products, as well as several minor version updates. Table 7 lists all major and minor releases.

Table 7: release date, version number, data date range, and production strategy for all CALIPSO lidar level 2 data products

Lidar Level 2: Half orbits (Night and Day)			
Release Date	**Version**	**Data Date Range**	**Production Strategy**
October 2025	5.00	June 13, 2006 to June 30, 2023	Standard
June 2023	4.51	June 13, 2006 to June 30, 2023	Standard
October 2020	4.21	July 01, 2020 to January 19, 2022	Standard

Lidar Level 2: Half orbits (Night and Day)			
Release Date	**Version**	**Data Date Range**	**Production Strategy**
October 2018	4.20	June 13, 2006 to June 20, 2020	Standard
November 2016	4.10	June 13, 2006 to September 30, 2020	Standard
October 2020	3.41	October 1, 2020 to June 30, 2023	Validated Stage 1
December 2016	3.40	December 1, 2016 to September 31, 2020	Validated Stage 1
April 2013	3.30	March 1, 2013 to November 30, 2016	Validated Stage 1
December 2011	3.02	November 1, 2011 to February 28, 2013	Validated Stage 1
May 2010	3.01	June 13, 2006 to October 31, 2011	Validated Stage 1
October 2008	2.02	September 14, 2008 to October 29, 2009	Provisional
January 2008	2.01	June 13, 2006 to September 13, 2008	Provisional
December 2006	1.10	June 13, 2006 to November 11, 2007	Provisional / Beta

Data Quality Summaries

Data Quality Statement for CALIPSO's Version 5.00 Lidar Level 2 Data Product Release

Data Version: **5.00**
Data Release Date: **1 October 2025**
Data Date Range: **June 13, 2006 to June 30, 2023**

The sections below highlight the most significant changes made in the CALIOP version 5.00 (V5.00) level 2 data products. The magnitude and effects of these changes are frequently illustrated with comparisons to the previous release of the version 4.51 (V4.51) data products.

Modifications for Low Energy Mitigation (LEM)

During final seven years of the CALIPSO mission, a slow leak in the laser canister (Hunt et al., 2009) reduced the internal pressure below the voltage breakdown limit described by Pachen's law. Once this occurred, intermittent coronal arcing across the Q switch caused the CALIOP laser to begin emitting an increasing number of low-to-no energy laser pulses. As seen in Figure 9, early on this behavior was confined almost exclusively to the South Atlantic Anomaly (SAA; Rodriguez et al., 2022) but toward the end of the mission the phenomenon occurred worldwide.

Because CALIOP profiles are time-averaged onboard the satellite prior to downlink (Hunt et al., 2009), the deleterious effects of individual low energy pulses are not localized, but instead cause a degradation in signal quality across multiple consecutive shots. To minimize these effects, the CALIPSO lidar science working group (LSWG) developed a family of low energy mitigation (LEM) algorithms (Tackett et al., 2025) that identify compromised level 1b data segments on small, targeted scales. Using a highly optimized data filtering scheme, these segments are subsequently excluded from all level 2 data analyses. The level 1 LEM algorithm corrects a pervasive low daytime calibration bias (3% to 4%) and reduces daytime calibration uncertainties by 20% to 40% in the SAA latitude band. In addition, the V5.00 level 1 energy normalization process now correctly compensates for the inclusion of no energy laser pulses in data averaged onboard the satellite. As demonstrated by Figure 10, this level 1 modification, in combination with the level 2 LEM algorithms, yields a substantial reduction in the number of false positive feature detections.

Note that averaged profiles containing one or more low energy pulses are not automatically excluded in the level 2 analyses. Horizontally averaged data segments that are "LEM-affected" (i.e., some low energy shots are present, but the filtered profile is still deemed acceptable for science retrievals) experience a signal-to-noise ratio reduction of 6–9 % which slightly increases the probability of false detections relative to unaffected data. However, as

illustrated by Figure 11, the median measured optical properties of the LEM-affected layers typically differ from the properties of unaffected layers by ~1.0% or less.

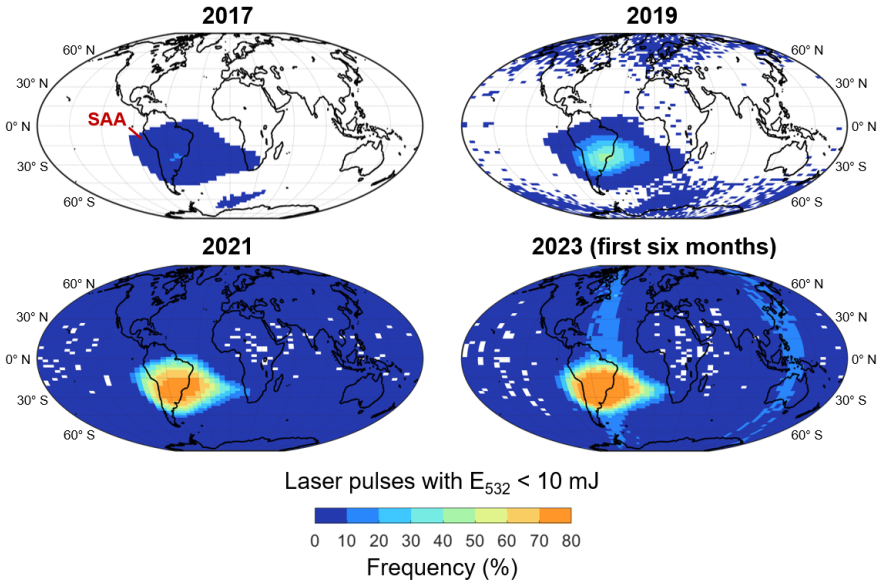

Figure 9: Global frequencies of laser pulses having 532 nm energies less than 10 mJ during 2017, 2019, 2021, and the first six months of 2023. The vertical bands of high frequencies seen in 2023 are caused by daytime granules having nearly continuous low energy pulses during May and June; e.g., see 2023-06-12T05-54-23ZD. (Figure from Tackett et al., 2025)

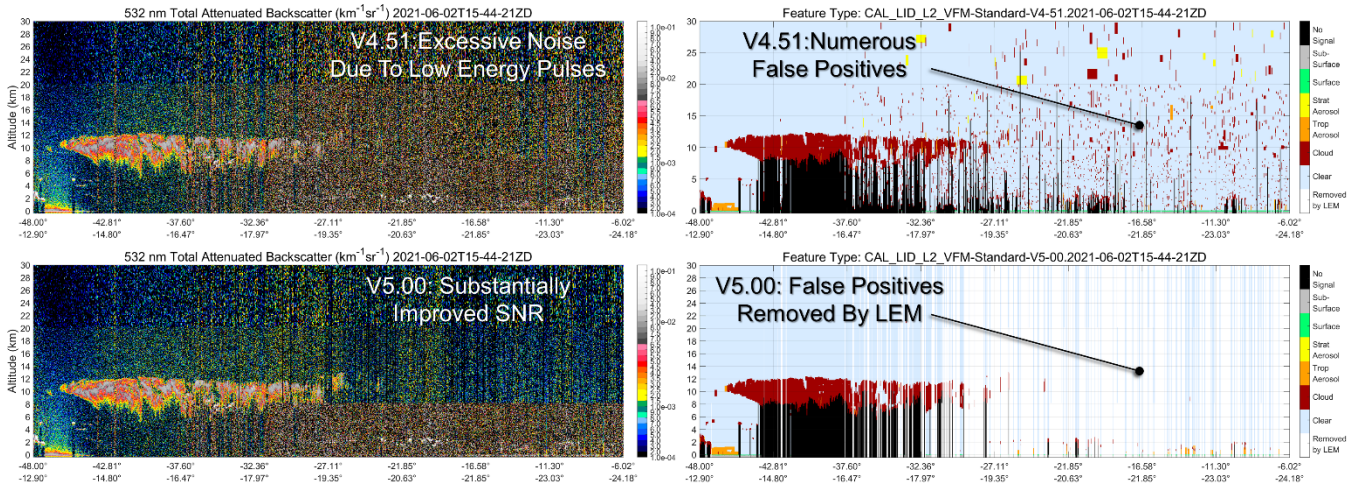

Figure 10: Top row shows the level 1 532 nm total attenuated backscatter (β'(z), left) and the corresponding level 2 vertical feature mask (VFM, right) from the V4.51 release for a granule strongly affected by low energy pulses on 02 June 2021 at 16Z. Similarly, the bottom row shows the same quantities for the V5.00 release. Relative to V4.51, the SNR above 8.2 km is noticeably higher in the LEM-filtered V5.00 532 nm β'(z) example. Similarly, the V5.00 VFM arguably eliminates all of the false positive feature detections seen in V4.51. (Figure adapted from Tackett et al., 2025.)

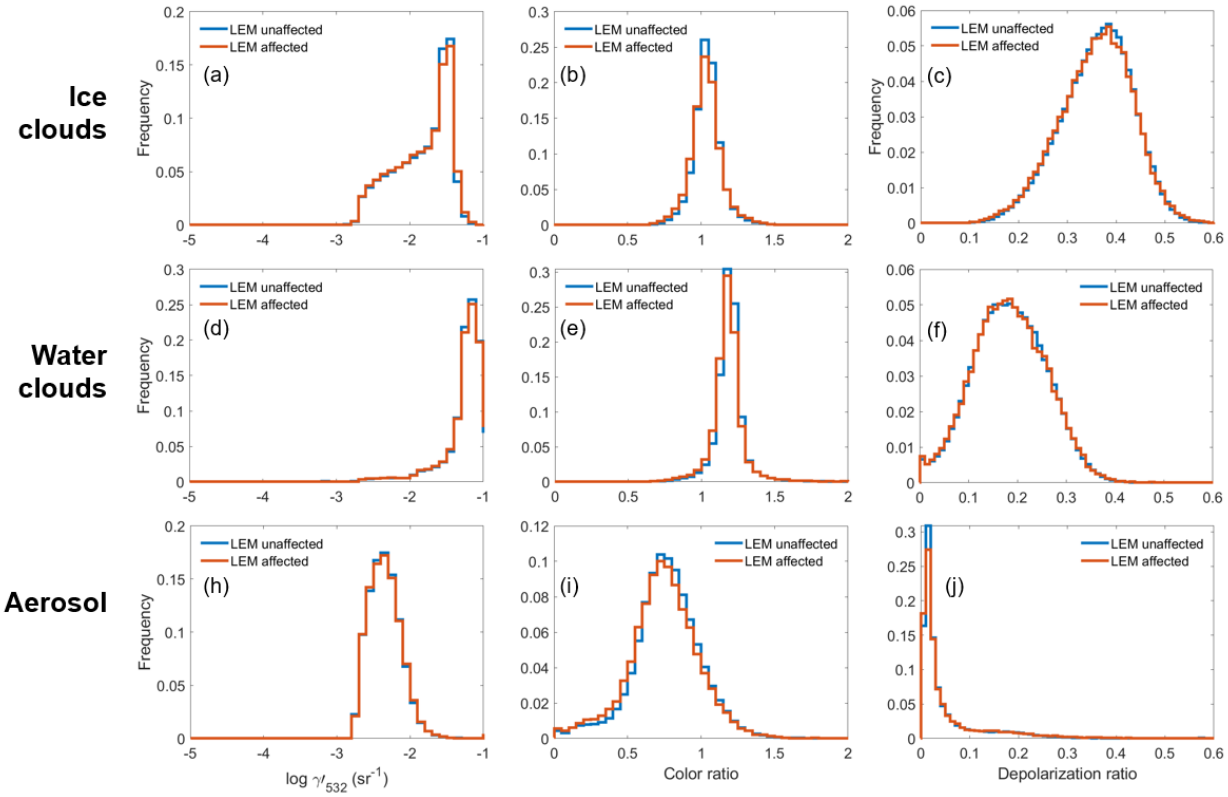

Figure 11: Frequency distributions of layer-integrated 532 nm attenuated backscatter (γ'_{532}), layer-mean attenuated backscatter color ratio ($\bar{\beta}'_{1064}/\bar{\beta}'_{532}$), and layer-integrated volume depolarization ratio for ice clouds (panels a-c), water clouds (panels d-f), and aerosol layers (panels h-j). Distributions from layers wholly unaffected by low energy pulses are shown in aqua. Distributions for LEM-affected layers are shown in orange. Statistics are computed from layers detected in nighttime measurements at 5 km horizontal resolution between 50°S-50°N, excluding the SAA, during all of 2021. (Figure from Tackett et al., 2025.)

To enable users to easily identify LEM-affected features and profiles that have been wholly excluded by the LEM algorithm, the CALIOP level 2 layer products and profile products now report a 'Low Energy Column QC Flag' for each atmospheric column in the respective data sets. These flags are bit-mapped 16-bit integers that indicate which columns contain low energy laser pulses, which columns have been wholly rejected as unusable, why rejected columns have been excluded, and which of CALIOP's altitude-dependent averaging regions contain LEM-rejected data. The interpretations of individual bits are given in Table 8. With the exception of the 333 m merged layer products, all layer products and profile products also report a Boolean 'Low Energy Mitigation Feature QC Flag'. When this flag is true, the corresponding feature (layer products) or range bin (profile products) contains either LEM-affected data, in which some low energy pulses were included in the data averaged onboard the satellite prior to downlink, or LEM-rejected data that have been wholly excluded from the level 2 analyses. The layer descriptions (e.g., top and base altitudes, integrated attenuated backscatter, etc.) in LEM-rejected columns are identified with a LEM flag value of -111.

LEM information is reported in the vertical feature mask (VFM) product via the new 'VFM Feature Detection Quality Flag'. Like the 'Feature Classification Flags', which have always been reported in the VFM files, the 'VFM Feature Detection Quality Flag' is an array of bit-mapped 16-bit integers, with one value reported for each element in the downlinked data stream. As shown in Table 9, these bits inform data users which range bins contain low energy shots, which have been rejected by LEM, and which feature finder averaging resolution was required for the feature to be detected.

Table 8: Interpretation of the individual bits in the Low Energy Column QC Flag; note that "a frame" consists of 15 consecutive laser pulses that have been averaged onboard the satellite to the vertical and horizontal spatial resolutions given in (Hunt et al., 2009). Bit 0 is the least significant bit.

Bit	Interpretation
0	Column contains LEM-affected data (data has been rejected or contains low energy pulses that LEM accepts)
1	Column belongs to a 5 km frame that has been rejected due to too many unusable profiles
2	Column belongs to a 5 km frame that has been rejected due to too many rejected subregions in altitude region 3
3	Column belongs to a 5 km frame that has been rejected due to too many rejected subregions in altitude region 4
4	Feature detection not performed at 20 km resolution in this column due to too many rejected frames
5	Feature detection not performed at 80 km resolution in this column due to too many rejected frames
6	Unused
7	Column has data rejected in altitude regions 1 and 2 (only reported at single-shot resolution)
8	Column has data rejected in altitude region 3 (only reported at single-shot resolution)
9	Column has data rejected in altitude region 4 (only reported at single-shot resolution)
10	Column does not have low energy, but data is rejected in regions 1 & 2 due to rejected data in altitude region 3 (only reported at single-shot resolution)
11–15	Unused

Table 9: bit interpretations for the 'VFM Feature Detection Quality Flag'; bit 0 is the least significant bit.

Bit	Interpretation
0	First single-shot profile has low energy
1	Second single-shot profile has low energy
2	Third single-shot profile has low energy
3	Fourth single-shot profile has low energy
4	Fifth single-shot profile has low energy
5	Bin in first single-shot profile is rejected by LEM
6	Bin in second single-shot profile is rejected by LEM
7	Bin in third single-shot profile is rejected by LEM
8	Bin in fourth single-shot profile is rejected by LEM
9	Bin in fifth single-shot profile is rejected by LEM
10	Contributed to feature detection at 1/3 km resolution
11	Contributed to feature detection at 1 km resolution
12	Contributed to feature detection at 5 km resolution
13	Contributed to feature detection at 20 km resolution
14	Contributed to feature detection at 80 km resolution
15	Unused

The effects of the low energy mitigation filtering are pervasive throughout the CALIPSO level 2 data products, particularly in the final years of the mission. To optimize the functioning of the LEM algorithms required several LEM-related changes to the lidar level 2 analyses.

- The feature classification flags (in the layer products and VFM) and the atmospheric volume descriptions (in the profile products) no longer include an "invalid" feature category. Previously, invalid features could be readily identified whenever the three least significant bits were all set to zero. Invalid features occurred extremely rarely – e.g., 872 of the 41,194,051 (~0.002%) of the unique atmospheric features detected during

all of 2012 we designated as invalid. These features were also assigned special cloud-aerosol discrimination (CAD) scores (Liu et al., 2019) to give users some insight into the failure mechanism that cause the layer to be identified as invalid. In V5.0, having the three least significant bits of a feature classification flag evaluate to zero no longer represents an 'invalid' classification of a detected layer, but instead indicates that data in the column has been rejected by the level 2 LEM filter. The spatial and optical properties within these columns (e.g., top and base altitudes, CAD scores, and optical depths) are all set to a special LEM flag value (–111). Features that were previously classified as invalid are now identified as zero-confidence clouds and they retain any of the special CAD scores that were assigned in previous data releases.

- Substantial modifications were required to add "LEM awareness" to the CALIOP boundary layer cloud clearing (BLCC) algorithm. The function of this procedure is to separate boundary layer clouds from the surrounding aerosols at single shot resolution so that the signal-to-noise ratios (SNR) of the aerosol data could be improved by large scale averaging, thus greatly reducing uncertainties in the aerosol extinction retrievals. Problems arose, however, when dense aerosols lay immediately above stratus decks. In these cases, the combined aerosol and cloud signals were often detected as a single, heterogenous feature in CALIOP's initial 5 km (15 shot) resolution profile scan (Vaughan et al., 2009). The clouds in these multi-type features were subsequently identified at single shot resolution. However, when 15 horizontally adjacent clouds were detected at single shot resolution within a single 5 km segment, a logic flaw in the BLCC scheme failed to separate these clouds from the overlying aerosol. This, in turn, introduced significant errors into the affected aerosol extinction retrievals. While this flaw was largely eliminated in the V4.51 data release (Tackett et al., 2022), some residual errors remained. When checking for the presence of 15 horizontally adjacent clouds detected at single shot resolution, the V4.51 BLCC did not account for contamination by low energy laser pulses. Since no clouds would be detected in these single shot low energy pulses, the count of horizontally adjacent clouds within the 5 km segment would fall below 15. As a consequence, these clouds were not properly separated from the overlying aerosol prior to calculating an extinction solution. Not surprisingly, the extinction solutions retrieved for these unintentionally heterogenous layers were completely unreliable. This situation is ameliorated in V5.00 by excluding low energy pulses when calculating the fraction of laser shots in which clouds are detected at single shot resolution.
- In concert with the above change to the BLCC, the calculation of the 'Single Shot Cloud Cleared Fraction' parameter reported in all 5 km averaged products was updated to correctly account for LEM-rejected profiles. As an example, if 5 clouds are detected at single shot resolution within a 5 km along-track segment that also included 5 low energy laser pulses, the single shot cloud cleared fraction in the V5.00 data products will be 5/10 = 0.5 versus 5/15 = 0.333 in the V4.51 products.
- To improve the accuracy of the surface detection algorithm and prevent spurious detections, the surface detection algorithm was modified to recognize and exclude LEM-rejected data.
- To accommodate the addition of the special LEM flag value (-111), the data types of the 'Cloud Layer Fraction', 'Aerosol Layer Fraction', and 'High Resolution Layers Cleared' scientific data sets (SDSs) were changed from unsigned integers to signed integers.

Changes to Aerosol Lidar Ratios

The Models, In situ, and Remote sensing of Aerosols (MIRA) working group was formed by an international team of aerosol research scientists shortly after the successful conclusion of the CALIPSO Version 5 Aerosol Lidar Ratio Workshop in March 2021. One of the primary goals initially identified by the MIRA group was to develop a solid empirical basis for creating a global set of spatially and seasonally varying Maps of Aerosol lidar ratios for CALIPSO (MAC). Based on in-depth analyses by MAC researchers, CALIPSO's V5.00 data release makes extensive changes to the default lidar ratios used to initiate extinction solutions for the marine and dusty marine aerosol types.

In all previous data releases, the CALIOP aerosol subtypes were characterized by a single, type specific, globally applicable lidar ratio, together with an associated uncertainty estimate that defined the lidar ratio's expected natural variability (Kim et al., 2018). For example, the lidar ratios for marine and dusty marine types were,

respectively, 23 ± 5 sr and 37 ± 15 sr. In preparation for the V5.00 release, the MAC team constructed tropospheric aerosol optical depth (AOD) estimates by subtracting the stratospheric AODs reported in CALIPSO's level 3 stratospheric aerosol product (Kar et al., 2019) from the full column AODs reported by MODIS. These tropospheric AODs were then paired with collocated CALIOP 532 nm attenuated backscatter profiles to retrieve aerosol lidar ratio estimates from constrained solutions of the lidar equation (Toth et al., 2025). Retrievals were limited to cloud-free scenes over oceans in which CALIPSO identified only a single aerosol type (i.e., either marine or dusty marine) within a 5 km averaged column. Solutions were calculated for all qualifying measurements obtained while CALIPSO flew in the A-Train with MODIS-Aqua, from June 2006 through August 2018. The retrieved lidar ratios for each of the two aerosol types were then aggregated into four seasonal maps (winter, spring, summer, and fall) having a spatial resolution of 2° latitude × 4.8° longitude. Grid cells having fewer than 50 samples – e.g., in polar winters, when the MODIS orbit does not allow for the daytime measurements necessary to retrieve AOD – are excluded from these maps. These excluded values are replaced with an approximation derived from the relationship between the constrained lidar ratios and the sea salt volume fraction (SSVF) computed using parameters reported by the Goddard Chemistry Aerosol Radiation and Transport (GOCART) model (Toth et al., 2025). For any V5.00 CALIOP footprint, the locally appropriate lidar ratio and its associated uncertainty are interpolated in both time and space from the map data.

Figure 12 shows the seasonal maps developed for marine aerosols. Seasonal and regional variations in marine lidar ratios are plainly visible and often show a marked difference from the 23 ± 5 sr value used globally in previous data releases. These differences highlight an important conceptual difference between the V5.00 marine lidar ratios and the marine lidar ratios in previous data releases. Previously, the marine lidar ratio represented our best approximation of "clean marine" conditions (e.g., see Kim et al., 2018). In V5.00, marine lidar ratios are assigned to aerosols detected over oceans that are dominated by marine constituents but that can also be mixed with other, mostly anthropogenic components. As seen in Figure 12, genuinely pristine marine aerosols are largely confined to the remote southern oceans. Coastal regions frequently exhibit a pronounced influence from other aerosol sources that elevates the lidar ratios to values significantly higher than those seen in the southern oceans.

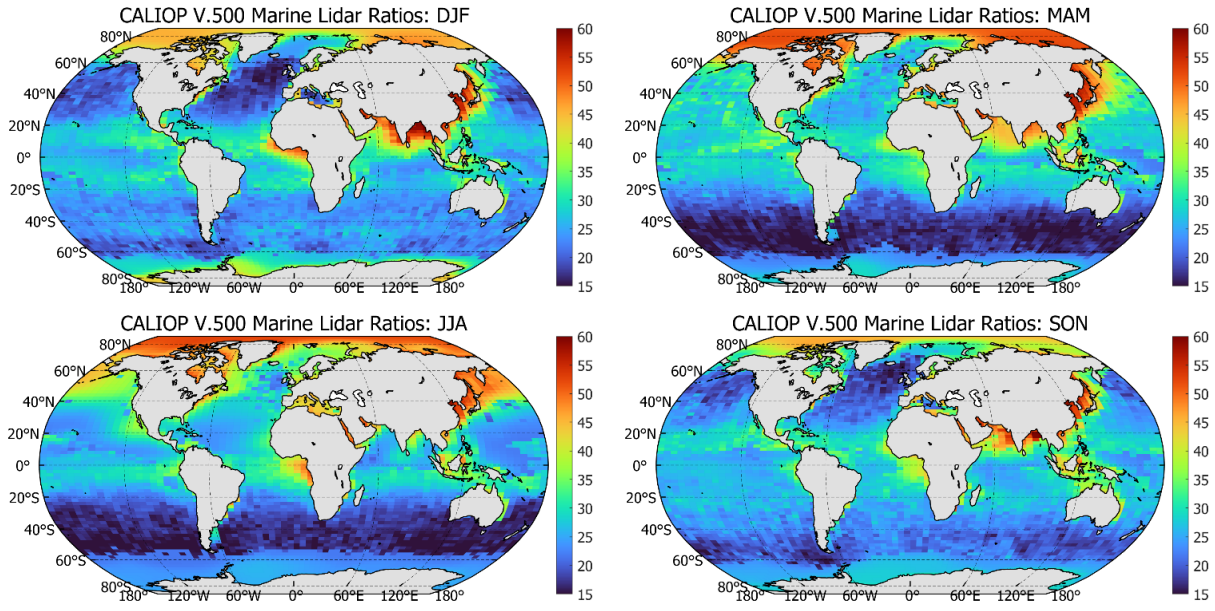

Figure 12: CALIOP initial marine lidar ratios (units = sr) derived from CALIOP 532 nm attenuated backscatter profiles constrained by collocated MODIS aerosol optical depths. The top left shows median values for the winter months (December, January, and February); the top right shows median values for the spring (March, April, and May); the bottom left shows median values for the summer (June, July, and August); and the bottom right shows median values for the fall (September, October, and November).

Our approach for constructing dusty marine maps was, with two notable exceptions, essentially identical to the method we used for marine aerosols. The first exception is that for the dusty marine maps we also included lidar

ratio solutions constrained by CALIOP's ocean-derived column optical depth (ODCOD; Ryan et al., 2024) retrievals. For the marine lidar ratios, ODCOD retrievals were excluded so that they could later be used to validate the MODIS constrained retrievals. However, for the dusty marine type, sun glint contaminating the collocated MODIS measurements precluded their use as an AOD constraint in important dust transport corridors (e.g., during boreal summers in the Caribbean and central western Atlantic). Consequently, we chose to include ODCOD constrained solutions in developing the dusty marine maps. The second exception is that, unlike the marine lidar ratio maps, the seasonal variability in the dusty marine maps is limited to the green shaded region shown in Figure 13. While other parts of the hydrosphere showed little, if any, seasonal variation (perhaps due to temporal changes in dust concentrations), significant seasonal variations in dusty marine lidar ratios were observed over the Mediterranean Sea, the Persian Gulf, the Arabian Sea, and the Bay of Bengal. Furthermore, the seasonal sample counts in these regions were large enough in each season to retrieve confident lidar ratio estimates. Neither of these conditions were met simultaneously in any other extended regions of the globe.

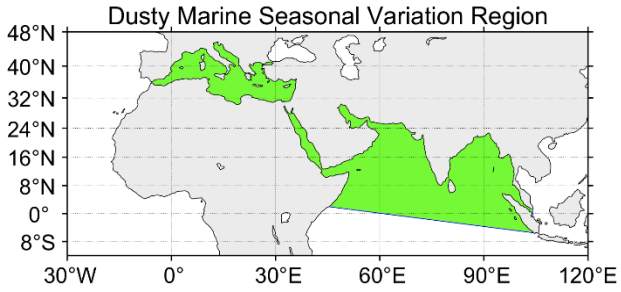

Figure 13: the green shaded area of the map indicates those regions where CALIOP's dusty marine lidar ratios are observed to vary seasonally.

The V5.00 dusty marine maps are shown in Figure 14. As expected, the dusty marine lidar ratios are uniformly larger than the marine lidar ratios. The spatial patterns of the two types are generally similar, simply because anthropogenic aerosol transport patterns are essentially identical for both types and the inclusion of anthropogenic aerosols elevates both sets of values.

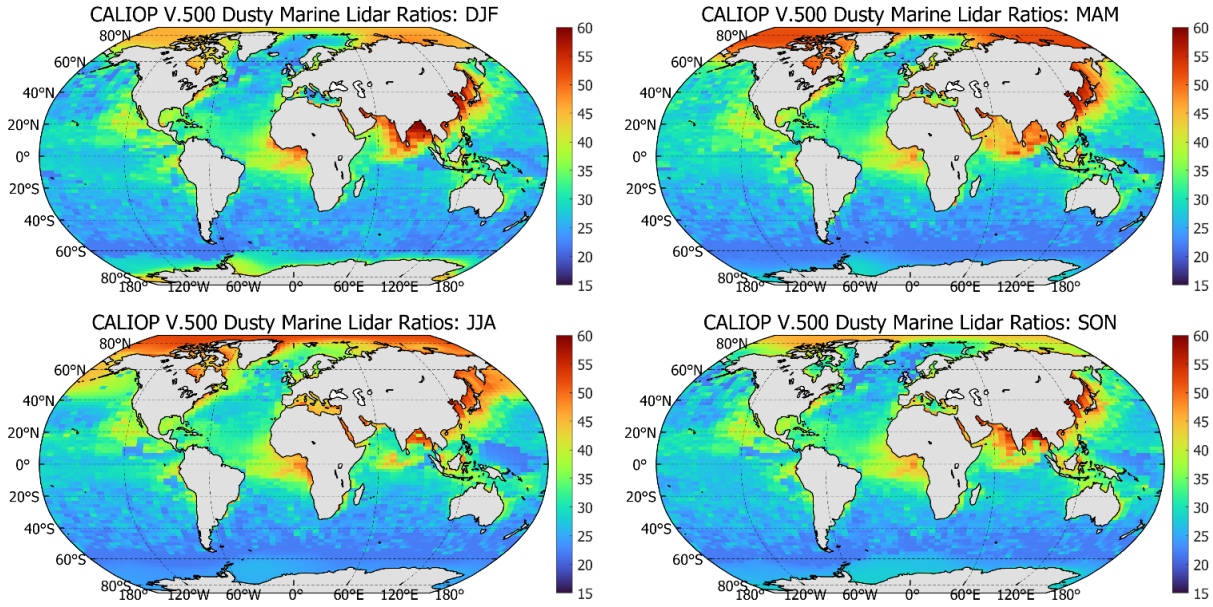

Figure 14: CALIOP initial dusty marine lidar ratios (units = sr) derived from CALIOP 532 nm attenuated backscatter profiles constrained by collocated aerosol optical depth measurements from MODIS and ODCOD. The top left shows median values for the winter months (December, January, and February); the top right shows median values

for the spring (March, April, and May); the bottom left shows median values for the summer (June, July, and August); and the bottom right shows median values for the fall (September, October, and November).

A second change to the CALIOP aerosol lidar ratios is the selection of a new value of 45 ± 24 sr for 1064 nm retrievals of clean continental aerosol. This change is based on field measurements of continental aerosol made by Haarig et al., 2025 using a 1064 nm rotational Raman lidar. The 532 nm lidar ratio for the clean continental type remains unchanged at 53 ± 24 sr.

Changes to Aerosol Type Identification

In addition to the MAC lidar ratio work, the V5.00 data set contains a second fairly substantial (albeit localized) change. CALIOP's V4.51 aerosol subtyping algorithm classified planetary boundary layer (PBL) aerosols located over ocean surfaces as marine, with ocean surfaces being identified using the CALIPSO land-water mask. In Arctic winter however, most of the "ocean surfaces" reported by the land-water mask are actually extended over-ocean ice sheets, and the aerosol above is not marine but instead some species of anthropogenic aerosol arriving in the polar regions via long range transport. In these cases, assigning a marine aerosol lidar ratio to the aerosol layer both misrepresents the true aerosol type and leads to sometimes substantial underestimates of aerosol optical depth. By expanding the surface type identification scheme to also include snow and ice data reported in the CALIOP level 1b files and by making small modifications to the aerosol subtyping flowchart (see Figure 15), the V5.00 CALIOP data product now more correctly classifies a large fraction of these "over frozen ocean" aerosols.

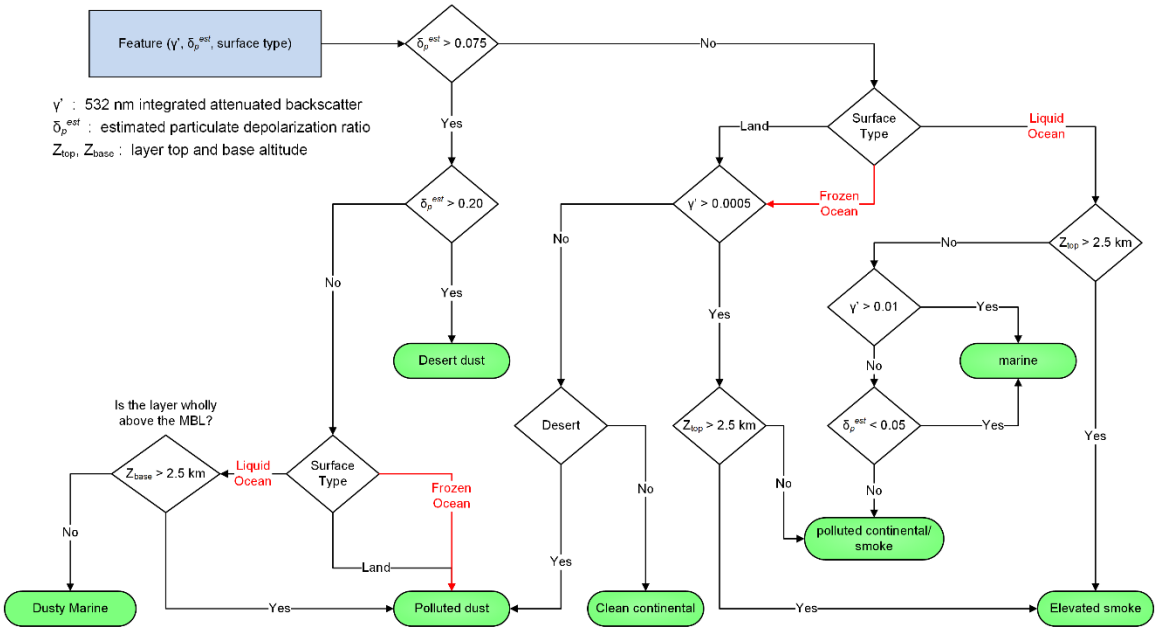

Figure 15: revised tropospheric aerosol subtyping flowchart; paths and labels in red were added for the V5.00 release.

New ODCOD Retrieval Confidence Flag

In response to data user requests, a new confidence flag has been added to the existing 'ODCOD QC Flag' SDS reported in the 'Ocean Derived Column Optical Depth' Vgroup included in all layer products and profile products. Table 11 describes how to interpret all of the bits used in the 'ODCOD QC Flag'. The new confidence flag (shown in orange) is reported in bit 6. In this new configuration, all valid ODCOD retrievals will have an 'ODCOD QC Flag' of 127 or less. All high confidence ODCOD retrievals will have an 'ODCOD QC Flag' value of 63 or less. Any of the following conditions will cause bit 6 to be toggled on, indicating a low confidence solution.

a) Wind speed out of range; the AMSR corrected MERRA-2 wind speed is less than 3 m/s or greater than 15 m/s

b) Surface integrated depolarization ratio is greater than 0.05, suggesting that the surface is not pure sea water

c) Surface integrated attenuated backscatter exceeds the upper bound specified in Table 10.

Table 10: maximum values of surface integrated attenuated backscatter for confident retrievals; higher values may include undetected surface saturation.

	Daytime	Nighttime
532 nm	0.0413 sr^{-1}	0.0353 sr^{-1}
1064 nm	0.0384 sr^{-1}	0.0325 sr^{-1}

d) The number of range bins shifted by the altitude registration algorithm (Powell et al., 2009) is not constant over all profiles used to create the averaged surface return. This is only a concern for averaged profiles where having multiple "bins shifted" will distort the shape of the spatially averaged surface return and degrade the quality of the fit to the CALIOP response model (CRM; Ryan et al., 2024). To aid in diagnosing the presence of non-constant bin shifts, a new SDS ('ssNumber Bins Shift') was added to the 'Single Shot Detection' Vgroup reported in the 5 km layer products.

Table 11: interpretation of the individual bits in the ODCOD QC flags (adapted from Ryan et al., 2024); bit 0 is the least significant bit.

Bit	Interpretation
0	Of the measurements provided to the ODCOD algorithm by the surface detection algorithm, ODCOD adjusted the CRM such that the first data point of the surface detection data was not the first point on the CRM
1	The surface detection algorithm provided surface measurements covering a range greater than 120 m
2	The ODCOD algorithm used range bins above the top of the detected surface altitude
3	The ODCOD algorithm used range bins below the base of the detected surface altitude
4	When solving for the alignment of the CRM, the first measurement that should fall on the CRM curve was not originally provided by the surface detection algorithm
5	ODCOD had to adjust the CRM such that the first measurement provided by the surface detection algorithm was not the first point on the CRM
6	ODCOD retrieval confidence flag; a value of 1 indicates a confident retrieval whereas 0 signals low confidence
7-9	Unused
10	The surface detection algorithm did not find a surface
11	The International Geosphere–Biosphere Programme (IGBP) surface type is not 17 for ocean
12	The depolarization ratio of the surface is greater than 0.15
13	The corrected MERRA-2 wind speed is outside of the inclusive range 0.025 m s^{-1} to 43 m s^{-1}
14	ODCOD has failed to find the time delay of the CRM from the surface measurements provided by the surface detection algorithm
15	The vertical extent of the detected surface contains too few samples to derive a time delay solution
16	When solving for the CRM area, the solution grew unrealistically large
17	A failure occurred while attempting to solve for the scale factor
18	Surface saturation was detected in the surface return
19	Negative signal anomaly was detected in the surface return
20	The detected surface contains negative or invalid backscatter measurements
21	Necessary input data is either fill or invalid
22	The surface detection algorithm had to resort to an alternative method of finding the surface when the surface return was averaged to coarser resolutions that may not be reliable for ODCOD

Bit	Interpretation
23–31	Unused

Wrong profile starts for a new chunk after missing data gap

The CALIOP level 2 processing ingests level 1 data in 80 km "chunks", equivalent to the largest horizontal averaging resolution used in the search for features. Each chunk contains 240 consecutive single-shot profiles distributed uniformly across 16 consecutive 5-km (15 shot) frames. If there are any missing data within these 240 consecutive profiles, the candidate chunk is discarded, and the level 2 processing resumes beginning with the first single shot profile in the first frame available after the data gap. However, the V4.51 and earlier level 2 code contained an "off by one" error that caused this processing restart to begin with the second profile in the frame instead of the first. As a consequence of eliminating this error, in granules containing data gaps – e.g., for planned activities such as boresight alignments and polarization gain ratio calibrations or for unplanned events such as the repeated ground station downlink anomalies that occurred between 21:20:46 UTC on 2020-12-12 and 00:12:12 UTC on 2020-12-13 – the level 2 chunks built following those data gaps will use a somewhat different collection of single shot profiles in V5.00 relative to all previous versions. Figure 16 shows an example of the kinds of changes that can occur due to this change in profiles averaged. The upper panel shows daytime data acquired in the southern Pacific Ocean on 2020-12-12 at ~22:27 UTC. On this day, data downlink from the satellite was intermittently interrupted by ground station errors. The white vertical strips in the upper panel show where individual frames were missing or irretrievably corrupt in the downlink data stream. The lower panel is a "red-green-black" diagram comparing feature detections in V4.51 to those in V5.00. The green areas represent features detected in both data processing versions, while the red areas show features that were detected in V4.51 but not V5.00 and the black areas show the opposite; i.e., features that were detected in V5.00 but not V4.51. Regions where no features were detected in either analysis are shown in white. The vertical gray bars show where chunks have been rejected by the level 2 processing due to the presence of missing data. In some cases – e.g., following the first to data gaps beginning at ~41.5°S and ~37.2°S – there are no layer detection changes. On the other hand, the region following the final data gap shows substantial changes, though not all of them can be attributed to the change in the selection of pseudo-single shot profiles to average. The red range bins not detected in V5.00 were eliminated by the LEM algorithm described above. In this and other segments, the intermittent detection changes in individual range bins adjacent to the Earth's surface occur due to V5.00 changes in VFM altitude registration, as described below in the Revised VFM Layer Detection Altitudes section. The additional aerosol detections highlighted by the black areas in this data segment are a fortuitous result of the combination of a shift in profiles averaged combined with LEM filtering. We note, however, that additional feature detections are not a guaranteed outcome of this code change.

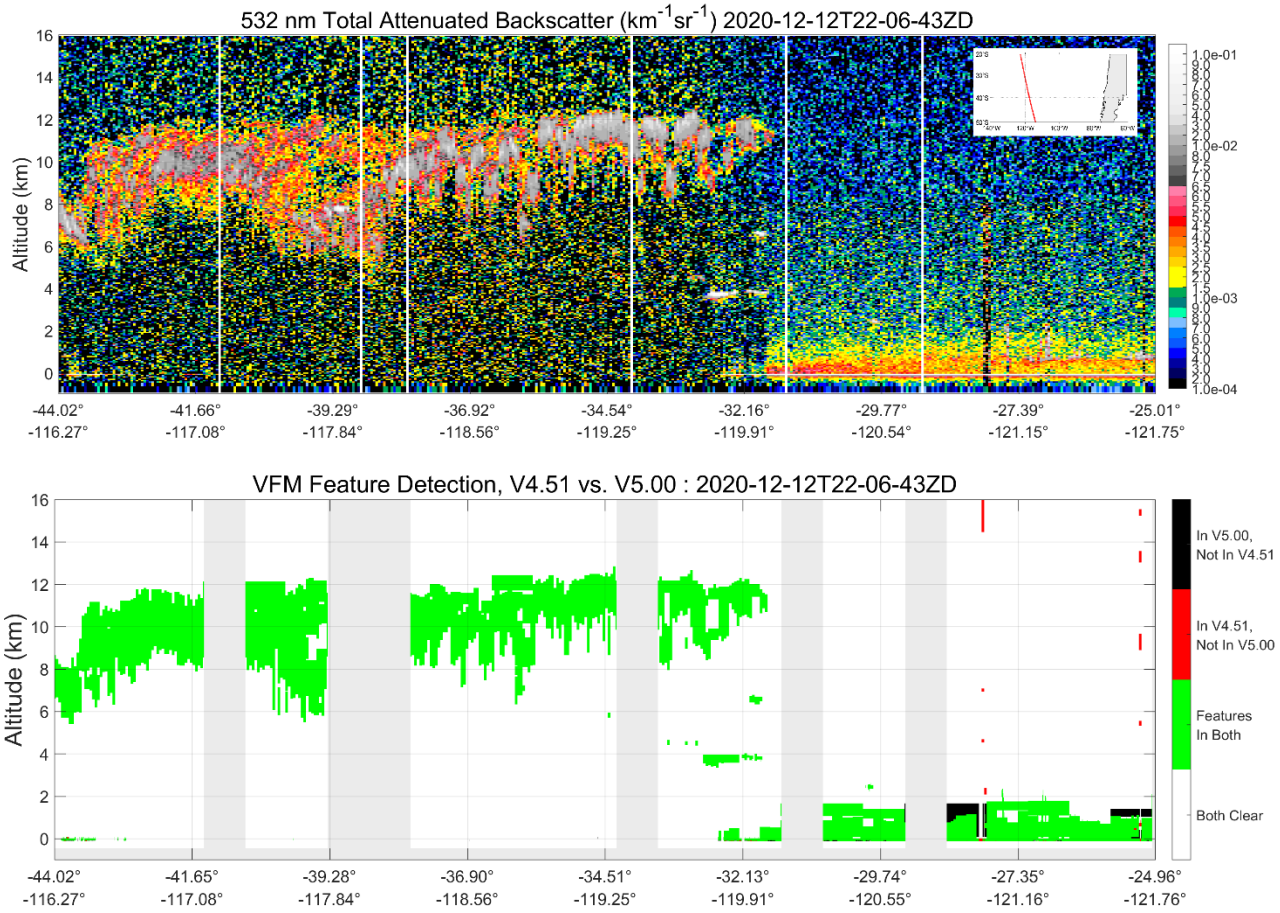

Figure 16: The upper panel shows 532 nm total attenuated backscatter coefficients measured in the southern Pacific Ocean on 2020-12-12 at ~22:27 UTC. The white vertical stripes in the image represent frames (i.e., 15 consecutive shots) containing missing data. The lower panel compares V4.51 and V5.00 VFM feature detections for the scene shown in the upper panel. The gray vertical stripes show where chunks (i.e., 240 consecutive shots) were rejected by the level 2 processing algorithms due to missing data in one or more included frames.

HDF File Changes

The V5.00 CALIPSO data products are distributed as Hierarchical Data Format Version 4 (HDF4) files, consistent with the EOS requirement in effect when CALIPSO launched in 2006. Since launch, there have been substantial technological advances in data discoverability and access to resources. To make CALIPSO data more readily accessible to the scientific community beyond the life of the mission and take advantage of newer data access capabilities, several modifications were made to the format and content of the CALIOP HDF files. These include:

- Updating all units to conform to NetCDF Climate and Forecast (CF) metadata conventions.
- Ensuring that all dimensions are named, to allow HDF to NCDF conversions using commercial off the shelf (COTS) tools that currently exist.
- Creating/expanding SDS attributes and comments to make the data products more self-documenting.

New Data Product: CAL_LID_L2_MLay_Diagnostic-Beta-V5-00*.hdf

The newly released CAL_LID_L2_MLay_Diagnostic-Beta-V5-00*.hdf data products are augmented versions of the standard CAL_LID_L2_05kmMLay_Standard-V5-00*.hdf products. The production strategy for these products is 'Beta', indicating that some of the included parameters have not been fully validated. In particular, these 'not fully validated' parameters include the cloud values reported in the 1064 nm derived optical properties SDSs (e.g.,

'Feature Optical Depth 1064'). While the Diagnostic Beta products contain all the information reported in the Standard products, they also contain the five SDSs listed below that are not reported in the Standard products.

1. Low Energy Mitigation Internal Column QC Flag – a 16-bit unsigned integer that offers extra insight into the internal workings of the LEM algorithm. Bit interpretations are given in Table 12.

2. Initial Integrated Attenuated Backscatter 532 – The standard 'Integrated Attenuated Backscatter 532' (γ'_{std}) values reported in all CALIOP lidar level 2 layer files are calculated assuming that the feature attenuated backscatter coefficients have been corrected for signal attenuation due to all layers detected above. The 'Initial Integrated Attenuated Backscatter 532' (γ'_{init}) values are recorded immediately after feature detection during the initial 5 km search for features. At this point in the processing, no single shot cloud clearing has been done nor have the layers been classified by the CAD algorithm. Assuming perfect detection and classification and perfect knowledge of layer lidar ratios and multiple scattering factors, $\gamma'_{init} = T^2_{above} \times \gamma'_{std}$, where T^2_{above} is the two-way transmittance of all overlying particulate layers. In special cases, when particulate layers lie above opaque water clouds, measurements of γ'_{init} can be used to derive estimates of T^2_{above} and hence obtain estimates of the overlying particulate optical depths (Hu et al., 2007). These measurements of γ'_{init} are an essential input required for calculating the 'Column Particulate Optical Depth Above Opaque Water Cloud 532' values reported in all layer products.

3. Initial Integrated Attenuated Backscatter Uncertainty 532 – uncertainty estimates for the 'Initial Integrated Attenuated Backscatter 532' which are subsequently used to calculate the 'Column Particulate Optical Depth Above Opaque Water Cloud Uncertainty 532' values.

4. Initial Integrated Attenuated Backscatter 1064 – this is the 1064 nm analog of the 'Initial Integrated Attenuated Backscatter 532'. Because CALIOP does not make depolarization ratio measurements at 1064 nm, this parameter is unused in the V5.00 analyses. In any (currently unforeseen) future version of the CALIOP data products, the 'Initial Integrated Attenuated Backscatter 1064' values could potentially be used in the algorithm proposed by Chand et al., 2008 to derive column Ångström exponents for particulates above opaque water clouds.

5. Initial Integrated Attenuated Backscatter Uncertainty 1064 – this is the 1064 nm analog of the 'Initial Integrated Attenuated Backscatter Uncertainty 532'. Because CALIOP does not make depolarization ratio measurements at 1064 nm, this parameter is unused in the V5.00 analyses.

Table 12: internal low energy mitigation (LEM) quality control flags set during LEM algorithm operations; bit 0 us the least significant bit

Bit	Interpretation
0	Single shot columns have data rejected in regions 1 and 2 but the 5 km resolution column was NOT rejected by LEM
1	Column has data rejected in altitude region 3 but the 5 km resolution column was not rejected by LEM
2	Column has data rejected in altitude region 4 but the 5 km resolution column was not rejected by LEM
3	Full column is rejected by LEM
4	Column rejected due to altitude region 3
5	Frame rejected due to too many low energy shots
6	Frame rejected due to too many rejected subregions in altitude region 3
7	Frame rejected due to too many rejected subregions in altitude region 4
8	Feature detection was not attempted at 20 km resolution due to too many LEM-rejected columns
9	Feature detection was not attempted at 80 km resolution due to too many LEM-rejected columns
10	Feature detection was not attempted at resolution 6 due to too many LEM-rejected columns
11	Column contains LEM affected data in altitude region 3
12	Column contains LEM affected data in altitude region 4
13-15	Unused

In addition to the new SDSs, the Diagnostic Beta products also contain an extra Vgroup. The '01 km Detection' Vgroup replicates the majority of the SDSs reported in the CAL_LID_L2_01kmCLay_Standard-V5-00*.hdf products. Information in the excluded SDSs is either (a) replicated in the 5 km SDS of the same name (e.g., 'Day Night Flag' and 'IGBP Surface Type') or (b) easily derived from the SDS of the same name reported in the 'Single Shot Detection' Vgroup (e.g., 'Solar Zenith Angle', 'Solar Azimuth Angle', and 'Troposphere Height').

Finally, the 'Ocean Derived Column Optical Depth' (ODCOD) Vgroup in the Diagnostic Beta products augments the information contained in the Standard products by reporting column particulate optical depth retrievals at 1064 nm. In addition, ODCOD Vgroup in the Diagnostic Beta products contains a wealth of diagnostic information and intermediate calculations for the ODCOD retrievals at both wavelengths. Comments in the HDF attributes for each SDS in this Vgroup describe the function of each parameter in the ODCOD calculation chain. Researchers considering using this information should first very thoroughly review the ODCOD retrieval technique described in Ryan et al., 2024.

Unique Layer IDs for Features Detected at 5 km, 20 km, and 80 km Resolutions

Within each granule, unique layer IDs are now assigned for all layers detected at 5 km, 20 km, and 80 km averaging resolutions. Unique layer IDs are unsigned 16-bit integers that enable unambiguous mapping between the integrated optical properties for the individual layers reported in the 5 km layer products and the corresponding profiles of vertically resolved optical properties reported in the 5 km profile products. Because extinction retrievals are not attempted for layers detected at single shot and 1 km resolutions, unique layer IDs are not assigned for the features reported in the 333 merged layer files and the 1 km cloud layer files.

In the 5 km aerosol, cloud, and merged layer files, unique layer IDs are reported in the same manner as layer optical properties. Recall that layer properties are reported at a uniform 5 km along-track resolution, and that for layers detected at 20 km and 80 km resolution, these properties are replicated over four 5 km columns for 20 km detections and sixteen 5 km columns for 80 km detections. Consequently, while a unique layer ID may appear as many as sixteen times in a single data file, these sixteen instances all reference the same layer, and the layer properties reported for all instances – e.g., top and base heights, integrated attenuated backscatters, and optical depths – will also replicated across all sixteen 5 km columns. In the 5 km profile products, unique layer IDs are reported at the same latitude, longitude, and time coordinates as in the layer products. But, instead of appearing once in each 5 km column, layer IDs are replicated over the full vertical extent of a layer. For example, for a 480 m thick aerosol layer detected at 80 km horizontal averaging in a rectangular region would extend over eight 60 m altitude bins and sixteen 5 km profile segments.

New 'Scene Flag' SDS Added to All Layer Products

To enable rapid identification of all columns containing specific feature types, the CALIPSO layer products now include a 'Scene Flag' SDS. The Scene Flag is implemented as a 32-bit integer with individual bit interpretations as defined in Table 13. Fill values (-9999) are used to identify columns that do not pass the LEM quality checks. Users are therefore warned to check the sign of the Scene Flags and discard/ignore any negative values before querying the flags to determine column feature types.

Table 13: Bit interpretations for positive values of the new 'Scene Flag' SDS. Bit 0 is the least significant bit.

Bit	Interpretation
0	column contains tropospheric aerosol, marine subtype
1	column contains tropospheric aerosol, dust subtype
2	column contains tropospheric aerosol, polluted continental/smoke subtype
3	column contains tropospheric aerosol, clean continental subtype
4	column contains tropospheric aerosol, polluted dust subtype
5	column contains tropospheric aerosol, elevated smoke subtype
6	column contains tropospheric aerosol, dusty marine subtype

Bit	Interpretation
7	column contains stratospheric aerosol, polar stratospheric aerosol subtype
8	column contains stratospheric aerosol, volcanic ash subtype
9	column contains stratospheric aerosol, sulfate subtype
10	column contains stratospheric aerosol, elevated smoke subtype
11	column contains stratospheric aerosol unclassified
12	column contains ice clouds composed of randomly oriented crystals
13	column contains ice clouds composed of horizontally oriented crystals
14	column contains water clouds
15	column contains clouds with unknown ice-water phase
16–31	Unused

More Readily Accessible Altitude Information

To make CALIOP altitude information easier to access, new 'Lidar Data Altitudes' SDSs have been added to all level 2 data products. The 'Lidar Data Altitudes' array reports the altitudes, relative to mean sea level, that specify the vertical midpoints of all range bins in the profile measurements downlinked from the CALIPSO satellite. In all previous versions of the CALIPSO lidar data products, the 583-element 'Lidar Data Altitudes' array was stored only in the file metadata. To ensure backward compatibility with existing software, the metadata copy of the 'Lidar Data Altitudes' is retained in all files.

In the V5.00 vertical feature mask (VFM) product, the altitude array now contains 545 elements instead of the 583 elements reported in all other products. Because the VFM product does not report layer detections in the highest (~30 km to ~40 km) or lowest (~-0.5 km to ~-2.0 km) CALIOP onboard averaging regions, the superfluous altitude bins were eliminated. Making this change now matches the VFM altitude array size to the vertical dimension of the (unpacked) 'Feature Classification Flags' SDS.

Revised VFM Layer Detection Altitudes

Some changes were made to the altitude registration of layer tops and bases in the VFM product to more accurately reflect the top and base altitudes reported in the CALIOP layer products. Differences between the V4.51 and V5.00 VFM files are small, confined to the high resolution (i.e., single shot) data regime between –0.5 km and 8.2 km, and typically no more than ±1 range bin. The images below show a particularly egregious example of altitude mismatches between V4.51 and V5.00. Approximately 1% of all range bins reporting feature detection in either V4.51 or V5.00 were detected only in V4.51. Similarly, approximately 0.4% were detected only in V5.00. This apparent altitude registration anomaly is, fortunately, confined solely to the VFM files. When comparing V4.51 data products versus V5.00, the layer top and base altitudes reported in the 333 m merged layer files, the 1 km cloud layer files, and the 5 km merged layer files are identical for all layers detected in this granule.

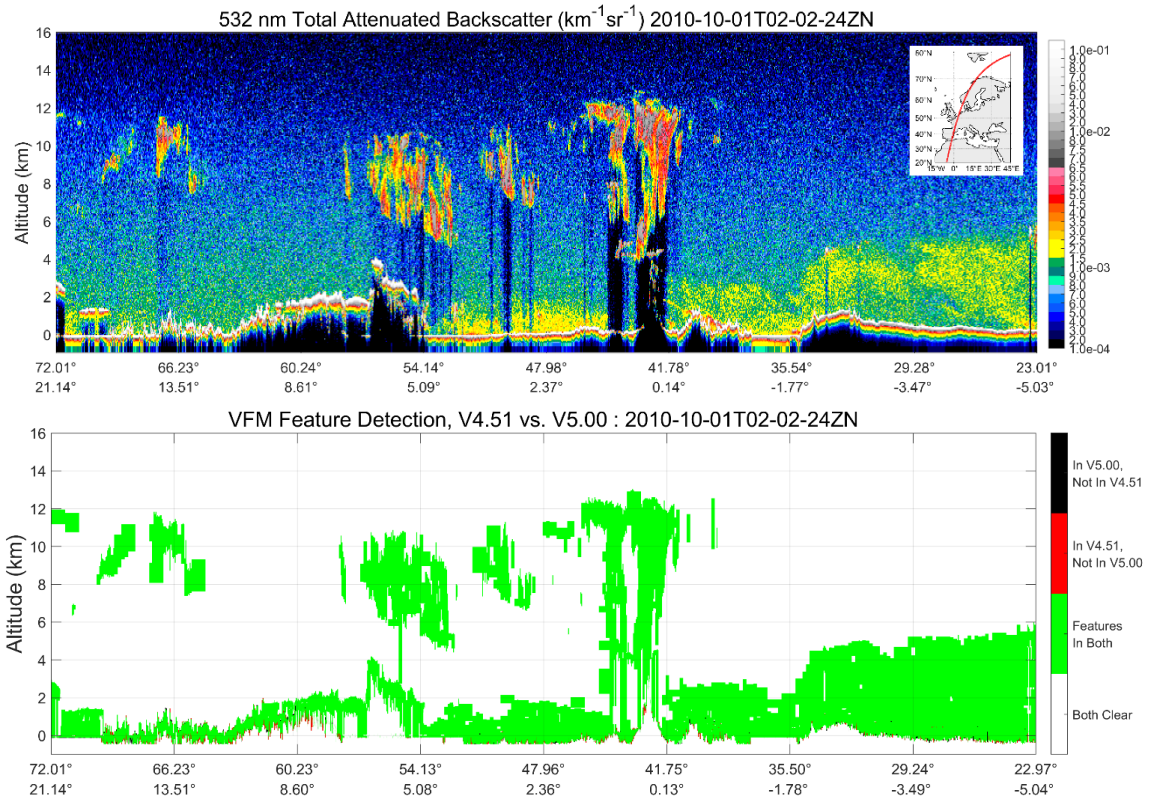

Figure 17: CALIOP nighttime observations of clouds and aerosols over Scandinavia, western Europe, and into northern Africa. These measurements were acquired on 2010-10-01 beginning at 02:02:42 UTC. The top panel shows attenuated backscatter coefficients measured at 532 nm. The bottom panel shows the VFM differences between V4.51 and V5.00. In the majority of the cases, V5.00 extends one range bin below the layer base altitude reported in the V4.51 analyses.

Summary of Newly Added and Removed SDSs

The tables below contain a comprehensive listing of all SDSs that were either added or removed. Included in the listing are SDSs that were renamed in the transition from V4.51 to V5.00.

Table 14: new scientific data sets reported in the CALIOP V5.00 lidar level 2 data products; horizontal resolution suffixes are A = aerosol, C = cloud, and M = merged layers (i.e., both aerosol and cloud).

	VFM	Layer					Profile	
SDS name		**1/3kmM**	**1kmC**	**5kmA**	**5kmC**	**5kmM**	**5kmA**	**5kmC**
Lidar_Data_Altitudes		✓	✓	✓	✓	✓	✓	✓
Low_Energy_Mitigation_Column_QC_Flag		✓	✓	✓	✓	✓	✓	✓
Low_Energy_Mitigation_Feature_QC_Flag			✓	✓	✓	✓	✓	✓
Scene_Flag		✓	✓	✓	✓	✓		
DEM_Surface_Elevation							✓	✓
Unique_Layer_ID				✓	✓	✓	✓	✓
VFM_Feature_Detection_Quality_Flag	✓							
Number_Bins_Shift		✓						
Extinction_QC_Flag_532				✓	✓	✓		
Extinction_QC_Flag_1064				✓	✓	✓		
Single_Shot_Detection::ssLow_Energy_-Mitigation_Column_QC_Flag			✓	✓	✓	✓	✓	✓
Single_Shot_Detection::ssScene_Flag			✓	✓	✓	✓	✓	✓

	VFM	Layer					Profile	
SDS name		1/3kmM	1kmC	5kmA	5kmC	5kmM	5kmA	5kmC
Single_Shot_Detection::ssNumber_-Bins_Shift			✓	✓	✓	✓	✓	✓

Table 15: scientific data sets removed from the CALIOP V5.00 lidar level 2 data products; horizontal resolution suffixes are A = aerosol, C = cloud, and M = merged layers (i.e., both aerosol and cloud).

	VFM	Layer					Profile	
SDS name		1/3kmM	1kmC	5kmA	5kmC	5kmM	5kmA	5kmC
Samples_Averaged							×	×
Surface_Elevation_Statistics							×	×
ExtinctionQC_532				×	×	×		
ExtinctionQC_1064				×	×	×		

Data Quality Statement for CALIPSO's Version 4.51 Lidar Level 2 Data Product Release

Data Version: **4.51**
Data Release Date: **June 1, 2023**
Data Date Range: **June 13, 2006 to June 30, 2023**

The new version 4.51 (V4.51) of the CALIPSO lidar (CALIOP) Level 2 (L2) data products contains a number of improvements and additions over the previous version (V4.2) that was released in October 2018. A summary of the major changes addressed in this release is detailed below, as well as a section highlighting known issues.

Improved Smoke Layer Accuracy above Clouds

The CALIOP L2 feature detection algorithm employs an iterative thresholding technique applied to profiles of 532nm attenuated scattering over differing horizontal resolutions to identify and vertically resolve layers (Vaughan et al., 2009). Rajapakshe et al., 2017 identified instances when CALIPSO was under-reporting the vertical extent of dense smoke layers above low-level clouds when compared with coincident observations made by the Cloud-Aerosol Transport System (CATS) lidar instrument. Figure 1 (a, c) shows one of those specific over-flights, in which the 532nm total attenuated backscatter (a) and vertical feature mask (c) show a clear delineation on the order of 1 km between the base of the upper-level smoke layer and the top of a marine cloud layer below. Further examination of this scene showed that this smoke layer was dense enough to rapidly attenuate the 532nm signal to such a degree that the CALIOP feature detection algorithm artificially elevated the layer base. This is confirmed by seeing that the rapid attenuation is not seen in the 1064 nm signal response (Figure 1b), where the aerosol extinction is not as great as that seen in the 532nm signal. The 1064 nm response, which appears to close the clear-air gap between the smoke and cloud layer, is also why CATS was able to fully identify the smoke layer as that instrument uses 1064 nm for feature detection. The inability of CALIPSO to fully detect these layers can have the consequence of underestimating global aerosol optical depths, critically important for the derivation and understanding of radiative forcings (Lu et al., 2018).

In the version 3 (V3) release of the CALIOP L2 data a technique was developed for the feature finder algorithm to extend the base of near-surface aerosol layers done to the surface. A variant of this same approach was applied for these overlying dense smoke layer cases. Several criteria need to be met before the layer could be extended, a summary of which are detailed in the V4.51 CALIOP layer level 2 data product description.

Figure 1d shows the application of this new technique, in which the clear-air gap has been closed. The mean 532nm optical depth of these extended smoke layers has also increased, from 0.94 to 0.122, an increase of nearly 30%. A global representation of all extended layers for the month of August 2016, seen in figure 2a, show a concentration in the south-eastern Atlantic during the African burn season, the same region noted in the CALIPSO/CATS comparisons previously documented. Figure 2b shows the impact on the 532nm optical depth for those extended smoke layers, where in a majority of those cases in which the layer was extended the optical depths increase. The

few outliers that exist have been traced to instances when the negative values of the 532nm extinction are included, which could happen during rapid attenuation of the signal.

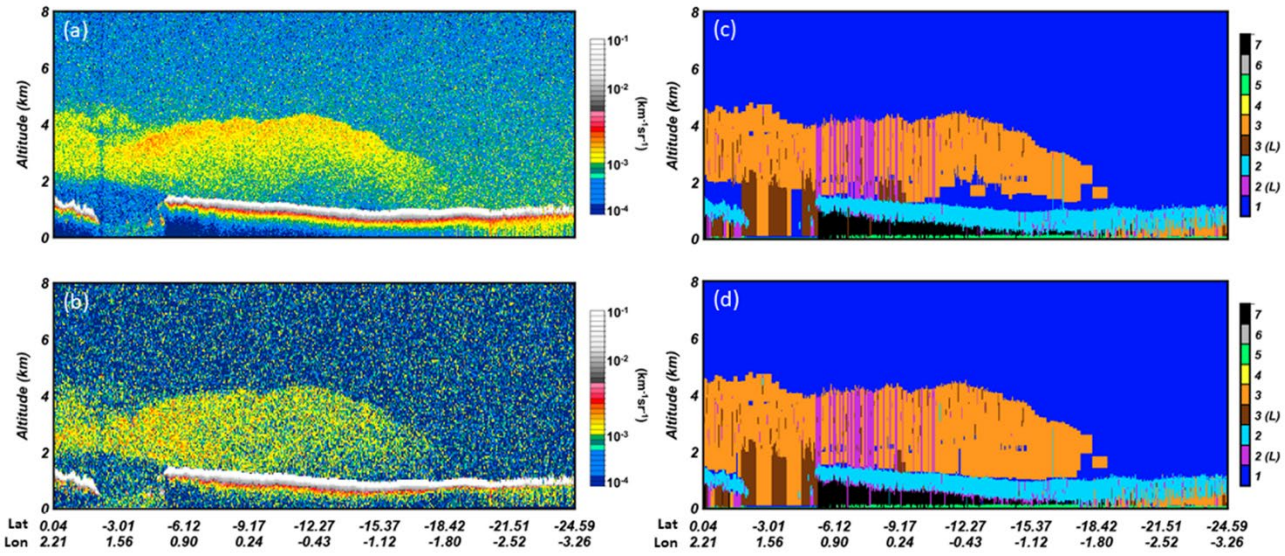

Figure 1: (a) 532 nm total attenuated backscatter from the V4.51 CALIOP Level 1B, (b) 1064 nm attenuated backscatter from the V4.51 CALIOP Level 1B, (c) feature type from the V4.21 CALIOP Level 2 Vertical Feature Mask (VFM), and (d) feature type from the V4.51 CALIOP Level 2 VFM between 1:35:03 and 1:41:44 on August 6th, 2016.

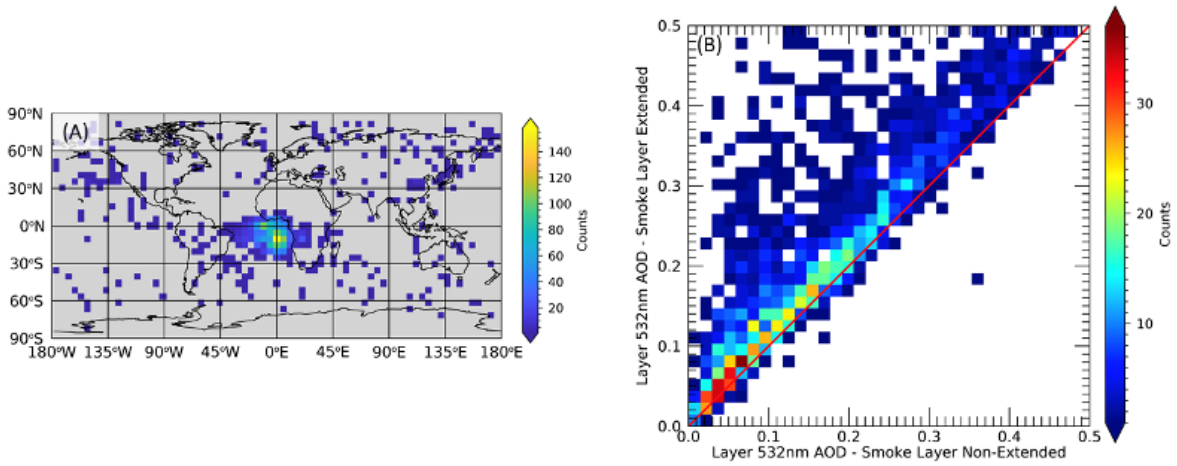

Figure 2: (a) Global distribution of all (day and night) extended smoke layers for August 2016 and (b) 532nm aerosol optical depth changes between extended (y-axis) and non-extended (x-axis) smoke layers. Data used to generate both plots were pulled from the V4.51 Lidar Level 2 5km Merged layer files. Non-extended smoke layers were created by running the V4.51 Lidar Level 2 algorithm but with the smoke extension turned off.

Improved Classifications for Stratospheric Aerosols

The stratospheric aerosol subtyping algorithm has been updated in V4.51 to improve the ability to discriminate between volcanic ash and depolarizing smoke from pyrocumulonimbus (pyroCb) injections, improve the fidelity of the sulfate classification, and to update the 532 nm volcanic ash lidar ratio to the current state of knowledge. The stratospheric aerosol subtypes are now: volcanic ash, sulfate, smoke, polar stratospheric aerosol, and unclassified. A full description of changes with the V4.51 algorithm are documented in Tackett et al., 2023a.

Summary of changes:

- The stratospheric aerosol subtyping algorithm now relies solely on depolarization and integrated attenuated backscatter (γ') to discriminated between volcanic ash, sulfate, and smoke. Removing the reliance on layer

color ratio that was included in the V4.2 subtyping algorithm allows more accurate identification of sulfate and less misclassification of sulfate as smoke.

- The estimated particulate depolarization ratio threshold used to discriminate between smoke from pyroCb injections and volcanic ash has been increased from 0.15 to 0.25 based on empirical analysis of recent major pyroCb events.
- The V4.2 "sulfate/other" stratospheric aerosol subtype has been separated into two subtypes in V4.51 - sulfate, and unclassified. Previously, the sulfate/other type included both aerosol layers likely to be sulfate and layers with low values of γ', representing the "other" component of the combined class. In V4.51, layers with low γ' are now reported separately as "unclassified".
- The 532 nm lidar ratio for volcanic ash has been increased to 61 ± 17 sr based on CALIOP-constrained retrievals of volcanic ash plumes.

Figure 3 demonstrates the improvements in stratospheric aerosol subtyping between V4.2 and V4.51. Panels in each row show the frequency of classification of each stratospheric aerosol subtype for manually identified layers associated with a dominant aerosol type. In V4.51, there are fewer misclassifications of volcanic ash as sulfate, more accurate classifications sulfate from true sulfate events, and fewer misclassifications of true smoke as volcanic ash. There remain some misclassifications of sulfate as smoke due to the difficulty of separating these types with CALIOP observables.

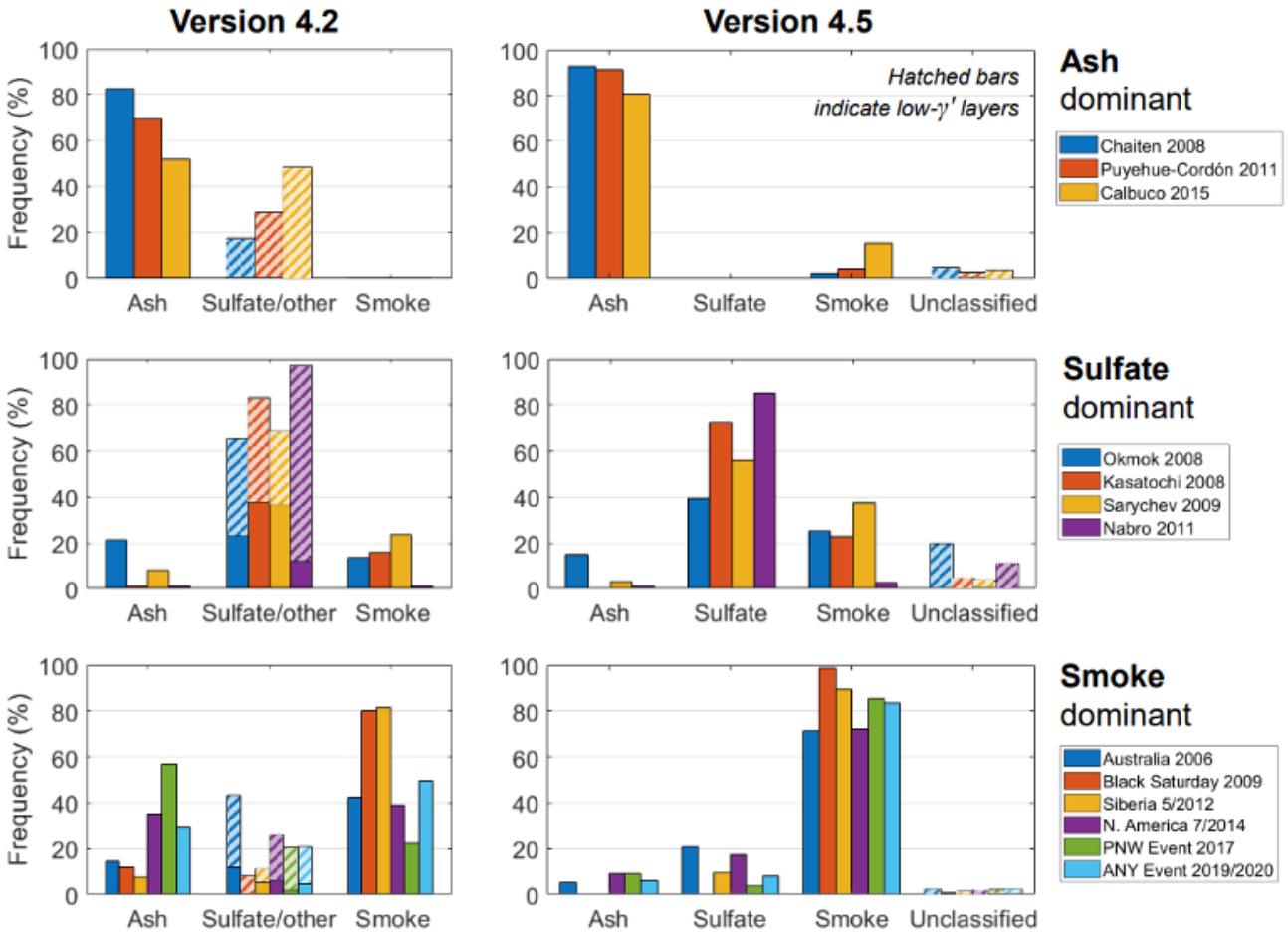

Figure 3: Stratospheric aerosol subtype classification frequency for events dominated by volcanic ash (top row), sulfate (middle row), and smoke (bottom row). V4.2 and V4.51 classifications are in the left and right columns, respectively. Taken from Tackett et al., 2023a.

Total Column Particulate Optical Depths Above Opaque Water Clouds

Hu et al., 2007 developed an approach to estimate 532nm total particulate optical depth above opaque water clouds. The 532nm layer integrated attenuated backscatter (γ′) for an opaque water cloud, assuming clear air-above, could be estimated as a function of the lidar ratio of the water cloud (S_0) and the multiple scattering factor. If there are features above, then γ′ will be reduced based on the overlaying two-way transmittance, which is a function of the optical depth (τ_{above}). Using this information an estimate of the above cloud optical depth can be inferred directly from current CALIPSO measurements, as seen in equation 1. The multiple scattering is a ratio of the layer integrated 532 nm volume depolarization ratio (δ_v), which along with γ′ are parameters that are already computed in the CALIOP L2 data products. An estimate of S_0 for opaque water clouds is assumed to be 19 sr.

$$\tau_{above} = -\frac{1}{2}\ln\left(2\left(\frac{1-\delta_v}{1+\delta_v}\right)^2 S_0\,\gamma'\right) \quad (1)$$

This new column particulate optical depth and uncertainty are detailed further in the V4.51 CALIOP Layer Level 2 data product description. These two new parameters are denoted as 'particulate', and do not differentiate between feature typing as seen in other column optical depth parameters in the CALIOP level 2 data product.

A comparison between this new approach and data collected from NASA Langley's High Spectral Resolution Lidar (HSRL-2) during a leg of the ORACLES-2 field campaign (Redemann et al., 2020) can be seen in Figure 4. This particularly scene, taken from September 18th, 2016, of a CALIPSO transit from 13:33:50 to 13:36: 52 UTC and coincident with the ER-2 over-flight, is in the south-eastern Atlantic Ocean off the coast of Africa and is characterized by an elevated smoke layer from seasonal biomass burning over a dense marine stratiform cloud layer. The 532nm aerosol optical depth derived from HSRL-2 (black triangles) compares favorably with the new depolarization ratio approach (blue circles) at 5km resolution. The particulate optical depth is also reported at 1km and 333m (single shot) resolution. Profiles of 532nm extinction reported in the Lidar Level 2 5km aerosol profile products were used to compute aerosol optical depths for this scene, using both the V4.51 (red) and V4.20 (green, previous version) data. These two optical depths do not track the depolarization approach as well, given that the profiles of extinction are for aerosol only, as determined by the level 2 typing algorithm, while the depolarization method uses the entire column. The differences between V4.20 and V4.51 aerosol optical depths, in which V4.51 is always greater than/equal to V4.21, is due to the increase in depth of layer associated with smoke base extension.

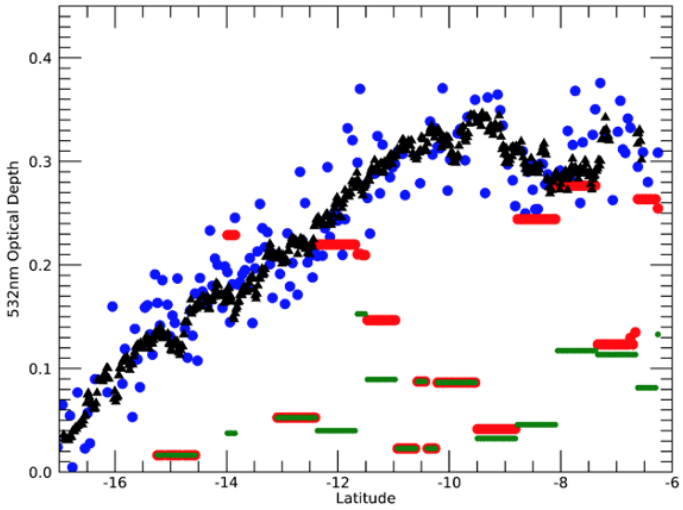

Figure 4: 532nm aerosol optical thickness above clouds from the HSRL-2 (black triangles), 532nm particulate optical depth above opaque water clouds at 5km resolution using the V4.51 Lidar Level 2 depolarization ratio technique (blue circles), and 532nm aerosol optical depth (V4.51 red circles, V4.20 green circles) computed by integration of aerosol profile extinction above opaque water clouds during CALIPSO over-flight of HSRL-2 track on September 18th, 2016, from 13:33:50 to 13:36:52 UTC in the south-east Atlantic Basin during the ORACLES-2 field campaign.

Total Column Particulate Optical Depths from Ocean Surface Returns

The Ocean Derived Column Optical Depth (ODCOD) product is an estimate of total column effective optical depth. ODCOD relates the measured magnitude of the lidar ocean surface return and the two-way transmittance overhead to a modelled ocean returned by the equation 2 below (Venkata and Reagan 2016).

$$T_p^2(z_s) = \frac{c\,A\,T_m^2(z_s)}{2\,R_\lambda} \tag{2}$$

In the relationship, $T^2(z_s)$ is the two-way transmittance at range z_s from the spacecraft where molecular/ozone and particulate components are denoted by the subscripts 'm' or 'p', respectively. Variable c is the speed of light, A is the area of the ocean surface return, and R_λ is the modelled backscatter reflectance from the ocean surface. The retrieval is for the total column, from the CALIOP top of the atmosphere calibration region to the lidar detected ocean surface. The estimate is an *effective* optical depth because no attempt is made to separate multiple scattering and single scattering from the cloud and aerosol particulates in the column (Ryan et al., 2024).

The V4.51 Lidar Level 2 algorithms only estimate 532 nm optical depths in regions of the column where clouds and aerosol are directly detected. The regions where no layers are detected are assumed to be particulate free. This assumption is known to yield an underestimate total column particulate optical depth by on the order of 0.03–0.05 (Toth et al., 2018). ODCOD compliments the CALIPSO data record by providing estimates of optical depth for the entire column including regions CALIOP does not detect particulate.

Figure 5 shows cloud screened seasonal difference of medians (ODCOD - MODIS) of the 5km ODCOD daytime retrieval to MODIS derived Effective Optical Depth Average Ocean interpolated to 532 nm and to the CALIOP 5km footprint midpoint. Generally, ODCOD shows good agreement in each season and over most of the globe with global median differences of 0.019 in December, January, and February; 0.025 in March, April, and May, 0.015 in June July and August; and 0.017 in September, October, November. Regionally, some parts of the globe see larger differences possibly due to uncertainties in wind speed and the surface reflectance model used.

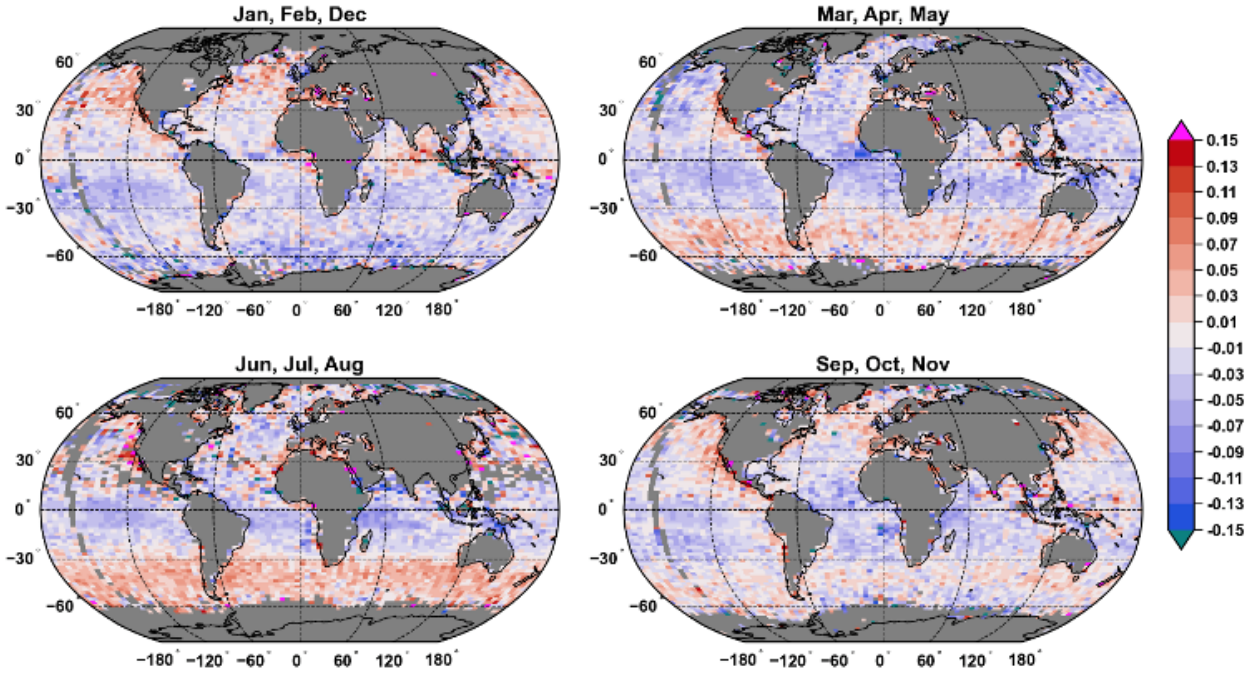

Figure 5: The four panels show cloud screened seasonal difference of medians (ODCOD - MODIS) comparisons of the 5km ODCOD daytime retrieval to MODIS derived Effective Optical Depth Average Ocean interpolated to 532 nm and to the CALIOP 5km footprint midpoint. OD ODCOD higher than MODIS is shown in red and ODCOD lower is shown in blue. Taken from Ryan et al., 2024.

Corrections to Single-Shot Cloud Clearing

An anomalous condition was identified in the CALIOP Level 2 Selective Iterated Boundary Layer (SIBYL) algorithm, in which 333m single shot clouds identified and retained in the boundary layer could inadvertently be reclassified as an aerosol. The V4.51 layer product description details the error and new approach used, in which a boundary layer scene could be broken apart and these newly defined layers reclassified based on a number of criteria.

Figure 6 illustrates this error and the resultant amelioration. In this scene a dense water cloud underlies a dust plume (Figure 6a). For a majority of this scene the V4.2 algorithm retains the 333m single shot water cloud layer, which occurs when the single shot clouds are detected throughout the entirety of each 5km block of data. The Cloud-Aerosol Discrimination (CAD; Liu et al, 2019) doesn't know that the clouds haven't been removed and reclassifies those bins as having aerosols, as seen in Figure 6b. The consequence of this error can be seen in Figure 6c, as the 532nm 'aerosol' extinction for that layer are clearly biased when compared with the overlying aerosol. When applying the corrected algorithm, the single shot layer remains as a cloud (Figure 6d) and the 532nm aerosol extinction bias has been eliminated (Figure 6e). Tackett et al, 2022 also detailed the consequence of this error, in which nearly 3% of all 5km resolution layers for June-August 2007, 2013, and 2014, clustered around regions of continental aerosol outflow (smoke or desert dust), were impacted.

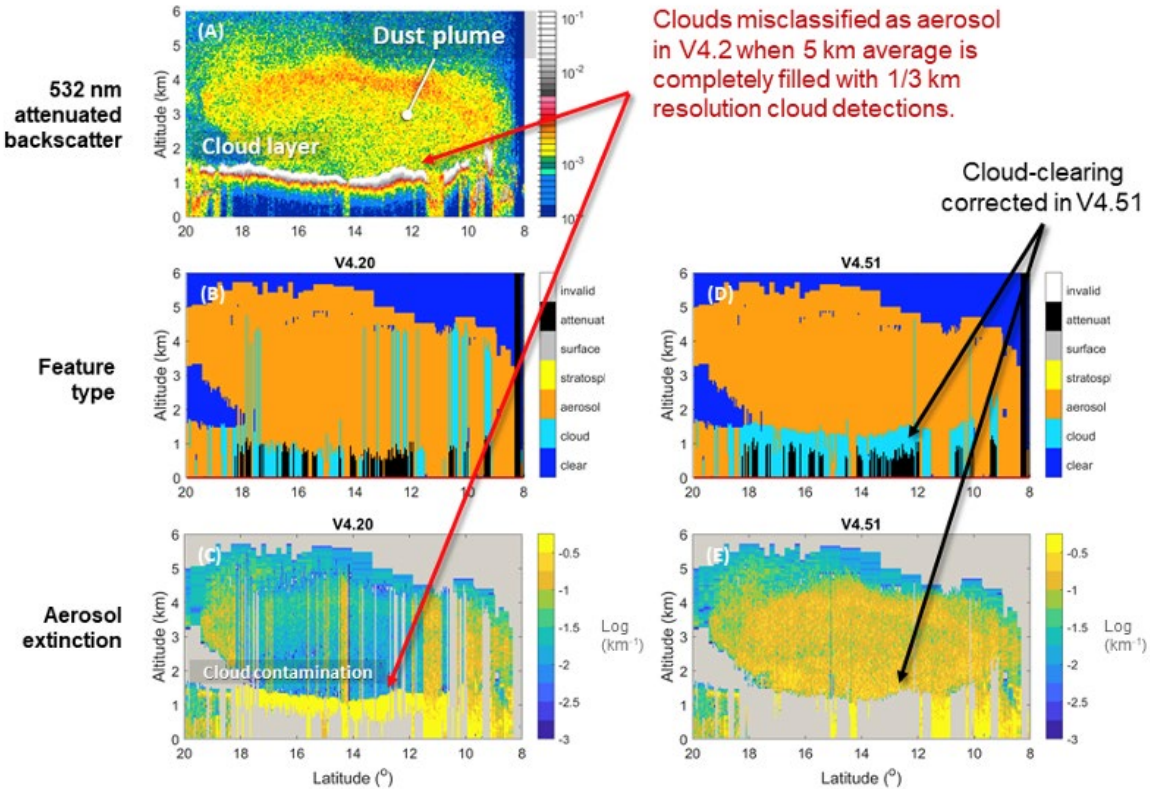

Figure 6: June 15th, 2013, scene in the eastern Atlantic Ocean between CALIOP V4.21 Level 1 and Level 2 data (a-c) and the V4.51 Level 2 data (d-e). The left most column shows the prescience of the low-level water cloud and the implications on extinction of the cloud layer being recast as an aerosol by the Cloud-Aerosol Discrimination algorithm. The right most column shows that the updated V4.51 algorithm now properly accounts for the cloud and the 532nm extinction bias has been eliminated. Taken from Tackett, 2023.

Table 1: new scientific data sets reported in the CALIOP V4.51 L2 data products

	VFM	Layer					Profile	
SDS name		**1/3kmM**	**1kmC**	**5kmA**	**5kmC**	**5kmM**	**5kmA**	**5kmC**
Surface_Wind_Speeds_02m				✓		✓	✓	✓

Data Quality Statement for CALIPSO's Version 4.21 Lidar Level 2 Data Product Release

Version: **4.21**
Data Release Date: **October 02, 2020**
Data Date Range: **October 01, 2020 to present**

A minor version bump (+0.01) has been applied to all CALIPSO data products due to a required upgrade to the operating system on the CALIPSO production cluster. All program executables were re-compiled to process in this new environment with no changes made to the underlying science algorithms or inputs.

Data Quality Statement for CALIPSO's Version 4.20 Lidar Level 2 Data Product Release

Data Version: **4.20**
Data Release Date: **October 10, 2018**
Data Date Range: **June 13, 2006 to September 30, 2020**

The Version 4.20 (V4) CALIOP Level 2 data product is identical to the V4.10 data product with the addition of several HDF science data sets (SDS) that provide information to the user for filtering out low laser energy shots. The technical advisory of this phenomena, shown below, was posted on the CALIPSO website in June of 2018.

Table 2: new scientific data sets reported in the CALIOP V4.20 L2 data products

	VFM	Layer				Profile	
SDS name		**1/3kmM**	**1kmC**	**5kmA**	**5kmC**	**5kmA**	**5kmC**
Minimum_Laser_Energy_532	✓	✓	✓	✓	✓	✓	✓

Data Release: June 12, 2018
CALIOP Instrument Anomaly Advisory: Low Energy Laser Shots
Dates Affected: September 01, 2016 – present
Applies to: CALIOP Level 1B and Level 2 Data Products, V4.10 and earlier

CALIOP (CALIPSO's LIDAR instrument) is experiencing an elevated frequency of low energy laser shots within the South Atlantic Anomaly (SAA) region due to decreased pressure inside the laser canister. The low energy laser shots began in September 2016 and have increased in frequency, particularly since the second half of 2017 (Fig. 1). Science quality of affected profiles within the SAA is degraded and these profiles should be excluded from scientific analyses. The document below provides guidance on how to identify affected profiles in CALIOP level 1B and level 2 products. Science quality of profiles with nominal laser energies is unaffected by this issue. The IIR (Imaging Infrared Radiometer) and the WFC (Wide Field Camera) instruments are also unaffected.

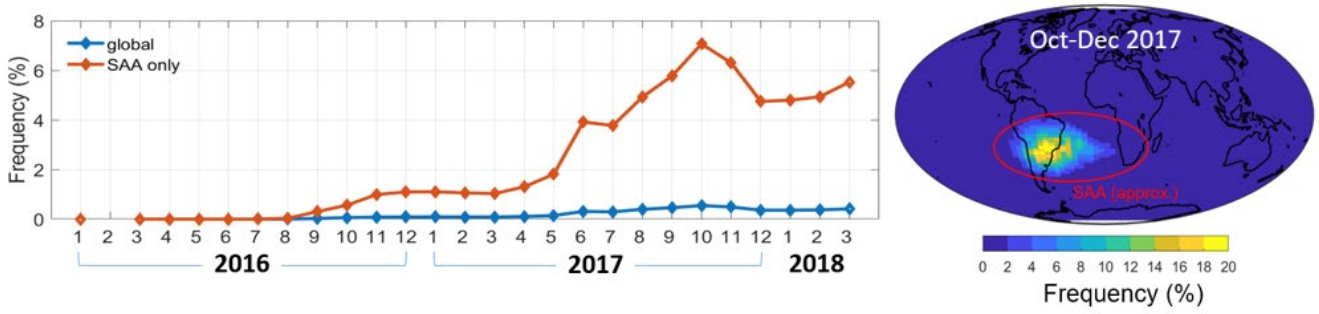

Figure 1 Monthly frequency of low energy laser shots (E_{532} < 80 mJ) from January 2016 to March 2018, globally and in the SAA region (left). Spatial distribution of low energy shot frequency from October to December 2017 (right).

Data Quality Statement for CALIPSO's Version 4.10 Lidar Level 2 Data Product Release

Data Version: **4.10**
Data Release Date: **November 8, 2016**
Data Date Range: **June 13, 2006 to May 31, 2018**

Version 4.10 (V4) is the first wholly new release of the CALIPSO lidar level 2 data products since the initial release of the Version 3 (V3) series of products in May 2010. As expected, V4.10 provides a substantial advance over V3 and earlier releases; known retrieval artifacts have been eliminated and numerous enhancements have been incorporated to increase the accuracy of the science data while simultaneously reducing uncertainties. The most significant code, algorithm, and data product changes include

- a stand-alone surface detection algorithm
- revised probability density functions (PDFs) for the cloud aerosol discrimination (CAD) algorithm
- application of the CAD algorithm to layers detected at single shot resolution and to layers detected in the stratosphere
- a major overhaul of the aerosol subtyping algorithms in which separate algorithms are now used to classify tropospheric and stratospheric aerosols
- improved cloud subtyping and ice-water phase determination
- temperature-dependent determination of multiple scattering factors for ice clouds
- multiple scattering factors for opaque water clouds derived from measured depolarization ratios
- updated extinction retrievals for opaque layers; improved uncertainty estimates and more in-depth quality assurance reporting for all extinction retrievals
- a new algorithm for deriving ice-water content from CALIOP extinction retrievals
- introduction of a new 5-km merged layer product that reports the spatial and optical properties of all cloud and aerosol layers detected in a single file
- new browses image showing cloud subtypes identified within each granule
- the addition of several new parameters in the data products files

Each of these is discussed in some detail in the sections below.

Lidar Surface Detection

In previous versions of the CALIOP level 2 (L2) data products, the altitude of the Earth's surface was determined using a general purpose layer detection scheme that scans lidar profiles from the top of the atmosphere downward, looking for significant positive excursions rising above an expected molecular backscatter signal. In general, this approach works well. However, in multi-layer scenes and/or highly turbid atmospheres the effectiveness of the top-down technique can be degraded by signal attenuation from intervening atmospheric layers that limit its ability to reliably detect surface returns. In the V4.10 data products, detection of the Earth's surface is accomplished using a dedicated, newly developed search routine that scans upward from the bottom of the profile using a derivative-based peak finding algorithm. This new technique demonstrates significant improvement over the V3 method in turbid atmospheres, while maintaining equal or better performance in clear skies. As a result of this improved detection scheme, there are fewer opaque layers identified in the V4.10 data than there were in V3, especially at night. Because regions below layers previously classified as opaque are now scanned for the presence of atmospheric features, there is also a slight increase in the number of cloud and aerosol layers reported. Signal strengths in these 'not previously scanned' regions tend to be quite low, and thus many of these newly detect layers will have low CAD scores.

The V4.10 data products report substantially more surface detection information than was available in V3. The Lidar_Surface_Elevation and Surface_Elevation_Detection_Frequency parameters reported in the V3 data products have been discontinued in V4.10. Instead, surface detection information is recorded in a multi-parameter Lidar_Surface_Detection Vgroup. In addition to the surface detection status (i.e., detected or not detected) and

surface altitude information provided in V3, this new Vgroup reports the following parameters at both 532 nm and 1064 nm.

- surface top and base altitudes
- integrated attenuated backscatter
- integrated volume depolarization ratio
- integrated attenuated backscatter color ratio
- where applicable, surface detections at finer spatial resolutions (i.e., 1/3 km and 1 km)

These additional parameters are expected to provide new insights into surface type (e.g., distinguishing between ice, liquid water and land) and, for measurements over oceans, total column optical depths at both 532 nm and 1064 nm.

Cloud and Aerosol Layer Detection

The CALIOP V4.10 level 1 (L1) data, first released in April 2014, significantly improved the calibration of the CALIOP attenuated backscatter coefficients at 532 nm (Kar et al., 2018; Getzewich et al., 2018) and especially at 1064 nm (Vaughan et al., 2019). In particular, the magnitude of the calibration coefficients at 532 nm decreased by ~3% to ~8%, depending on latitude and season, resulting in the concomitant increase in the 532 nm attenuated backscatter coefficients. This increase in backscatter magnitude translates directly into a slightly greater layer detection frequency. When combined with the layer detection increases obtained from the new surface detection algorithm, the V4.10 data products show a net cloud fraction gain of ~5% relative to V3.

Cloud Aerosol Discrimination (CAD)

The magnitude of the calibration changes introduced in the CALIOP V4.10 L1 data necessitated substantial revisions to the V3 level 2 (L2) CAD algorithm. Accordingly, a new set of CAD probability distribution functions (PDFs) was developed and subsequently used to generate the V4.10 L2 data. The V4.10 CAD PDFs are still 5-dimensional, but now have increased latitude resolution (5° intervals vs. 10° in V3) which has led to an overall improvement in CAD reliability. The revised PDFs were specifically designed to be more sensitive to the presence of lofted aerosols. As a consequence, the V4.10 data products show significant improvements in the classification of high-altitude smoke plumes and Asian dust layers, which in earlier versions were often classified as cirrus clouds.

Application of the V4.10 CAD algorithm differs from previous versions in these important aspects:

1. In V3 and earlier, the CAD algorithm was applied only to tropospheric layers, and layers detected above the tropopause were classified as “stratospheric” features. In V4.10 the “stratospheric” feature type has been eliminated. Instead, the CAD algorithm is applied everywhere, to all layers detected. The CAD scores for stratospheric clouds and aerosols are generally robust within a few kilometers of the tropopause. However, at very high altitudes, the general paucity of samples available for the training set as well as falling SNR may affect the reliability of the CAD.

   For in-depth scientific analyses of polar stratospheric clouds (PSCs), users are strongly advised to use CALIPSO’s dedicated PSC products. For less demanding applications, PSCs are also reported in the standard L2 data products. While the V4.10 CAD algorithm classifies the majority of the polar stratospheric layers as clouds, some aerosol layers are also identified. The spatial distribution of these polar stratospheric aerosol layers is similar to the distribution of STS (i.e., the supercooled ternary solution of nitric acid, sulfuric acid and water) obtained from the dedicated CALIPSO PSC product.

2. Unlike V3, the V4.10 CAD algorithm is also applied to those strongly scattering layers that can be detected at single shot resolution (333 m). In the past these layers were classified as clouds by default and were systematically removed before averaging over the weaker signals. In V4.10, layers detected at single shot resolution that are classified as aerosols are no longer removed from coarser resolution averages, and thus can be expected to increase peak aerosol optical depths in the regions where they occur. The bulk of the single shot layers classified as aerosols in V4.10 are found within the dust belt region of the globe. However, it should

be noted that optical properties of these layers were not used in building the V4.10 CAD PDFs, which may affect the overall CAD performance when classifying single shot layers.

While the CAD algorithm is applied to all layers detected, there are two anomalous situations where layers are subsequently reclassified using additional analysis. The first occurs when dense smoke plumes extend over stratus decks and other water clouds. The differential attenuation of the signals at 1064 nm and 532 nm by the smoke can lead to very high color ratios in the clouds below, which in turn can result in artificially low CAD scores. In such cases, the color ratio of the underlying clouds is reset to an empirically derived mean value and the CAD scores are recalculated. Both the original CAD score and the revised CAD score are recorded in the layer products. In the second case, the similarity of the scattering signatures of faint, isolated layers of lofted dust and weakly depolarizing cloud fragments makes them largely indistinguishable in the CAD domain. To achieve reliable separation, a sequence of spatial proximity tests is applied to identify those layers which may in fact be "fringes" of previously identified large scale ice clouds. Layers identified as "cirrus fringes" are assigned a special CAD score of 106.

Figure 1 shows the pattern of changes in CAD scores from V3 to V4.10. Most of the high confidence samples in V3 are also classified as the same type (cloud or aerosol) in V4.10 with similar high confidence. However, as seen in the lower right quadrant of Figure 1, a small fraction of layers classified as clouds in V3 are classified as aerosols in V4.10. Some of these have optical properties that fall in the grey zone between aerosols and clouds and may actually be misclassified clouds. These cases occur most often over the polar regions. Because they typically have low CAD scores, they can be identified and removed at the users' discretion.

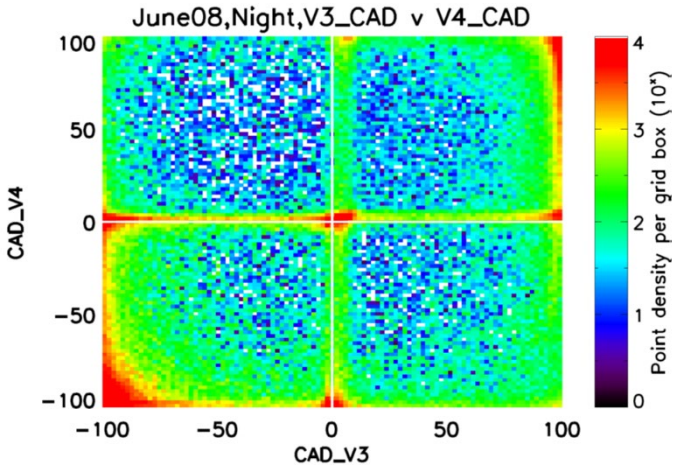

Figure 1: Comparison of CAD scores of the same samples between V3.30 and V4.10 using the L2 profile products.

After acquisition and analysis of over 10 years of space-based lidar data, the CALIPSO team has gained a much improved understanding of the physical and optical properties of the different types of aerosols and clouds that occur in different altitude regimes. As a result, the V4.10 PDFS are more representative and more physically realistic than earlier versions, in which the occurrence frequency of aerosols at higher altitudes was noticeably underestimated. One result of modifying the PDFs to achieve more accurate aerosol identification is an across the board decrease in the magnitude of the CAD scores reported in V4.10; i.e., the mean magnitude of CAD scores for all aerosols detected in V4.10 is lower than the mean magnitude in V3. Likewise, the mean magnitude of the cloud CAD scores is lower in V4.10 than in V3. In retrospect, the higher CAD scores in V3 should be seen as overly optimistic; the slightly lower V4.10 scores now provide a more realistic assessment of CAD classification confidence.

Aerosol Subtyping Changes

Several improvements to aerosol subtyping have been implemented in V4.10. The most fundamental change is that aerosol layers are now classified as either tropospheric aerosol or stratospheric aerosol feature types, depending on the location of the attenuated backscatter centroid relative to the MERRA2 reanalysis tropopause height. In previous versions, aerosol was only identified below the tropopause. Given that the CAD algorithm is applied at all altitudes in V4.10, aerosol layers detected above the tropopause are classified as stratospheric

aerosols and are assigned subtypes commonly found in the stratosphere. Figure 2 compares distributions of tropospheric aerosol subtypes between V3 and V4.10.

Tropospheric aerosol subtyping improvements

1. A new "dusty marine" aerosol subtype has been added. Dusty marine layers are mixtures of dust and marine aerosol identified as moderately depolarizing aerosol layers having base altitudes within the marine boundary layer (assumed to be at 2.5 km). In previous versions these layers would have been classified as polluted dust. The dusty marine lidar ratio is more representative of a dust/marine aerosol mixture and its characteristic lidar ratio is ~33% smaller than that of polluted dust. The geographic distribution of dusty marine layers agrees well with known locations of dust subsidence into the marine boundary layer, though some ambiguity occurs in regions where anthropogenic pollution, dust, and marine aerosol co-exist. These layers are classified as dusty marine, yet it is not always clear whether they should be typed instead as polluted dust.
2. Smoke layer identification and nomenclature has been revised. As in previous versions, elevated non-depolarizing aerosols are assumed to be smoke which is injected above the planetary boundary layer (PBL) due to combustion-induced buoyancy. The definition for "elevated" is revised in V4.10 to mean layers with tops higher than 2.5 km above ground level (i.e., a simple PBL approximation). For clarity, the nomenclature for the smoke aerosol subtype is changed to "elevated smoke". Owing to the revised "elevated" definition and the introduction of a new algorithm to vertically homogenize aerosol subtyping for weakly scattering fringes detected at the base of extended plumes, elevated smoke layers which were misclassified as marine aerosol in V3 are now correctly classified as elevated smoke.
3. Within the PBL, it is difficult to discriminate smoke due to biomass burning from polluted continental aerosol arising from anthropogenic pollution using CALIOP measurements. Therefore, the description of the polluted continental subtype is revised to "polluted continental/smoke" to clarify that either aerosol type could be present.
4. In previous versions, aerosol detected over snow, ice, or tundra were subtyped as either clean continental or polluted continental. Given that transport pathways exist for smoke, dust and other aerosol types to reach the Arctic, this condition has been removed in V4.10 and all species are allowed. Users are cautioned to treat aerosol detected over Antarctica carefully and to exercise prudence when interpreting aerosol subtyping in this region. Often aerosol layers in the Antarctic are classified as dust or polluted dust due to their elevated depolarization. Despite that transport pathways do exist for dust to reach Antarctica (from Patagonia for example), data users are cautioned that layers classified as aerosol may actually be misclassified clouds or blowing snow rather than true dust.
5. Calculation of the particulate depolarization ratio estimates using in the aerosol subtyping scheme now correctly accounts for signal attenuation due to overlying layers. Making this change greatly reduces the over-abundance of polluted dust in identified in V3.
6. Tropospheric aerosol lidar ratios and lidar ratio uncertainties have been updated for the marine, dust, clean continental, and elevated smoke subtypes to reflect the current state of knowledge based on observations by NASA Langley Airborne High Spectral Resolution Lidar, EARLINET, AERONET, CALIPSO and synergistic multi-sensor retrievals.

Stratospheric aerosol subtypes introduced

Stratospheric aerosol subtypes have been introduced in V4.10 for ash, sulfate/other, smoke and polar stratospheric aerosol. The V4.10 stratospheric aerosol subtyping algorithm performs well at identifying volcanic ash and sulfate above the tropopause based on manual verification. Note that below the tropopause, ash and sulfate plumes are given tropospheric aerosol subtypes: volcanic ash is often classified as dust or polluted dust and volcanic sulfate is often classified as elevated smoke. As a result, contiguous aerosol features crossing the tropopause will have aerosol subtypes which switch from tropospheric to stratospheric subtypes, depending on the relationship between the attenuated backscatter centroid altitude of the layer identified by the feature finder and the tropopause altitude. Weakly scattering stratospheric aerosol layers which are not classified as polar stratospheric

aerosol are classified as “sulfate/other”. Therefore, layers that are, in fact, ash and/or smoke could be misclassified as “sulfate/other” if they are weakly scattering (layer integrated attenuated backscatter less than 0.001 sr^{-1}).

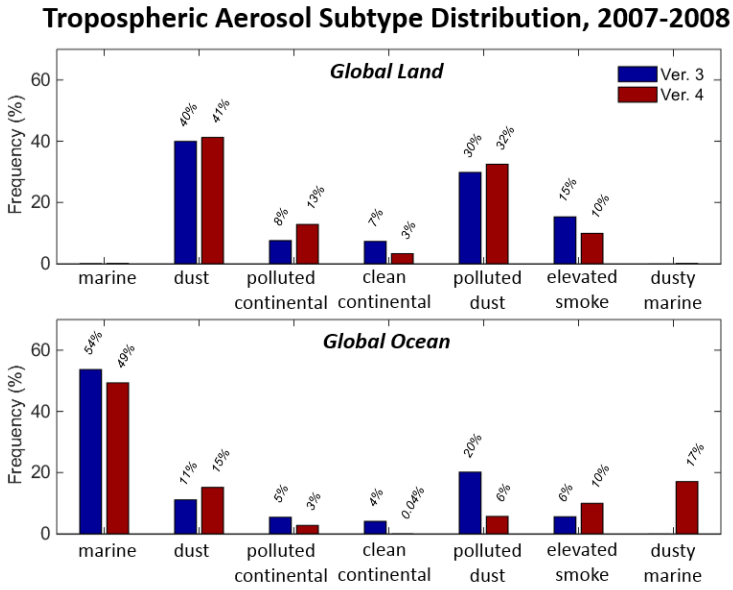

Figure 2: Comparison of global tropospheric aerosol subtype distributions between V3 and V4.10 for 2007-2008, day and night. Over land, elevated smoke is reduced in favor of polluted continental/smoke as a consequence of revised “elevated” definition. Over ocean, dusty marine replaces a substantial portion of polluted dust classifications.

Cloud Subtyping Changes

The CALIPSO cloud subtyping algorithm uses cloud top pressure, cloud opacity and cloud fraction to identify eight cloud types. A bug in the V3 analysis code caused a systematic underestimate of all categories of opaque clouds; in fact, no low overcast opaque clouds were reported in any of the V3 data products. As seen in Figure 3, this defect has been remedied in V4.10, and thus, relative to V3, the V4.10 data products show a large increase in the fraction of low opaque cloud types and a corresponding decrease in the fraction of low transparent clouds.

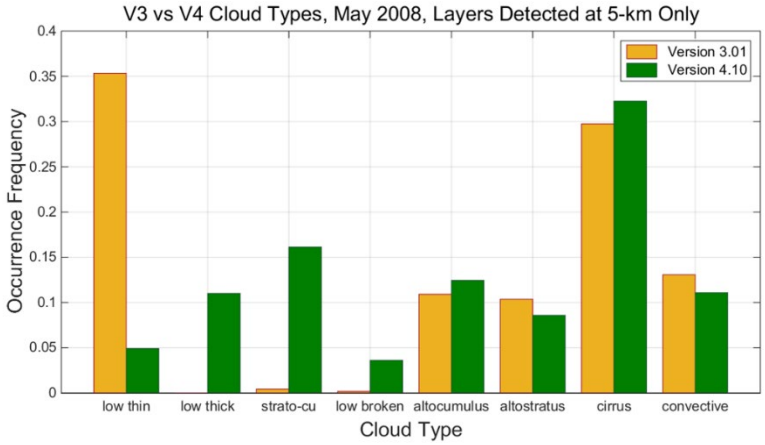

Figure 3: distribution of cloud subtypes in V3 (orange) and V4.10 (green) for all layers detected at a 5-km horizontal averaging resolution during May 2008

Cloud Ice-Water Phase Discrimination Changes

Layers identified as clouds by the CAD algorithm are further classified according to thermodynamic phase as either water, randomly oriented ice (ROI), horizontally oriented ice (HOI) or unknown phase. The phase algorithm

primarily uses an objective sorting algorithm based on the clustering of relationships between the layer-integrated attenuated backscatter (IAB) and the layer-averaged depolarization. This technique relies on fundamental CALIOP L1 measurements, and in V4.10 confidently identifies the thermodynamic phase (ice vs. water) of at least 75% (nadir pointing) and 85% (tilted) of cloud layers, globally.

On November 28, 2007, the initial CALIOP viewing angle of 0.3° (nadir) was permanently changed to 3° (tilted), to repress specular reflections from hexagonal plates. These plates, with crystal faces perpendicular to the CALIOP laser beam, cause specular reflections which can be identified in nadir viewing data by abnormally large integrated attenuated backscatter with essentially zero depolarization. The V3 phase algorithm included a scheme for recognizing HOI that identified numerous instances of these ice clouds. However, in-depth comparisons of the V3 nadir and tilted data determined that very few true specular reflections were occurring in the tilted data, and so HOI testing of ice clouds initially identified as ROI was eliminated. In the V4.10 phase algorithm only water clouds observed in the nadir view are tested. Clouds that mainly consist of ROI may also have water or HOI occurring at warmer temperatures at the bottom of the layer, and these are now identified by the dominant cloud particle phase, which is ROI. Additional details about the change of off-nadir angle from 0.3° to 3.0° are given in Appendix 1 at the end of this document. Table 1 characterizes V3 to V4.10 changes in the volume of cloud phases globally, for both nadir and tilted viewing angles.

Table 1: Cloud volume occurrence frequency (5 km x 60 m bins) in percent; nadir statistics computed using all data from January through November 2007 (excluding off-nadir tests); tilted statistics computed using all data from January through November 2008 (MC = mid-confidence).

Cloud Phase	Phase Flag	Confidence Flag	V3 Nadir (0.3°)	V4.10 Nadir (0.3°)	V3 Tilted (3.0°)	V4.10 Tilted (3.0°)
ROI	1	3	48	53	64	67
Water	2	3	18	20	18	19
HOI	3	3	6	5	< 1	< 1
Unknown	0	0	9	13	6	10
Fringe	1	0	N/A	3	N/A	3
MC-HOI	3	2	17	5	10	N/A
MC-ROI	1	2	3	< 1	< 1	< 1

A non-zero, but negligible, amount of low- and mid-confidence water layers are also identified at each viewing angle. As these phase classifications account for less than 1% of all cloud bins, they are not shown in this table.

In V4.10, between 65-70% of the range bins identified as atmospheric features by CALIOP are classified as clouds. The population of water clouds identified at horizontal averages of 5 km or more remains very stable between V3 and V4.10, at about 18%. The ROI population is larger in tilted data than in nadir data and is 10-15% larger in V4.10 than in V3. The additional V4.10 ROI bins were mainly classified as clear air, mid-confidence HOI or stratospheric features in V3. Unknown phase clouds increase in V4.10 due to generally lower CAD scores and the detection of more thin cloud layers with weak backscatter and depolarization signals. The reduction in V4.10 HOI is due to the elimination of a spatial coherence test in the phase algorithm. About 3% of the cloud population in V4.10 are identified as “cirrus fringes”. Since the composition of cloud populations varies regionally and seasonally, these numbers should be used only for guidance in understanding the changes between V3 and V4.10.

Lidar Ratios and Multiple Scattering Factors for Ice Clouds

In V3 and earlier, ice clouds were assigned a constant multiple scattering factor of $\eta_{532} = 0.6$. In V4.10, the multiple scattering factor is instead implemented as a sigmoid approximation function of the layer attenuated backscatter centroid temperature, with η_{532} increasing from 0.46 at 270 K to 0.76 at 190 K.

This approximation function was derived from extensive analysis of collocated measurements acquired by the CALIPSO lidar and the CALIPSO IIR, which reconciled observed and theoretical ratios of 532 nm optical depths

derived from V3 CALIOP measured two-way transmittances to the absorption optical depth retrieved from IIR measurements at 12.05 μm. The theoretical ratios are computed assuming severely roughened aggregated columns.

In V3 and earlier, ice cloud extinction retrievals that could not be constrained by the direct measurement of the two-way transmittance (i.e., "unconstrained" retrievals) were assigned an initial default lidar ratio of 25 sr. For semi-transparent clouds, comparisons with IIR absorption optical depth at 12.05 μm and a radiative closure experiment using MODIS 11 μm radiances both showed, on average, quite good agreement with V3 CALIOP constrained retrievals, but substantially worse agreement with unconstrained retrievals, thus demonstrating that the initial default lidar ratio was generally too small.

To ensure full consistency between unconstrained and constrained retrievals in semi-transparent clouds, initial ice cloud lidar ratios in V4.10 are derived from the statistical analysis of several years of constrained retrievals, using only those clouds identified as high-confidence randomly oriented ice. Like the multiple scattering factor, the V4.10 initial ice cloud lidar ratio is estimated using a sigmoid approximation function based on the layer attenuated backscatter centroid temperature. Default lidar ratio values decrease from ~35 sr to ~20 sr as the cloud centroid temperature decreases. This initial lidar ratio is only used for semi-transparent ice clouds when constrained retrievals are not possible. For opaque clouds and constrained retrievals of semi-transparent clouds, the extinction retrievals are initialized using a lidar ratio derived directly from the CALIOP L1 measurements and the temperature-dependent multiple scattering factor.

Multiple Scattering Factors for Water Clouds

In V3 and earlier, all water clouds were assigned a constant multiple scattering factor of $\eta_{532} = 0.6$. In V4.10, η_{532} for transparent water clouds remains fixed at 0.6. For opaque layers, however, layer-effective water cloud multiple scattering factors are computed from the measured layer integrated volume depolarization ratios. As a consequence, under the appropriate conditions (e.g., single layer clouds in otherwise clear skies), estimates of water cloud lidar ratios can now be obtained from the multiple scattering factors and the 532 nm layer integrated attenuated backscatter estimates.

Extinction and Optical Depths

The particulate backscatter and extinction profiles and layer optical depths reported in the CALIOP V4.10 data products are produced by a modified and substantially enhanced version of the hybrid extinction retrieval algorithm used in earlier releases. Several developments are particularly noteworthy.

- Analysis of Opaque Layers

  The extinction retrieval used for opaque layers is entirely different. In V3 and earlier, the lidar ratios used for opaque layers were assigned by the scene classification algorithms based on layer type (i.e., cloud vs. aerosol) and subtype (e.g., ice vs. water, dust vs. smoke, etc.). In V4.10, initial estimates of the lidar ratios for opaque layers are computed directly from the measured integrated attenuated backscatter, and refined as necessary within the extinction solver to ensure that extinction coefficients are calculated through the full vertical extent of the layer. This procedure yields highly precise and accurate layer-effective lidar ratios, which translate directly into more realistic extinction coefficient estimates and eliminate many artifacts previously seen in CALIOP optical depth distributions.

- Increased Number of Constrained Retrievals

  Constrained retrievals use measurements of clear air above and below a lofted layer to directly estimate layer optical depth. These optical depths provide a constraint on the solution of the lidar equation, allowing the layer lidar ratio to be retrieved from the data rather than estimated a priori. In retrospect, the approach used in V3 and earlier was perhaps too timid, in that constrained solutions were only attempted for lofted layers with optical depths greater than ~0.3. In V4.10 constrained solutions (and hence lidar ratio estimates) are derived for all layers having valid two-way transmittance measurements. Uncertainties in the lidar ratio estimates are

now reported for all retrievals. While lidar ratios derived from layers with small optical depths can have large random uncertainties, the extinction retrievals are unbiased.

- More Precise Reporting of Retrieval Success

  For each extinction profile retrieved, information about the termination state of the extinction algorithm is provided in the extinction QC flags. These flags are implemented as 16-bit unsigned integers. Multiple bits can be toggled within each extinction QC flag, with each bit conveying a specific piece of information. In V3, 10 of the 16 bits were used. The V4.10 algorithm uses 14 bits and is both more verbose and more rigorous in its assessment of retrieval quality. As a consequence, users will encounter many more distinct QC flags in V4.10 than in V3. For example, for all data collected in 2008 V3 reported only 19 different extinction QC flags at 532 nm. By contrast, V4.10 is expected to report in the neighborhood of 75 different values for the same time period. The most reliable retrievals have extinction QC flags of 0, 1, 2, 16 or 18. Data flagged with other values should be treated with varying degrees of suspicion. In aberrant cases, the extinction retrieval can fail. The backscatter and extinction coefficients reported for these failed retrievals are set to a fill value of -333.

- Improved Estimates of Extinction Uncertainties

  During the V4.10 development, considerable attention was given to providing more accurate estimates of the uncertainties reported for the CALIOP extinction coefficients and optical depths. In particular, V4.10 lidar ratio uncertainty estimates are now verified and adjusted as appropriate on a layer-by-layer basis. In the V3 processing these uncertainty estimates were always specified a priori and never varied thereafter.

  While layer-effective multiple scattering factors for opaque water clouds can be reliably estimated, the known range dependence of water cloud multiple scattering is not accounted for in the V4.10 CALIOP retrieval algorithm. Furthermore, the V4.10 extinction retrieval does not attempt to compensate for the loss of ranging information introduced by pulse stretching. As a result, beyond the first range bin (and frequently within the first range bin) the V4.10 CALIOP extinction retrievals in opaque water clouds should be considered entirely unreliable. To reinforce this notion, the uncertainties for opaque water clouds are not calculated, but instead are assigned a uniform fill value of -29.

- Summary of Extinction Changes from V3 to V4.10

  The changes described above will have considerable impact on the magnitude of the V4.10 backscatter and extinction coefficients, their attendant uncertainties, and in those parameters subsequently derived from these values. However, it is critically important for data users to understand that the extinction and optical depth changes from V3 to V4.10 cannot be attributed wholly to changes in the extinction algorithm. Changes in the a priori specifications of layer multiple scattering factors and/or layer lidar ratios can by themselves introduce considerable changes in the retrieved values of extinction and optical depth. Similarly, changes in the calibration coefficients from V3 to V4.10 result in small increases in the L1 attenuated backscatter coefficients, which in turn yield concomitant but nonlinear increases in particulate backscatter and extinction coefficients.

Revised Ice-Water Content Algorithm

Cloud ice water content (IWC) is reported for all ice clouds detected by CALIOP. As in V3, IWC is a provisional data product calculated as a parameterized function of the CALIOP 532 nm extinction coefficients retrieved within ice clouds. In V4.10, the parameterization has been modified to include a temperature-dependent particle size relationship that approximates the observations compiled in an expanded set of aircraft microphysical data. Due to the cumulative impact of multiple factors, including the new ice mass parameterization and improved V4.10 calibration and extinction coefficient retrievals, users can expect V4.10 IWC to be significantly larger than V3 IWC; e.g., up to 6-8 times as large for thick ice clouds at warm temperatures. At cold temperatures, the V4.10 IWC calculated for a given extinction coefficient is smaller than in V3. However, since the extinction coefficients are larger in V4.10, the resulting change in IWC from V3 to V4.10 is relatively small.

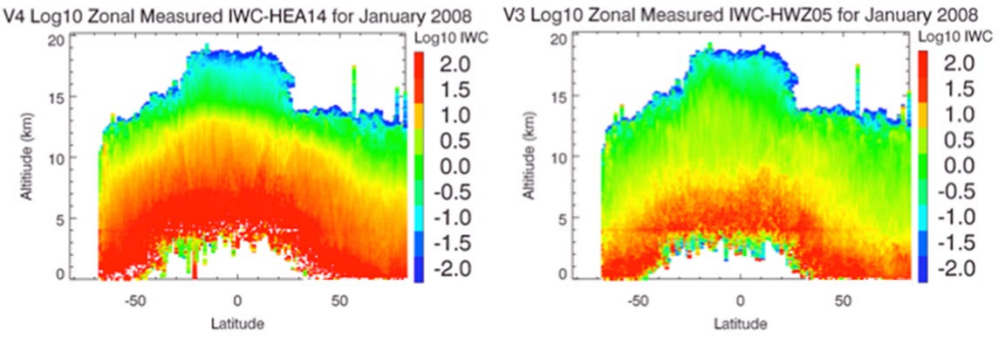

Figure 4: zonal mean IWC for January 2008 calculated from V4.10 data (left panel) and V3.01 data (right panel).

CALIOP IWC is a highly derived data product. Besides the cloud particle area-to-mass parameterization, it relies on cloud feature determination (CAD), cloud phase determination, specification of lidar ratios and multiple scattering factors and the ensuing extinction retrieval. Uncertainty in cloud ice water content is affected by the accuracy of the microphysical parameterization. However, the IWC uncertainty reported in the CALIOP data products reflects only the uncertainty in the extinction coefficient retrieval. Because IWC is parameterized from ice particle extinction, it follows that data screening criteria for valid IWC should be similar to those used to identify valid extinction coefficients. Best results will likely be obtained by using only those data with high CAD scores that have also been classified as ice with high confidence.

New Data Product: 5-km Merged Layer Product

In response to numerous end-user requests, the V4.10 data release includes a new 5-km merged layer product that aggregates all of the information found in the existing 5-km cloud layer product and 5-km aerosol layer product and packages it into a single file. The 5-km merged layer product also contains a comprehensive subset of the data reported in the single shot layer product (as do the V4.10 5-km cloud and aerosol layer products), so that unambiguous cloud clearing information will always be immediately available. This new product offers several advantages to users of the CALIPSO layer products. In particular, (a) the spatial relationships between clouds and aerosols detected at varying averaging resolution in any column are fully specified and (b) the optical influences between layers of different types (e.g., the uncertainties in cloud optical depth retrievals for cirrus clouds lying above aerosol layers) can be readily appreciated and fully characterized. A complete specification of all parameters included in the 5-km merged layer product is given in the latest release of the CALIPSO Data Products Catalog.

Browse Image Improvements

The CALIOP browse images have been augmented in the V4.10 release with new plots showing the cloud subtypes identified within each granule. The aerosol subtyping plots have been updated to reflect changes in aerosol subtyping and the addition of the stratospheric aerosol subtypes.

New Version 4.10 Data File Parameters

Table 2 lists all new parameters that have been added to the V4.10 data products. Of particular note is the inclusion of single shot layer detection information in all 5-km layer products.

Table 2: new scientific data sets reported in the CALIOP V4.10 L2 data products

	VFM	Layer				Profile	
SDS name		**1/3kmM**	**1kmC**	**5kmA**	**5kmC**	**5kmA**	**5kmC**
Lidar Surface Detection (Vgroup)		✓	✓	✓	✓	✓	✓
Single Shot Detection (Vgroup)	✓			✓	✓		
Profile ID	✓					✓	✓
CAD Score		✓					
“Was Cleared” Flag		✓					
Opacity Flag		✓	✓				

	VFM	Layer				Profile	
SDS name		1/3kmM	1kmC	5kmA	5kmC	5kmA	5kmC
Layer Centroid Temperature		✓	✓		✓		
Initial CAD Score		✓	✓		✓		
Attenuated Scattering Ratio Statistics, 532 nm		✓	✓	✓	✓		
High Resolution Layers Cleared				✓	✓		
Final Lidar Ratio Uncertainty, 532 nm				✓	✓		
Final Lidar Ratio Uncertainty, 1064 nm					✓		
Ozone Number Density						✓	✓
IGBP Surface Type						✓	✓

Data Quality Statement for CALIPSO's Version 3.41 Lidar Level 2 Data Product Release

Data Version: **3.41**
Data Release Date: **October 02, 2020**
Data Date Range: **October 01, 2020 to present**

Version 3.41 marks a change in the data products due to a required upgrade of the operating system on the cluster computer used to generate CALIPSO's publicly distributed data products. All program executables were re-compiled to process in this new environment with no changes made to the underlying science algorithms or inputs.

Data Quality Statement for CALIPSO's Version 3.40 Lidar Level 2 Data Product Release

Data Version: **3.40**
Data Release Date: **December 14, 2016**
Data Date Range: **December 01, 2016 to September 30, 2020**

Version 3.40 release reflects an update of the Forward Processing – Instrument Teams (FP-IT) meteorological data provided by the Global Modeling and Assimilation Office (GMAO) from version 5.9.1 to version 5.12.4. No changes were made to the program executables.

Data Quality Statement for CALIPSO's Version 3.30 Lidar Level 2 Data Product Release

Data Version: **3.30**
Data Release Date: **April 19, 2013**
Data Date Range: **March 1, 2013 to November 30, 2016**

Version 3.30 data products incorporate new versions of two important ancillary data products: (1) updated GMAO FP-IT meteorological data and (2) the enhanced Air Force Weather Authority (AFWA) snow and ice data set as ancillary inputs. Based on comparisons of CALIOP V3.02 data to the newly generated CALIOP V3.30 products, the transition to the new GEOS-5 FP-IT data is predicted to have only minimal effects on the science data products. Production of the V3.30 data set began with March 1, 2013.

Layer Detection

GEOS-5 molecular number densities increased in the CALIOP night and day calibration regions, which lowered the calibration coefficients and increased the attenuated backscatter coefficients, which in turn caused the number of layers detected to increase slightly. A two month of V3.02 to V3.30 showed that the number of aerosol and cloud layers increased by < 0.8% and < 0.2%, respectively.

Layer Classification

The GEOS-5 tropopause heights decreased by ~1 km between 30°S and 40°N. Since CALIOP classifies layers detected above the tropopause as stratospheric features, 3%–5% of the features formerly classified as stratospheric were reclassified as either cloud or aerosol. Over Antarctic in September 2011, tropopause heights decreased between 1.0 km and 1.5 km, causing all of cloud and aerosol layers with bases above the revised tropopause heights to be reclassified as stratospheric features. This effect may occur seasonally over Antarctica.

Data Quality Statement for CALIPSO's Version 3.02 Lidar Level 2 Data Product Release

Data Version: **3.02**
Data Release Date: **December 12, 2011**
Data Date Range: **November 1, 2011 to February 28, 2013**

Version 3.02 represents a transition of the Lidar, IIR, and WFC science data processing and browse image production to a new cluster computing system. No algorithm changes were introduced, and only very minor changes were observed between V3.01 and V3.02 as a result of the compiler and computer architecture differences.

Data Quality Statement for CALIPSO's Version 3.01 Lidar Level 2 Data Product Release

Data Version: **3.01**
Data Release Date: **April 28, 2010**
Data Date Range: **June 13, 2006 to October 31, 2011**

Version 3.01 of the Lidar Level 2 data products is a significant improvement over the previous version. Major code and algorithm improvements include:

- the elimination of a bug in the cloud clearing code that caused a substantial overestimate of low cloud fraction in earlier data releases (details given in Vaughan et al., 2010);
- enhancements to the cloud-aerosol discrimination algorithm that increase the number of diagnostic parameters used to make classification decisions (details given in Liu et al., 2010);
- improved daytime calibration procedures, resulting in more accurate estimates of layer spatial and optical properties (details given in Powell et al., 2010); and
- an entirely new algorithm for assessing cloud thermodynamic phase (details given in Hu et al., 2009).

Layer Detection

As in previous versions, the layer boundaries reported in the Lidar Level 2 Cloud and Aerosol Layer Products appear to be quite accurate. Some false positives are still found beneath optically thick layers; these, however, can generally be identified by their very low CAD scores (e.g., |CAD score| ≤ 20). In opaque layers, the lowest altitude where signal is reliably observed is reported as the base. In actuality, this reported base may lie well above the true base. Opaque layers are denoted by an opacity flag. In this release, the layers which are reported represent a choice in favor of high reliability over maximum sensitivity. Weakly scattering layers sometimes will go unreported, in the interest of minimizing the number of false positives.

Cloud-Aerosol Discrimination

Figure 1 (below) compares the distributions of CAD scores derived from four months of version 3 test data to the corresponding version 2.01 data. The V3 curve shows a smoother distribution and generally has fewer low CAD values (i.e., values less than ~|95|), reflecting the better separation of clouds and aerosols when using the version 3 5-D PDFs as compared to the separation provided by 3-D PDFs in previous versions. One notable exception to this observation is the bump between -10 and 20 in the V3 test curve, which accounts for ~ 6% of the total features.

The CAD scores in this region identify both outlier features whose optical/physical properties are not correctly measured or derived, and those features whose attributes fall within the overlap region between the cloud and aerosol PDFs. In contrast, these outliers are populated over the entire CAD span in the V2 release.

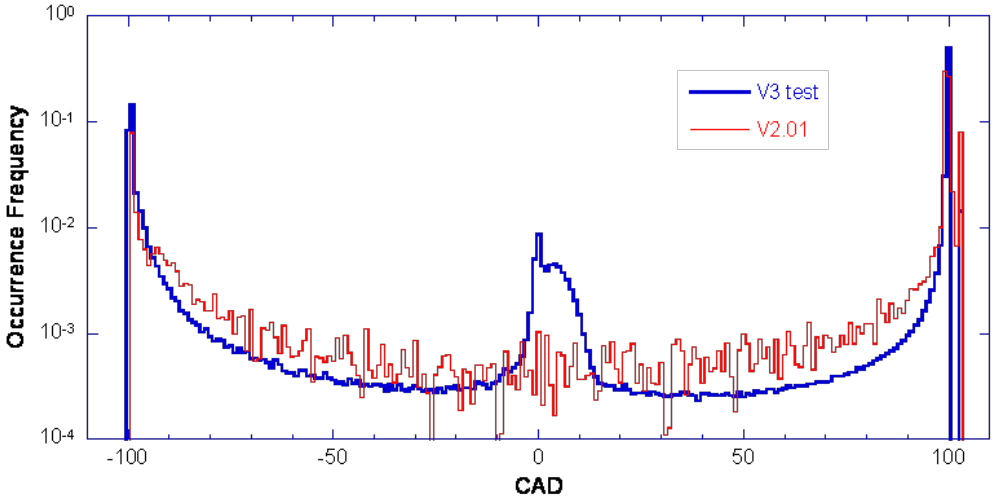

Figure 1: Histograms of CAD scores for Version 2 (red) and Version 3 (blue).

Figure 2 (below) presents the relationship between the CAD score and the layer IAB QA factor, which provides a measure of the integrated attenuated backscatter overlying a cloud or an aerosol layer. A layer IAB QA factor close to 1 indicates that the atmosphere above the layer under is clear. Decreasing values indicate the increasing likelihood of overlying layers that have attenuated the signal within the layer under consideration, and thus decreased the SNR of the measurement. A layer IAB QA factor of 0 would indicate total attenuation of the signal. As seen in the figure, the IAB QA is highest for high magnitude CAD scores and slopes down gradually for small CAD score magnitudes. This relationship reflects the fact that the presence of overlying features tends to add difficulty to the cloud-aerosol classification task, and therefore reduces the confidence of the classifications made. The dip between -10 and 20 represents features that are outliers in the 5-D CAD PDFs and indicates that these outliers most often lie beneath other relatively dense features. The cloud layers with special CAD scores (103 and 104) have the smallest IAB QA values. The relatively big value at CAD = 0 corresponds to the features having zero CAD values at high altitudes where the probability of the presence of overlying features is low. At high altitudes the separation of clouds and aerosols is not as good as at low altitudes because of the presence of subvisible cirrus clouds.

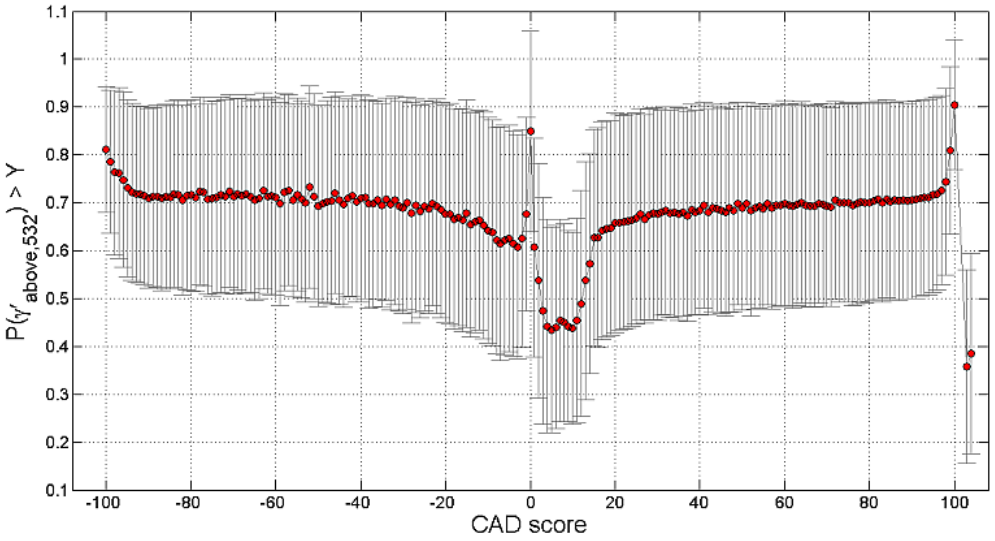

Figure 2: Relationship between CAD score and Layer IAB QA Factor

Overall, because of the better separation between clouds and aerosols in the 5D space, the 5D CAD algorithm significantly improves the reliability of the CAD scores. These improvements include:

1. Dense aerosol layers (primarily very dense dust and smoke over and close to the source regions), which are sometimes labeled as cloud in the V2 release, are now correctly identified as aerosol, largely because of the addition of the integrated volume depolarization ratio to the diagnostic parameters used for cloud-aerosol discrimination. In addition, in the open oceans, dense aerosols that were previously classified as clouds are now frequently observed in the marine boundary layer. Improvements are also seen for these maritime aerosols. Note, however, dense dust/smoke layers found at single-shot (0.333 km) resolution will be classified as cloud by default. This issue will be revisited for post-V3 releases.
2. Because the V2 CAD algorithm used a latitude-independent set of 3D PDFs, a class of optically thin clouds encountered in the polar regions that can extend from the surface to several kilometers were sometimes misclassified as aerosols. In version 3, these features are now correctly classified as cloud.
3. Correct classification of heterogeneous layers is always difficult. An example of a heterogeneous layer would be an aerosol layer that is vertically adjacent to a cloud or contains an embedded cloud, but which is nonetheless detected by the feature finder as a single entity in the V2 release. By convention, heterogeneous layers should be classified as clouds. The version 3 feature finding algorithm has also been improved greatly and can now much better separate the embedded or adjacent single-shot cloud layers from the surrounding aerosol. This improvement in layer detection contributes significantly to the improvement of the CAD performance.
4. Some so-called features identified by the layer detection scheme are not legitimate layers, but instead are artifacts due to the noise in the signal, multiple scattering effects, or to artificial signal enhancements caused by non-ideal detector transient response or an overestimate of the attenuation due to overlying layers. These erroneous "pseudo-features" are neither cloud nor aerosol and are distributed outside of the cloud and aerosol clusters in the PDF space. The V3 CAD algorithm can better identify these outlier features by assigning a small CAD score (the bump between -10 and 20 in the V3 CAD histogram) and classify most of them as cloud by convention. A CAD threshold of 20 can effectively filter out these outliers.

Some misclassifications may still occur with the 5D algorithm. For example, dust aerosols can be transported long distance to the Arctic. When moderately dense dust layers are occasionally transported to high latitudes, where cirrus clouds can present even in the low altitudes, they may be misclassified. This is also the case for moderately dense smoke aerosols occasionally transported to the high latitudes. Smoke can be mixed with ice particles during the long range transport, which makes the smoke identification even more difficult. When moderately dense dust and smoke are transported vertically to high altitudes, even at low latitudes, misclassifications can occur due to the presence of cirrus clouds. Volcanic aerosol that is newly injected into the high altitudes may have a large cross-polarized backscatter signal and thus may be misclassified as cloud.

Aerosol Type Identification

The main objective of the aerosol subtyping scheme is to estimate the appropriate value of the aerosol extinction-to-backscatter ratio (S_a) to within 30% of the true value. S_a is an important parameter used in the determination of the aerosol extinction and subsequently the optical depth from CALIOP backscatter measurements. S_a is an intensive aerosol property, i.e., a property that does not depend on the number density of the aerosol but rather on such physical and chemical properties as size distribution, shape, and composition. These properties depend primarily on the source of the aerosol and such factors as mixing, transport, and, in the case of hygroscopic aerosols, hydration.

The extinction products are produced by first identifying an aerosol type and then using the appropriate values of S_a and the multiple scattering factor, $\eta(z)$. Note that multiple scattering corrections have not yet been implemented for the current data release, so that $\eta(z) = 1$ for all aerosol types. The accuracy of the S_a value used in the lidar inversions depends on the correct identification of the type of aerosol. In turn, the accuracy of the subsequent optical depth estimate depends on the accuracy of S_a.

The underlying paradigm of the type classification is that a variety of emission sources and atmospheric processes will act to produce air masses with a typical, identifiable aerosol type. This is an idealization, but one that allows us to classify aerosols based on observations and location in a way to gain insight into the geographic distribution of aerosol types and constrain the possible values of S_a for use in aerosol extinction retrievals.

The aerosol subtype product is generated downstream of the cloud-aerosol discrimination (CAD) scheme and, therefore, depends on the cloud-aerosol classification scheme in a very fundamental way. If a cloud feature is misclassified as aerosol, the aerosol subtype algorithm will identify this 'aerosol' as one of the aerosol subtypes. The user must exercise caution where the aerosol subtype looks suspicious or unreasonable. Such situations can occur with some frequency in the southern oceans and the polar regions.

Cloud Ice/Water Phase Discrimination

The cloud phase algorithm used in Version 2 has been replaced with a new, completely different approach. The V3 algorithm classifies detected cloud layers as water, randomly-oriented ice (ROI), or horizontally-oriented ice (HOI) based on relations between depolarization, backscatter, and color ratio (Hu et al. 2009). These classifications have not yet been rigorously validated, which is difficult, but many of the obvious artifacts found in the V2 data have been eliminated.

The V2 algorithm included a rudimentary ability to identify a specific subset of high confidence instances of HOI. These clouds were classified as ice clouds and flagged with a 'special CAD score' of 102, indicating that they had been further classified as HOI. The new version 3 algorithm implements a much more sophisticated scheme for recognizing HOI that correctly identifies many more instances of these clouds. The special CAD score of 102 is no longer used to identify these layers. Instead, the "ice cloud" and "mixed phase cloud" classifications have been eliminated and replaced as shown in Table 1 below. Associated QC flags are given in Table 2.

Table 1: Updated Ice/Water Phase Flags

Value	V2 Interpretation	V3 Interpretation
0	unknown/not determined	unknown/not determined
1	ice	randomly oriented ice (ROI)
2	water	water
3	mixed phase	horizontally oriented ice (HOI)

Table 2: Updated Ice/Water Phase QC Flags

Value	V2 Interpretation	V3 Interpretation
0	no confidence	no/low confidence
1	low confidence	phase based on temperature only
2	medium confidence	medium confidence
3	high confidence	high confidence

A confidence flag of QA=1 indicates the phase classification is based on temperature. Initial classification tests are based on layer depolarization, layer-integrated backscatter, and layer-average attenuated backscatter color ratio. Layers classified as water with temperatures less than -40 C are forced to ROI and given confidence flags of QA=1. Layers classified as ROI or HOI with temperatures greater than 0 C are forced to water and also given confidence flags of QA=1. Clouds for which the phase is 'unknown/not determined' are assigned confidence values of 0 (no/low confidence).

Layers classified as HOI based on anomalously high backscatter and low depolarization are assigned QA=3. These layer characteristics are rarely detected after the CALIOP viewing angle was changed to 3° in November 2007. The V3 algorithm computes the spatial correlation of depolarization and integrated backscatter and uses this as an additional test of cloud phase. Layers classified as HOI using this test are assigned QA=2. The spatial correlation test is responsible for the majority of the layers classified as HOI. These layers typically have higher backscatter than ROI but similar depolarization and are common even at a viewing angle of 3°. We interpret this as clouds with

significant perpendicular backscatter from ROI but containing enough HOI to produce enhanced backscatter. These layers tend to be found at much colder temperatures than the high confidence HOI (see Hu et al. 2009).

Cloud and Aerosol Optical Depths

The reliability of cloud and aerosol optical depths reported in the V3 data products is considerably improved over the V2 release. Whereas the V2 optical depths were designated as a beta quality product, and not yet suitable for use in scientific publications, the maturity level of the V3 optical depths has been upgraded to provisional. Several algorithm improvements and bugs fixes factored into the decision to upgrade the maturity level. Among these were the addition of the aerosol layer base extension algorithm, which greatly improves AOD estimates in the planetary boundary layer (PBL), and several significant improvements to the code responsible for rescaling the attenuated backscatter coefficients in lower layers to compensate for the beam attenuation that occurs when traversing transparent upper layers.

Data Quality Statement for CALIPSO's Version 2.02 Lidar Level 2 Data Product Release

Data Version: **2.02**
Data Release Date: **October 2008**
Data Date Range: **September 14, 2008 to October 29, 2009**

Version 2.02 of the Level 2 data products is a maintenance release that implements the following changes.

- Corrections were made to the code used to interpolate the GMAO meteorological data products to the CALIPSO orbit tracks.
- The Cabanes backscattering cross-sections used to derive the molecular scattering models used for the Level 1 and Level 2 analyses were revised downward by ~0.8%.
- A typographical error was identified in the runtime script that controls the behavior of the aerosol subtyping algorithm in the Level 2 analyses.

The impacts of these changes on the Level 2 data products are as follows.

Layer Detection

As a result of the first two changes, the 532 nm and 1064 nm calibration constants are larger, on average, by ~1%, resulting in corresponding decreases in the magnitudes of the attenuated backscatter coefficients at both wavelengths. These changes in the level 1 data result in only small changes to the layer detection statistics. For example, the difference in the total number of layers detected by the two different versions on August 12, 2006 was 4: 9680 layers were detected by the V2.01 code versus 9676 layers detected by the V2.02 code.

Cloud-Aerosol Discrimination

With one exception, there were only minimal changes in cloud-aerosol discrimination results. The exception occurs in the polar regions when PSCs are present. For the August 12, 2006 test case, corrections to the interpolation algorithms applied to the GMAO data result in a slight upward shift in the tropopause heights and hence more clouds and fewer stratospheric layers are identified in the V2.02 results.

Cloud Ice/Water Phase Discrimination

Because this classification is based on depolarization ratio and temperature no substantial changes, there were no substantial changes in the assessments of cloud thermodynamic state.

Aerosol Subtype Identification

Correcting the level 2 runtime script error will reduce the number of layers identified as smoke and increase the number of layers identified as sea salt.

Cloud and aerosol extinction profiles and optical properties

Changes in backscatter and extinction coefficients at the tops of layers are small and proportional to the changes in the calibration coefficients. However, due to the cumulative nature of error propagation in the extinction retrieval, differences between V2.02 and V2.01 increase with increasing penetration depths, and can grow large when optical depths are large (i.e., > 3).

Data Quality Statement for CALIPSO's Version 2.01 Lidar Level 2 Data Product Release

Data Version: **2.01**
Data Release Date: **January 2008**
Data Date Range: **June 13, 2006 to September 13, 2008**

Layer Detection

Given the accuracy of the CALIPSO altitude registration, the layer heights reported in the Lidar Level 2 Cloud and Aerosol Layer Products appear to be quite accurate. In optically dense layers, the lowest altitude where signal is reliably observed is reported as the base. In actuality, this reported base may lie well above the true base. In this release, the layers which are reported represent a choice in favor of high reliability over maximum sensitivity. Weakly scattering layers sometimes will go unreported, in the interest of minimizing the number of false positives.

Cloud-Aerosol Discrimination

Based on the initial CALIOP measurements, an improved version of the cloud-aerosol discrimination (CAD) algorithm has been implemented for this release. Overall, the updated algorithm works well in most cases; manual verification of the classifications for a full day of data suggests that the success rate is in the neighborhood of 90% or better. Nevertheless, several types of misclassifications are still occurred with some frequency. Among these, the most prevalent are:

- Dense aerosol layers (primarily very dense dust and smoke over and close to the source regions) are sometimes labeled as cloud. Because the CAD algorithm operates on individual layers, without a contextual awareness of any surrounding features, it can happen that small but strongly scattering regions within an extended aerosol layer can occasionally be labeled as cloud. This occurs because the optical properties (backscatter and color ratio) within the region are similar to what would be expected for the relatively faint clouds that fall within the PDF overlap region. These misclassifications are often apparent from studying the Level 1 browse images. Based on the initial analysis of the CALIOP measurements, the cloud and aerosol distributions show variabilities that depend on season and on geophysical location. The globally averaged PDFs used in the current release will have a larger overlap between the cloud and aerosol than would occur for more regionally specific statistics. For future versions of the CAD algorithm, we expect to develop and deploy PDFs that will correctly reflect both seasonal and latitudinal variations.
- Many optically thin clouds, both ice and water, are encountered in the polar regions. The current CAD PDFs do not work as well in the polar regions as at lower latitudes and misclassifications of clouds as aerosol are more common. In particular, thin ice clouds which can extend from the surface to several kilometers in altitude, are sometimes misclassified as aerosol.
- Correct classification of heterogeneous layers is always difficult, and the process can easily go awry. An example of a heterogeneous layer would be an aerosol layer that is vertically adjacent to a cloud or contains an embedded cloud, but which is nonetheless detected by the feature finder as a single entity. By convention, heterogeneous layers should be classified as clouds. However, depending on the relative strengths of the components, these layers are sometimes erroneously identified as aerosol.

Some so-called features identified by the layer detection scheme are not legitimate layers, but instead are artifacts due to the noise in the signal, multiple scattering effects, or to artificial signal enhancements caused by non-ideal detector transient response or an overestimate of the attenuation due to overlying layers. These erroneous

"pseudo-features" are neither cloud nor aerosol; however, because they are not properly interdicted in the processing stream, the CAD algorithm nonetheless attempts to assign them to one class or the other. Very frequently these layers can be identified by their very low CAD scores (typically less than 20).

Cloud Ice/Water Phase Discrimination

Cloud phase is determined using a depolarization/backscatter relation, together with temperature and backscatter thresholds. Complete descriptions of the algorithm mechanics and underlying theory are given in Section 6 of the CALIPSO Scene Classification ATBD. The algorithm implemented for the version 2.01 release identifies obvious water and ice clouds and clear cases of oriented ice crystals. Improvements for recognizing mixed phase clouds are planned for future release.

Aerosol Subtype Identification

The main objective of the aerosol subtyping scheme is to estimate the appropriate value of the aerosol extinction-to-backscatter ratio (Sa) to within 30% of the true value. Sa is an important parameter used in the determination of the aerosol extinction and subsequently the optical depth from CALIOP backscatter measurements. Sa is an intensive aerosol property, i.e., a property that does not depend on the number density of the aerosol but rather on such physical and chemical properties as size distribution, shape and composition. These properties depend primarily on the source of the aerosol and such factors as mixing, transport, and in the case of hygroscopic aerosols, hydration.

The extinction products are produced by first identifying an aerosol type and then using the appropriate values of Sa and the multiple scattering factor, $\eta(z)$. Note that multiple scattering corrections have not yet been implemented for the current data release, so that $\eta(z) = 1$ for all aerosol types. The accuracy of the Sa value used in the lidar inversions depends on the correct identification of the type of aerosol. In turn, the accuracy of the subsequent optical depth estimate depends on the accuracy of Sa . The underlying paradigm of the type classification is that a variety of emission sources and atmospheric processes will act to produce air masses with a typical, identifiable aerosol 'type'. This is an idealization, but one that allows us to classify aerosols based on observations and location in a way to gain insight into the geographic distribution of aerosol types and constrain the possible values of Sa for use in aerosol extinction retrievals. The aerosol subtype product is generated downstream of the cloud-aerosol discrimination (CAD) scheme and, therefore, depends on the cloud-aerosol classification scheme in a very fundamental way. If a cloud feature is misclassified as aerosol, the aerosol subtype algorithm will identify this 'aerosol' as one of the aerosol subtypes. The user must exercise caution where the aerosol subtype looks suspicious or unreasonable. Such situations can occur with some frequency in the southern oceans and the polar regions.

Cloud and aerosol extinction profiles

The CALIOP cloud and aerosol profiles of extinction and backscatter are released as beta products. Cloud profiles are reported at a horizontal resolution of 5 km; aerosol profiles are reported at a horizontal resolution of 40 km. These products contain a number of known errors and, in their current form, cannot be used as standalone products. The current products contain no data quality information, and hence must be used in conjunction with the Cloud and/or Aerosol Layer Products and/or the Vertical Feature Mask Product, which contain data quality parameters and confidence flags. Data assessment and screening procedures have not yet been developed. Because of this, the profile data product is considered to be not appropriate for scientific publication but is released to users for evaluation and to provide feedback to the CALIOP algorithm development team. PLEASE NOTE: users of the CALIOP extinction and backscatter profile data should read and thoroughly understand the information provide in the Profile Products Data Quality Summary. This summary contains an expanded description of the extinction retrieval process from which the layer optical depths are derived and provides essential guidance in the appropriate use of all CALIOP extinction-related data products. Validation and improvements to the profile products QA are ongoing efforts, and additional data quality information will be included with future releases.

Cloud and aerosol optical depths

Because comprehensive data assessment and screening procedures have not yet been developed, the CALIOP cloud and aerosol optical depths reported in the V2.01 data release are not considered appropriate for scientific publication. The data is being released as a beta quality product, for evaluation by the user community, and to provide feedback to the CALIOP algorithm development team.

Data Quality Statement for CALIPSO's Version 1.10 Lidar Level 2 Data Product Release

Data Version: **1.10**
Data Release Date: **December 8, 2006**
Data Date Range: **June 13, 2006 to November 11, 2007**

The CALIPSO vertical feature mask (VFM) data product reports a single 16-bit integer for each lidar altitude resolution element in the data stream downlinked from the satellite. Upon decoding each of these bit-mapped integers, users will obtain information describing layer location (both vertically and horizontally), layer type, and the amount of horizontal averaging required for the layer to be detected.

Given the accuracy of the CALIPSO altitude registration, the layer heights reported in the Lidar Level 2 Cloud and Aerosol Layer Products and the VFM appear to be quite accurate. In optically dense layers, the lowest altitude where signal is observed is reported as the base. In actuality, this point may lie well above the true base. In this release, the layers which are reported represent a choice in favor of high reliability over maximum sensitivity. Weakly scattering layers sometimes will go unreported, in the interest of minimizing the number of false positives.

A preliminary version of the algorithm to discriminate cloud and aerosol has been used in this release. Overall, the algorithm performance is fairly good at labeling cloud as cloud and somewhat less successful in labeling aerosol as aerosol. Several types of misclassifications are fairly common and should be watched for. The most common misclassification is portions of dense aerosol layers being labeled as cloud. The algorithm operates on individual profiles, so small regions within an aerosol layer are sometimes labeled as cloud. These misclassifications are often apparent from study of Level 1 browse images. Actual clouds occurring within aerosol layers appear to be correctly classified as cloud most of the time. Additionally, portions of the bases of some cirrus clouds are mislabeled as aerosol, and some tropospheric polar clouds are erroneously labeled as aerosol. Improvements to the cloud/aerosol discrimination algorithm are underway and misclassifications should be greatly reduced in future data releases.

Appendix 1

Prior to November 28, 2007, CALIPSO was nominally pointed in a 'near nadir' direction (actually at ~0.3° off nadir, to avoid the full force of specular reflections from still waters and horizontally oriented ice crystals). In that pointing configuration, the CALIOP browse images – as shown below – correctly represented both the spatial distribution of clouds and aerosols, and the optical effects of overlying layers on the atmosphere below.

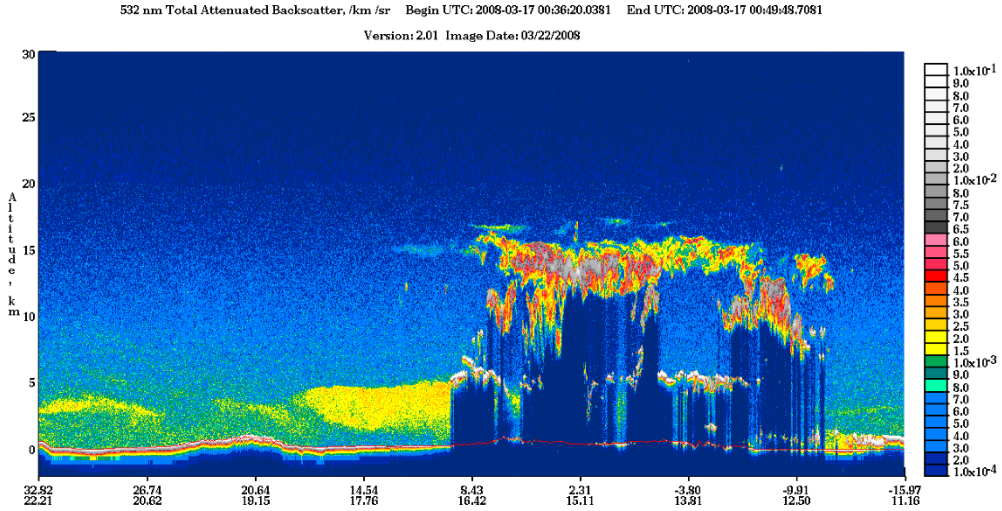

As a result of the change to pointing 3° off-nadir, with the tilt being in the same plane as the satellite velocity vector (i.e., along track, rather than cross track), the spatial distribution of layers is not exactly what is shown in the standard browse images. A more faithful representation might look like this…

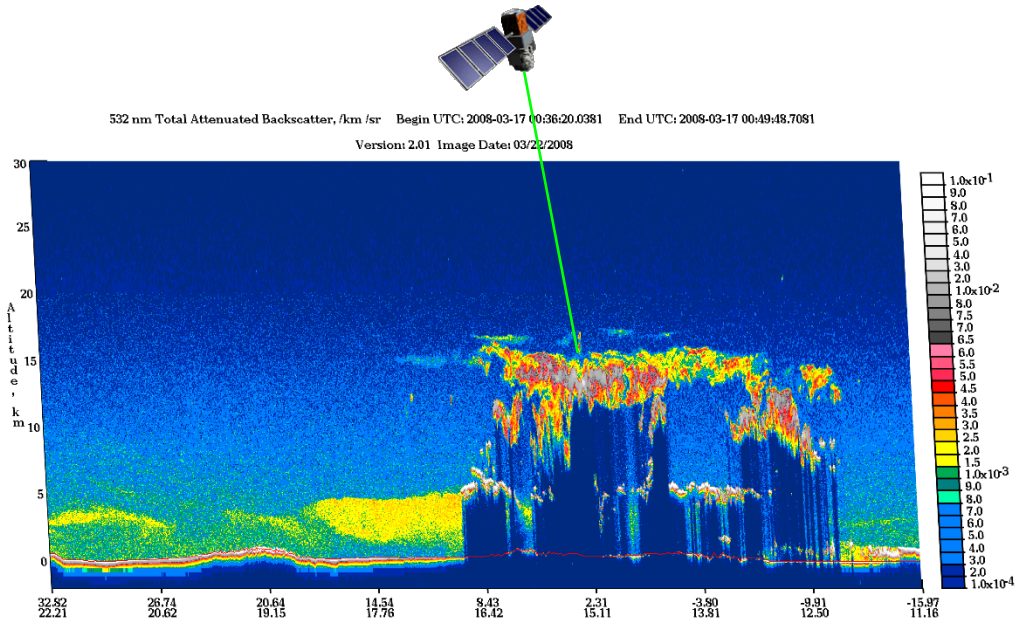

There are several aspects of this change that could be of interest to data users:

1. While there is now a 3° vertical shear in the spatial distribution of clouds and aerosols (i.e., as shown above), the optical effects of overlying layers are still correctly represented by the original, upright images that are being shown on our web pages.
2. The altitudes reported in all products are still measured with respect to a nadir viewing instrument, and thus users need not (and should not) make any corrections for pointing angle.
3. The laser footprint locations reported in the data products give the latitude and longitude coordinates of the beam location on the Earth at mean sea level.
4. The horizontal offset between any two points in the vertical can be computed using 'triangle trig'. If the vertical distance is V, the horizontal offset, Δh, between the upper and lower points is $\Delta h = V \cdot \tan(3°)$.
5. Version 2 of the data products includes a new 'Spacecraft_Position' SDS that contains all of the spacecraft attitude information required to vertically collocate the CALIPSO and CloudSat profiles. This was included at the request of the CloudSat team, specifically for the continued production of their GeoProf products.
6. In general, the optical properties reported for measurements of aerosols and water clouds are not expected to change as a function of the change in pointing angle. However, the properties reported for individual ice clouds will change by some varying amount, depending on the concentration of horizontally aligned ice crystals present in the cloud. Among the changes that can be anticipated are
   - a reduction in the maximum values of integrated attenuated backscatter measured at both wavelengths;
   - an increase in the minimum depolarization ratios associated with strongly scattering ice clouds;
   - a small change in the proportion of clouds classified as ice versus those classified as water; and
   - an increase in the minimum lidar ratios retrieved for strongly scattering ice clouds.

References

Avery, M. A., R. A. Ryan, B. J. Getzewich, M. A. Vaughan, D. M. Winker, Y. Hu, A. Garnier, J. Pelon, and C. A. Verhappen, 2020: CALIOP V4 Cloud Thermodynamic Phase Assignment and the Impact of Near-Nadir Viewing Angles, *Atmos. Meas. Tech.*, **13**, 4539–4563, https://doi.org/10.5194/amt-13-4539-2020.

Burton, S. P., R. A. Ferrare, M. A. Vaughan, A. H. Omar, R. R. Rogers, C. A. Hostetler, and J. W. Hair, 2013: Aerosol Classification from Airborne HSRL and Comparisons with the CALIPSO Vertical Feature Mask, *Atmos. Meas. Tech.*, **6**, 1397–1412, https://doi.org/10.5194/amt-6-1397-2013.

Chand, D., T. L. Anderson, R. Wood, R. J. Charlson, Y. Hu, Z. Liu, and M. Vaughan, 2008: Quantifying above-cloud aerosol using spaceborne lidar for improved understanding of cloudy-sky direct climate forcing, *J. Geophys. Res.*, **113**, D13206, https://doi.org/10.1029/2007JD009433.

Haarig, M., R. Engelmann, H. Baars, B. Gast, D. Althausen and A. Ansmann, 2025: Discussion of the spectral slope of the lidar ratio between 355 nm and 1064 nm from multiwavelength Raman lidar observations, *Atmos. Chem. Phys.*, **25**, 7741–7763, https://doi.org/10.5194/acp-25-7741-2025.

Heymsfield, A. J., D. Winker, and G.-J. van Zadelhoff, 2005: Extinction-ice water content-effective radius algorithms for CALIPSO, *Geophys. Res. Lett.*, **32**, L10807, https://doi.org/10.1029/2005GL022742.

Heymsfield, A., D. Winker, M. Avery, M. Vaughan, G. Diskin, M. Deng, V. Mitev, and R. Matthey, 2014: Relationships between Ice Water Content and Volume Extinction Coefficient from In Situ Observations for Temperatures from 0° to -86°C: Implications for Spaceborne Lidar Retrievals, *J. Appl. Meteor. Climatol.*, **53**, 479–505, https://doi.org/10.1175/JAMC-D-13-087.1.

Holz, R. E., S. Platnick, K. Meyer, M. Vaughan, A. Heidinger, P. Yang, G. Wind, S. Dutcher, S. Ackerman, N. Amarasinghe, F. Nagle, and C. Wang, 2016: Resolving ice cloud optical thickness biases between CALIOP and MODIS using infrared retrievals, *Atmos. Chem. Phys.*, **16**, 5075–5090, https://doi.org/10.5194/acp-16-5075-2016.

Hu, Y. M. Vaughan, Z. Liu, B. Lin, P. Yang, D. Flittner, W. Hunt, R. Kuehn, J. Huang, D. Wu, S. Rodier, K. Powell, C. Trepte, and D. Winker, 2007: The depolarization-attenuated backscatter relation: CALIPSO lidar measurements vs. theory, *Opt. Express*, **15**, 5327–5332, https://doi.org/10.1364/OE.15.005327.

Hu, Y., M. Vaughan, Z. Liu, K. Powell, and S. Rodier, 2007: Retrieving Optical Depths and Lidar Ratios for Transparent Layers Above Opaque Water Clouds From CALIPSO Lidar Measurements, *IEEE Geosci. Remote Sens. Lett.*, **4**, 523–526, https://doi.org/10.1109/LGRS.2007.901085.

Hunt, W. H, D. M. Winker, M. A. Vaughan, K. A. Powell, P. L. Lucker, and C. Weimer, 2009: CALIPSO Lidar Description and Performance Assessment, *J. Atmos. Oceanic Technol.*, **26**, 1214–1228, https://doi.org/10.1175/2009JTECHA1223.1.

Kar, J., K.-P. Lee, M. A. Vaughan, J. L. Tackett, C. R. Trepte, D. M. Winker, P. L. Lucker, and B. J. Getzewich, 2019: CALIPSO Level 3 Stratospheric Aerosol Product: Version 1.00 Algorithm Description and Initial Assessment, *Atmos. Meas. Tech.*, **12**, 6173–6191, https://doi.org/10.5194/amt-12-6173-2019

Kim, M.-H., A. H. Omar, J. L. Tackett, M. A. Vaughan, D. M. Winker, C. R. Trepte, Y. Hu, Z. Liu, L. R. Poole, M. C. Pitts, J. Kar, and B. E. Magill, 2018: The CALIPSO Version 4 Automated Aerosol Classification and Lidar Ratio Selection Algorithm, *Atmos. Meas. Tech.*, **11**, 6107-6135, https://doi.org/10.5194/amt-11-6107-2018.

Liu, Z., R. Kuehn, M. Vaughan, D. Winker, A. Omar, K. Powell, C. Trepte, Y. Hu, and C. Hostetler, 2010: The CALIPSO Cloud And Aerosol Discrimination: Version 3 Algorithm and Test Results, 25th International Laser Radar Conference (ILRC), 5–9 July 2010, St. Petersburg, Russia; see https://www.researchgate.net/publication/285685007.

Liu, Z., J. Kar, S. Zeng, J. Tackett, M. Vaughan, M. Avery, J. Pelon, B. Getzewich, K.-P. Lee, B. Magill, A. Omar, P. Lucker, C. Trepte, and D. Winker, 2019: "Discriminating Between Clouds and Aerosols in the CALIOP Version 4.1 Data Products", *Atmos. Meas. Tech.*, **12**, 703–734, https://doi.org/10.5194/amt-12-703-2019.

Lopes, F. J. S., E. Landulfo, and M. A. Vaughan, 2013: Evaluating CALIPSO's 532 nm lidar ratio selection algorithm using AERONET sun photometers in Brazil, *Atmos. Meas. Tech.*, **6**, 3281–3299, https://doi.org/10.5194/amt-6-3281-2013.

Lu, X., Y. Hu, Z. Liu, S. Rodier, M. Vaughan, C. Trepte, and J. Pelon, 2017: Observations of Arctic snow and sea ice cover from CALIOP lidar measurements, *Remote Sens. Environ.*, **194**, 248–263, https://doi.org/10.1016/j.rse.2017.03.046.

Lu, Z., X. Liu, Z. Zhang, C. Zhao, K. Meyer, C. Rajapakshe, C. Wu, Z. Yang and J. E. Penner, 2018: Biomass smoke from southern Africa can significantly enhance the brightness of stratocumulus over the southeastern Atlantic Ocean, *PNAS*, **115**, 2924–2929, https://doi.org/10.1073/pnas.1713703115.

Mace, G. G., S. Benson and Y. Hu, 2020: On the Frequency of Occurrence of the Ice Phase in Supercooled Southern Ocean Low Clouds Derived from CALIPSO and CloudSat, *Geophys. Res. Lett.*, **47**, e2020GL087554, https://doi.org/10.1029/2020GL087554.

McGill, M. J., M. A. Vaughan, C. R. Trepte, W. D. Hart, D. L. Hlavka, D. M. Winker, and R. Kuehn, 2007: Airborne validation of spatial properties measured by the CALIPSO lidar, *J. Geophys. Res.*, **112**, D20201, https://doi.org/10.1029/2007JD008768.

Papagiannopoulos, N. and 15 coauthors, 2016: CALIPSO climatological products: evaluation and suggestions from EARLINET, *Atmos. Chem. Phys.*, **16**, 2341–2357, https://doi.org/10.5194/acp-16-2341-2016.

Platt, C. M. R., D. M. Winker, M. A. Vaughan and S. D. Miller, 1999: Backscatter-to-Extinction Ratios in the Top Layers of Tropical Mesoscale Convective Systems and in Isolated Cirrus from LITE Observations, *J. Appl. Meteor. Climatol.*, **38**, 1330–1345, https://doi.org/10.1175/1520-0450(1999)038<1330:BTERIT>2.0.CO;2.

Powell, K. A., C. A. Hostetler, Z. Liu, M. A. Vaughan, R. E. Kuehn, W. H. Hunt, K. Lee, C. R. Trepte, R. R. Rogers, S. A. Young, and D. M. Winker, 2009: CALIPSO Lidar Calibration Algorithms: Part I - Nighttime 532 nm Parallel Channel and 532 nm Perpendicular Channel, *J. Atmos. Oceanic Technol.*, **26**, 2015–2033, https://doi.org/10.1175/2009JTECHA1242.1.

Powell, K. A., M. A. Vaughan, R. R. Rogers, R. E. Kuehn, W. H. Hunt, K-P. Lee, and T. D. Murray, 2010: The CALIOP 532-nm Channel Daytime Calibration: Version 3 Algorithm, 25th International Laser Radar Conference (ILRC), 5–9 July 2010, St. Petersburg, Russia; see https://www.researchgate.net/publication/391011856.

Rajapakshe, C., Z. Zhang, J. E. Yorks, H. Yu, Q. Tan, K. Meyer, S. Platnick and D. M. Winker, 2017: Seasonally Transported Aerosol Layers over Southeast Atlantic are Closer to Underlying Clouds than Previously Reported, *Geophys. Res. Lett.*, **44**, https://doi.org/10.1002/2017GL073559.

Redemann, J. and 68 coauthors, 2021: An overview of the ORACLES (ObseRvations of Aerosols above CLouds and their intEractionS) project: aerosol–cloud–radiation interactions in the southeast Atlantic basin, *Atmos. Chem. Phys.*, **21**, 1507–1563, https://doi.org/10.5194/acp-21-1507-2021.

Rodriguez, J. V., R. C. Verhappen, C. Weimer, C. R. Trepte and T. E. Cayton, 2022: Charged Particle Fluxes Associated with CALIPSO Low Laser Energy Shots, *IEEE T. Nucl. Sci.*, **69**, 2146–2153, https://doi.org/10.1109/TNS.2022.3204715.

Ryan, R. A., M. A. Vaughan, S. D. Rodier, J. L. Tackett, J. A. Reagan, R. A. Ferrare, J. W. Hair, and B. J. Getzewich, 2024: Total Column Optical Depths Retrieved from CALIPSO Lidar Ocean Surface Backscatter, *Atmos. Meas. Tech.*, **17**, 6517–6545, https://doi.org/10.5194/amt-17-6517-2024.

Tackett, J., M. Vaughan, J. Lambeth, and A., Garnier, 2022: Critical Improvements to CALIOP Boundary Layer Cloud-Clearing in Version 4.5, 2022 CALIPSO/CloudSat Science Team Meeting, 12–14 September 2022, Fort Collins, CO USA, https://ntrs.nasa.gov/citations/20220013563.

Tackett, J. L., J. Kar, M. A. Vaughan, B. Getzewich, M.-H. Kim, J.-P. Vernier, A. H. Omar, B. Magill, M. C. Pitts, and D. Winker, 2023: The CALIPSO version 4.5 stratospheric aerosol subtyping algorithm, *Atmos. Meas. Tech.*, **16**, 745–768, https://doi.org/10.5194/amt-16-745-2023.

Tackett, J. L., R. A. Ryan, A. E. Garnier, J. Kar, B. Getzewich, X. Cai, M. A. Vaughan, C. R. Trepte, R. Verhappen, D. M. Winker and K.-P. A. Lee, 2025: Mitigating Impacts of Low Energy Laser Pulses on CALIOP Data Products, *EGUsphere* [AMTD], https://doi.org/10.5194/egusphere-2025-2376, accepted for publication.

Toth, T. D., J. Zhang, J. R. Campbell, J. S. Reid, Y. Shi, R. S. Johnson, A. Smirnov, M. A. Vaughan, and D. M. Winker, 2013: Investigating Enhanced Aqua MODIS Aerosol Optical Depth Retrievals over the Mid-to-High Latitude Southern Oceans through Intercomparison with Co-Located CALIOP, MAN, and AERONET Datasets, *J. Geophys. Res.*, **118**, 4700–4714, https://doi.org/10.1002/jgrd.50311.

Toth, T. D., J. R. Campbell, J. S. Reid, J. L. Tackett, M. A. Vaughan, J. Zhang, and J. W. Marquis, 2018: Minimum Aerosol Layer Detection Sensitivities and their Subsequent Impacts on Aerosol Optical Thickness Retrievals in CALIPSO Level 2 Data Products, *Atmos. Meas. Tech.*, **11**, 499–514, https://doi.org/10.5194/amt-11-499-2018.

Toth, T. D., M. Clayton, Z. Li, D. Painemal, S. Rodier, J. Kar, T. Thorsen, R. Ferrare, M. Vaughan, J. Tackett, H. Bian, M. Chin, A. Garnier, E. Welton, R. Ryan, C. Trepte and D. Winker, 2025: Mapping CALIPSO Marine and Dusty Marine Aerosol Lidar Ratios using MODIS AOD Constrained Retrievals and GOCART Model Simulations, *EGUsphere* [AMTD], https://doi.org/10.5194/egusphere-2025-2832, accepted for publication.

Vaughan, M., K. Powell, R. Kuehn, S. Young, D. Winker, C. Hostetler, W. Hunt, Z. Liu, M. McGill, and B. Getzewich, 2009: Fully Automated Detection of Cloud and Aerosol Layers in the CALIPSO Lidar Measurements, *J. Atmos. Oceanic Technol*., **26**, 2034–2050, https://doi.org/10.1175/2009JTECHA1228.1.

Vaughan, M., R. Kuehn, J. Tackett, R. Rogers, Z. Liu, A. Omar, B. Getzewich, K. Powell, Y. Hu, S. Young, M. Avery, D. Winker, and C. Trepte, 2010: Strategies for Improved CALIPSO Aerosol Optical Depth Estimates, 25th International Laser Radar Conference (ILRC), 5–9 July 2010, St. Petersburg, Russia, https://ntrs.nasa.gov/citations/20100026019

Vaughan, M., K.-P. Lee, A. Garnier and B. Getzewich, 2016: Improvements to the CALIOP Surface Detection Algorithm, CALIPSO CloudSat Science Team Meeting, 1-3 March 2016, Newport News, VA USA, https://doi/org/10.13140/RG.2.2.21628.04481.

Venkata, S. L. and J. A. Reagan, 2016: Aerosol Retrievals from CALIPSO Lidar Ocean Surface Returns, *Remote Sens.*, **8**, 1006, https://doi.org/10.3390/rs8121006.

Yang, P., L. Bi, B. A. Baum, K.-N. Liou, G. W. Kattawar, M. I. Mishchenko, and B. Cole, 2013: Spectrally Consistent Scattering, Absorption, and Polarization Properties of Atmospheric Ice Crystals at Wavelengths from 0.2 to 100 µm, *J. Atmos. Sci.*, **70**, 330–347, https://doi.org/10.1175/JAS-D-12-039.1.